SPRINGER BRIEFS IN ELECTRICAL AND COMPUTER ENGINEERING · CONTROL, AUTOMATION AND ROBOTICS

Alexander Scheinker
Miroslav Krstić

Model-Free Stabilization by Extremum Seeking

Springer

SpringerBriefs in Electrical and Computer Engineering

Control, Automation and Robotics

More information about this series at http://www.springer.com/series/10198

Alexander Scheinker · Miroslav Krstić

Model-Free Stabilization by Extremum Seeking

Springer

Alexander Scheinker
Low-Level RF Control Group
Los Alamos National Laboratory
Los Alamos, NM
USA

Miroslav Krstić
Department of Mechanical and Aerospace Engineering
University of California, San Diego
La Jolla, CA
USA

ISSN 2191-8112 ISSN 2191-8120 (electronic)
SpringerBriefs in Electrical and Computer Engineering
ISSN 2192-6786 ISSN 2192-6794 (electronic)
SpringerBriefs in Control, Automation and Robotics
ISBN 978-3-319-50789-7 ISBN 978-3-319-50790-3 (eBook)
DOI 10.1007/978-3-319-50790-3

Library of Congress Control Number: 2016959805

Mathematics Subject Classification (2010): 93-01, 93-02

Printed on acid-free paper

This Springer imprint is published by Springer Nature
The registered company is Springer International Publishing AG
The registered company address is: Gewerbestrasse 11, 6330 Cham, Switzerland

Preface

Originating in 1922, in its 95-year history, extremum seeking has served as a tool for model-free real-time optimization of stable dynamic systems. We introduce a paradigm in which not only is the system being optimized allowed to be time varying and open-loop **unstable**, but also the very goal of extremum seeking is to stabilize the system. The cost function and the control Lyapunov function (CLF) play interchangeable roles, with the unknown optimal set point being implicitly defined through the cost/CLF and coinciding with the equilibrium to be stabilized.

Our "extremum seeking for stabilization" (ESS) consists of employing the CLF as the cost function in a slightly modified extremum seeking algorithm. The goal is to minimize the CLF, i.e., to drive the CLF value to zero over time, which amounts to asymptotic stabilization. Unlike conventional CLF-based stabilization approaches, which employ the knowledge of the system model in the feedback law (Sontag's formula being a "universal" and a particularly clear example of such a feedback law), our ESS approach does not rely on the system model and does not require its knowledge. Instead, ESS employs periodic perturbation signals, along with the CLF. The same effect as that of CLF-based feedback laws that imply the modeling knowledge is achieved, but in a time-average sense.

Averaging is an important tool in the analysis of ESS controllers. Rather than standard averaging, which utilizes integrals of the system's vector field, we employ Lie bracket-based (i.e., derivative-based) averaging, based on weak limits of combinations of dithering terms and their integrals. As results based on averaging are of "approximate" nature, so are the stability properties that we achieve. For instance, in contrast to global stability properties that are achieved by CLF-based control laws that employ the full modeling knowledge, our model-free ESS controllers achieve stability that is semiglobal and "practical" asymptotic (or exponential). This is an acceptable price we pay for achieving model-free stabilization with very simple control algorithms.

In addition to developing simple robust/adaptive model-free stabilizing controllers, we develop new extremum seeking algorithms, which employ bounded updates. One of the corollaries of our effort is also that we provide alternative and

more generally applicable solutions to the problem of controlling systems with unknown signs of high-frequency gains (the Morse–Nussbaum problem). While standard adaptive solutions require the high-frequency gains (and their signs) to be constant, our perturbation-based extremum seeking solution allows the high-frequency gain to vary with time and even its sign to change.

Our exposition is mathematically self-contained. We present many illustrative examples and even several experimental applications. The intended audience for this brief ranges from theoretical control engineers and mathematicians to practicing engineers in various industrial areas and in robotics. Chapter 1 motivates the problems considered and gives the overview of the topics. Chapter 2 presents the mathematical foundations on which the rest of the brief is built. Chapters 3–8 present the control designs and their mathematical properties established through theorems. In particular, Chap. 8 demonstrates the generality of our weak-limit averaging approach in utilizing discontinuous and non-differentiable dithers. Chapter 9 presents experimental applications and provides design guidelines.

Alexander Scheinker thanks his parents, Vladimir Scheinker and Anna Gazumyan, and his wife Reeju Pokharel, for their support and encouragement and his brother David Scheinker for his collaboration on the weak-limit averaging Theorem 2.3, which is the main theoretical result upon which many of the results of this work are based. Miroslav Krstić thanks Hans-Bernd Durr for his innovative connection of Lie bracket averaging with extremum seeking.

Los Alamos, NM, USA
La Jolla, CA, USA
November 2016

Alexander Scheinker
Miroslav Krstić

Contents

Chapter 1
Introduction

1.1 Motivation

The main focus of this book is the stabilization and optimization of unknown, nonlinear, time-varying systems, by utilizing an extremum seeking (ES) approach directly as the feedback controller itself.

Our "extremum seeking for stabilization" (ESS) consists of employing the control Lyapunov function (clf) as the cost function in a slightly modified extremum seeking algorithm. The goal is to minimize the clf, i.e., to drive the clf value to zero over time, which amounts to asymptotic stabilization. Unlike conventional clf-based stabilization approaches, which employ the knowledge of the system model in the feedback law (Sontag's formula being a 'universal' and a particularly clear example of such a feedback law), our ESS approach does not rely on the system model and doesn't require its knowledge. Instead, ESS employs periodic perturbation signals, along with the clf. The same effect as that of clf-based feedback laws that imply the modeling knowledge is achieved, but in a time-average sense.

Averaging is an important tool in the analysis of ESS controllers. Rather than standard averaging, which utilizes integrals of the systems vector field, we employ weak limit-based averaging. As results based on averaging are of "approximate" nature, so are the stability properties that we achieve. For instance, in contrast to global stability properties that are achieved by clf-based control laws that employ the full modeling knowledge, our model-free ESS controllers achieve stability that is semiglobal and "practical" asymptotic (or exponential). This is an acceptable price we pay for achieving model-free stabilization with very simple control algorithms.

In addition to developing simple robust/adaptive model-free stabilizing controllers, we develop new extremum seeking algorithms, which employ bounded updates. One of the corollaries of our effort is also that we provide alternative and more generally applicable solutions to the problem of controlling systems with unknown signs of high-frequency gains (the Morse-Nussbaum problem). While standard adaptive solutions require the high-frequency gains (and their signs) to be constant, our

A. Scheinker and M. Krstić, *Model-Free Stabilization by Extremum Seeking*,
SpringerBriefs in Control, Automation and Robotics,
DOI 10.1007/978-3-319-50790-3_1

perturbation-based extremum seeking solution allows the high-frequency gain to vary with time and even its sign to change.

For illustration, we also consider problems such as source seeking with unknown, open-loop unstable systems, in which an unknown trajectory is followed based only on signal-strength measurements. We also consider many parameter systems which must both be stabilized and tuned in order to optimize an analytically unknown, time-varying cost function, based only on noise-corrupted measurements of the unknown function, so that the system operates in a stable, optimal manner.

This chapter introduces a few general examples of the types of systems that we can handle with our ESS method. Many of the results presented in this book are based on the authors' recent publications, including initial development of ESS for feedback stabilization [125, 126, 128], ESS for tracking [127], high voltage converter modulator optimization [129], automated particle accelerator tuning [130], a self-turning off version of ESS in which the dithers die out as equilibrium is approached [131], a bounded form of ESS [132], utilizing ESS for electron beam property prediction in a particle accelerator [133], a general form of ESS with non-periodic, discontinuous, non-differentiable dithers [134], ESS for systems not affine in control [135], and ESS for particle accelerating cavity resonance control [136, 137].

Scalar Linear Systems

A simple first example is the open-loop unstable scalar system

$$\dot{x} = x + b(t)u, \tag{1.1}$$

with unknown control direction $b(t)$. For such a system, standard controllers would fail if the sign of $b(t)$ was guessed incorrectly or if $b(t)$ passed through zero, changing sign, such as, for example, $b(t) = \sin(2\pi f t)$. However, under the action of the ES controller:

$$u = \sqrt{\alpha\omega}\cos(\omega t + kx^2),$$

for large ω, the dynamics of system (1.1) are, on average

$$\dot{\bar{x}} = \left(1 - k\alpha b^2(t)\right)\bar{x}. \tag{1.2}$$

The most important feature of system (1.2) is that the unknown control direction, $b(t)$, has been replaced with $b^2(t) \geq 0$ [126]. Therefore, if $b(t)$ is non-zero often enough, as discussed in more detail in the chapters that follow, for large enough $k\alpha > 0$, we can stabilize the system without worrying about the sign of $b(t)$.

Vector-valued Nonlinear Systems

For vector-valued, time-varying, nonlinear systems, of the form

$$\dot{x} = f(x,t) + g(x,t)u, \tag{1.3}$$

where the functions $f, g : \mathbb{R}^{n+1} \to \mathbb{R}^n$ are unknown and the system is possibly open-loop unstable, we utilize the scalar controller

$$u = \sqrt{\alpha\omega}\cos\left(\omega t + kV(x,t)\right), \tag{1.4}$$

where $V(x,t)$ is a Lyapunov-type function of our choice (such as $\|x\|^2$), we get the average dynamics

$$\dot{\bar{x}} = f(\bar{x},t) - \frac{k\alpha}{2} g(\bar{x},t) g^T(\bar{x},t) \left(\nabla_{\bar{x}} V(\bar{x},t)\right)^T, \tag{1.5}$$

where $\nabla_{\bar{x}}$ is the gradient with respect to $\bar{x}$. Again, the unknown control direction ambiguity is removed with $g(\bar{x},t)g^T(\bar{x},t) \geq 0$, or, more precisely, for $\nabla_{\bar{x}} V g \left(\nabla_{\bar{x}} V g\right)^T$, and for large enough $k\alpha > 0$ relative to $\nabla_{\bar{x}} V f$, the system performs a gradient descent of $V(\bar{x},t)$.

Vector-valued Nonlinear Systems Not Affine in Control

In the following chapters, we will show that this approach is not limited to systems affine in control, and is applicable to systems such as

$$\dot{x} = f(x,t) + g(x,t,u), \tag{1.6}$$

where $g(x,t,u)$ is a polynomial in u, with dominant odd-powered terms and allowable small even-powered perturbations of the form $\varepsilon g_{n,e}(x,t)u^{2n}$, for $|\varepsilon| \ll 1$, of the form

$$g(x,t,u) = \sum_{n=1}^{m_o} g_{n,o}(x,t)u^{2n+1}(x,t) + \varepsilon \sum_{n=1}^{m_e} g_{n,e}(x,t)u^{2n}(x,t). \tag{1.7}$$

This general result is important because many common nonlinear systems, such as those with dead-zone and saturation, can be approximated arbitrarily accurately by odd-powered polynomials over compact sets. Applying the ES controller

$$u(x,t) = \left(\sqrt{\alpha\omega}\right)^{\frac{1}{2m_0+1}} \cos(\omega t + kV(x,t)), \tag{1.8}$$

results in average dynamics of the form

$$\dot{\bar{x}} = f(\bar{x},t) - \frac{k\alpha}{2} G^2(\bar{x},t) \frac{\partial V(\bar{x},t)}{\partial \bar{x}}, \tag{1.9}$$

where $G(x,t)$ is a function which depends on the form of $g(x,t,u)$.

Stabilization and Optimization

When considering the type of problem most often associated with extremum seeking, one in which a system has an unknown output function whose value is to be maximized or minimized, our approach extends the standard ES results to noisy, open-loop unstable, time-varying, unknown systems of the form

$$\dot{x} = f(x,t) + g(x,t,u(y,t)), \quad y = h(x,t) + n(t), \tag{1.10}$$

where the output function $h(x,t)$ is analytically unknown, y is its noise corrupted measurement, $n(t)$ is bounded noise, and $g(x,t,u)$ is a polynomial in u as in (1.7). We replace $V(x,t)$ with y in (1.8) and apply the controller

$$u(x,t) = \left(\sqrt{\alpha\omega}\right)^{\frac{1}{2m_0+1}} \cos(\omega t + ky). \tag{1.11}$$

The resulting average dynamics are

$$\dot{\bar{x}} = f(\bar{x},t) - \frac{k\alpha}{2} G(\bar{x},t) G^T(\bar{x},t) \left(\nabla_{\bar{x}} h(\bar{x},t)\right)^T, \tag{1.12}$$

a gradient descent of the actual, unknown function $h(\bar{x},t)$ with respect to $\bar{x}$.

Example 1.1 As a simple example considered the open-loop unstable system

$$\dot{x} = \underbrace{x + 0.25\sin(t)x^2}_{f(x,t)} + \underbrace{0.5xu(y) + \sin(3t)u^3(y)}_{g(x,t,u)}, \quad y = \underbrace{(x - \sin(3t))^2}_{h(x,t)} + \underbrace{n(t)}_{\text{noise}}. \tag{1.13}$$

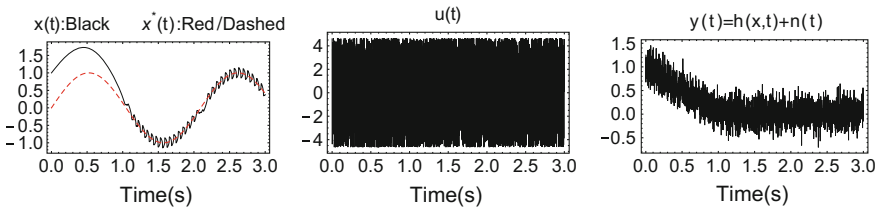

Fig. 1.1 Despite noisy measurements, $x(t)$ tracks the minimizing value, $x^\star(t)$, of unknown $h(x,t)$

We utilize a controller based only on the noisy measurement y:

$$u(y) = \left(\sqrt{\alpha\omega}\right)^{\frac{1}{3}} \cos(\omega t + ky), \tag{1.14}$$

which minimizes the unknown $h(x, t)$, with average system dynamics:

$$\dot{\bar{x}} = \bar{x} + 0.25\sin(t)\bar{x}^2 - \sin^2(3t)\frac{5}{16}k\alpha\frac{\partial h(\bar{x}, t)}{\partial \bar{x}}, \quad \bar{x}(0) = x(0). \tag{1.15}$$

The simulation results are shown in Fig. 1.1.

Multiparameter Optimization

Consider the problem of locating an extremum point of the function $J(\theta) : \mathbb{R}^n \to \mathbb{R}$, for $\theta = (\theta_1, \ldots, \theta_n) \in \mathbb{R}^n$. We assume that $J(\theta)$ has a global extremum such that there exists a unique $\theta^\star$ for which:

$$\nabla J|_{\theta^\star} = 0 \quad \text{and} \quad \nabla J \neq 0, \quad \forall \theta \neq \theta^\star. \tag{1.16}$$

We utilize the following extremum seekers:

$$\dot{\theta}_i = \sqrt{\alpha_i \omega_i}\cos\left(\omega_i t + k_i J(\theta)\right), \tag{1.17}$$

where $\omega_i = \omega\hat{\omega}_i$ such that $\hat{\omega}_i \neq \hat{\omega}_j \; \forall i \neq j$ and J satisfies (1.16). On average, the parameters θ_i will evolve according to a gradient descent of the unknown function $J(\theta)$:

$$\dot{\bar{\theta}} = -\frac{k\alpha}{2}\left(\nabla J\right)^T, \tag{1.18}$$

where $k\alpha$ is the diagonal matrix with entries $k_i\alpha_i$.

The results presented here, for a large class of systems, perform what is classically done with ES, with the added benefit that we can handle unstable and time-varying systems without having a-priori available stabilizing controllers. A quick summary of the differences between ES for stabilization and classical ES is provided in Fig. 1.2.

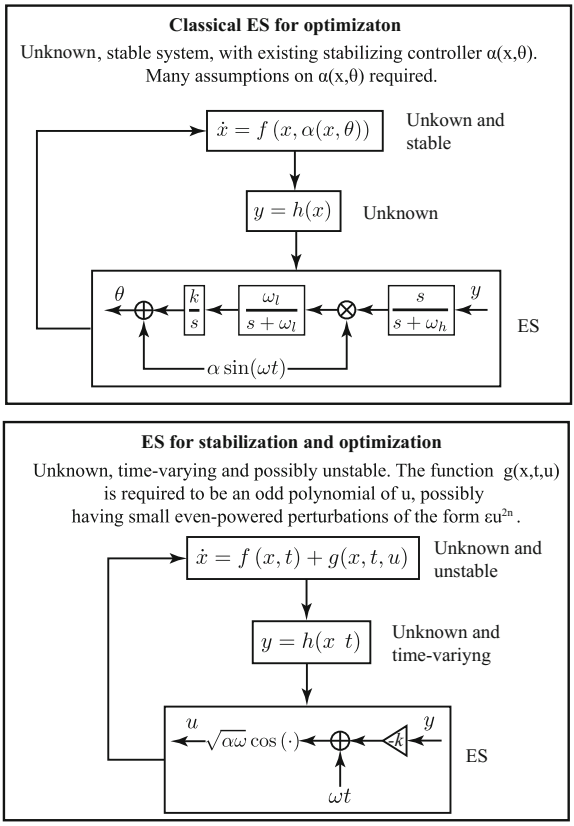

Fig. 1.2 Comparison of traditional ES for optimization (*top*) and the ES-based feedback for stabilization and optimization presented in this book (*bottom*)

1.2 Classical ES Background

Classical extremum seeking, a perturbation driven method for optimization, was developed for use as a tool for finding and maintaining the extremum value of an unknown function, which may be the output of a known dynamic system. This approach was first proposed in the 1922 paper of Leblanc [83]. In his paper, Leblanc reported on a new method for maintaining maximum power transfer from a transmission line to a tram car. Leblanc's paper was a description of an ingenious engineering design, but there was no mathematical analysis of the scheme's dynamics. Eventually, Leblanc's simple, powerful method became a popular tool for maximizing or minimizing unknown output functions for stable, known dynamic systems.

The intuitive explanation of why Leblanc's method works is very simple. Starting with some initial condition, $x(0)$ the system's input is perturbed in the form

$$x(t) = x(0) + \cos(\omega t),$$

which results in a perturbation of some unknown output function, $F(x(t)) = F(x(0) + \cos(\omega t))$. If $F(x)$ has an extremum point near $x(0)$ then $F(x(t))$ will be in or out of phase with the perturbing term $\cos(\omega t)$ as shown in Fig. 1.3. The phase of the output function, relative to the perturbing term then gives the controller an idea of which way to move the parameter in order to approach the extremum point. By mixing and filtering this process is made into an automated feedback loop which drives a system's output towards its minimum.

This simple and effective optimization scheme gained further attention in Russia starting in the 1940s [66, 67]. In the U.S. the scheme was introduced in the 1950s [30] for optimization of the performance of an internal combustion engine. In the 1950s and 1960s the algorithm was modified and its performance for specific problems was analyzed [97, 98, 112, 117], but rigorous performance and design analysis had not taken place. In 1971 a Lyapunov based stability analysis of a particular extremum seeking system was performed [95].

In 2000 the first general stability analysis of the extremum seeking method was performed by Krstić and Wang [76], for stable dynamic systems, with unknown output functions. What follows is an intuitive description of principle of operation of the ES scheme. For detailed analysis, which is an interesting combination of standard averaging and singular perturbation theory, one should consult the reference.

The dynamic system is given by $\dot{x} = f(x, u)$ for which a locally exponentially stabilizing family of controllers, parametrized by θ, in the form of $u = \alpha(x, \theta)$, is known and there exists a unique equilibrium map $l(\theta)$ such that $\dot{x} = 0$ if and only of $x = l(\theta)$. Furthermore, the unknown output function, $y = h(x)$ is assumed to have a minimum at some value of $\theta = \theta^\star$, such that $h(l(\theta))$ satisfies some usual minimization characteristics at $\theta = \theta^\star$ such as, for example $\frac{dh}{d\theta}\big|_{\theta^\star} = 0$.

In this setup a dithering term $a\sin(\omega t)$ is used to perturb the value of θ, in order to search for the optimal control which will minimize the output function $h(l(\theta))$. The value of the output function, $y = h(x)$ is first passed through the high pass filter, whose Laplace transform is represented as $\frac{s}{s+\omega_h}$ in order to remove any constant terms. The filtered signal is then mixed with the same term, $a\sin(\omega t)$, and then low pass filtered, a process which after some averaging analysis results in a few oscillating terms, one of which is of the form $\sin^2(\omega t)$ and proportional to $-\frac{dh}{d\theta}$, the gradient of the unknown output map. Upon integration, or low pass filtering through

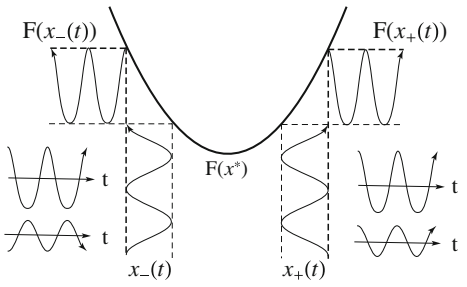

Fig. 1.3 In searching for the minimum of $F(x) = x^2$, depending on whether $x(0)$ is greater than or less than $x^\star = 0$ the value of the perturbed function $F(x(t))$ will be in or out of phase with the perturbing signal, allowing for an estimate of the gradient for minimization

$\frac{k}{s}$ all oscillatory terms average to zero, except for the $-k\frac{dh}{d\theta}\sin^2(\omega t)$ term, resulting in θ following a gradient descent towards the minimizing value $\theta^\star$ of the unknown function $y = h(x) = h(l(\theta))$.

The work of Krstić and Wang sparked renewed interest in the field. Since 2000 the extremum seeking method, as a real-time non-model-based optimization approach, has seen significant theoretical advances [6, 20, 124], with extension to semi-global convergence [147], development of scalar Newton-like algorithms [99, 107], inclusion of measurement noise [144], extremum seeking with partial modeling information [2, 3, 28, 35, 47], and learning in noncooperative games [37, 143].

Extremum seeking has also been used in many diverse applications with unknown/uncertain systems, such as steering vehicles toward a source in GPS-denied environments [22, 23, 157], active flow control [12, 13, 15, 58, 70, 71], aeropropulsion [104, 151], cooling systems [88, 89], wind energy [25], photovoltaics [87], human exercise machines [159], optimizing the control of nonisothermal continuously stirred tank reactors [46], reducing the impact velocity of an electromechanical valve actuator [119], controlling Tokamak plasmas [18, 19], and enhancing mixing in magnetohydrodynamic channel flows [94].

Recent developments include application for control of uncertain nonlinear systems [44], a non-gradient approach to global extremum seeking [109], a multivariable Newton-based ES scheme, for the power optimization of photovoltaic microconverters [42], Newton-based stochastic extremum seeking [93], a proportional integral ES approach [52], time-varying extremum-seeking control approaches for discrete-time systems [48, 50], many approaches to maximum power point tracking [10, 14, 16, 17, 59, 84–86, 90, 91, 123, 155], Newton-like ES for thermoacoustic instability control [101], ES for Weiner-Hammerstein plants [102], semi-global analysis of ES for Hammerstein plants [103], torque maximization of motors [5], optimization of variable CAM timing engine operation [121], global ES in the presence of local extrema [149], various dithering choices [148], multivariable Newton-based ES [41], ES for cascaded Raman optical amplifiers [29], multi unit systems with sampled data [69], ES with parameter uncertainties [108], application to nonlinear systems [57], bioreactor control [45], constrained ES [49], multi-objective ES [51], decentralized ES [80–82], ES for plants of arbitrary degree [61, 118], output-feedback ES with sliding modes [113], and ES with delays [113–116]. A broad review of developments of ES is summarized in [100, 161].

As described, extremum seeking is a control framework that has traditionally been developed as a methodology for optimizing steady states for known stable systems. The ES method has seen many alterations, a major simplification and a first effort towards applying ES to unstable plants was presented by Zhang et al. [158], but only for simple linear examples and only for problems where instability is an obstacle to achieving optimization, rather than stabilization being the goal. The new scheme was for velocity actuation of vehicles for minimization of the unknown output function $f(x, y)$. Because the position of a vehicle is the integral of its velocity, $x(t) = x(0) + \int_0^t v(\tau)d\tau$, the ES scheme was simplified by removal of the filter designated as $\frac{k}{s}$, with this low pass filtering now being performed by the vehicles

themselves. Furthermore, the addition of the ω as a gain of the dithering signal and the use of $\sin(\omega t)$ and $-\cos(\omega t)$ as mixing signals for dithering signals $\omega\cos(\omega t)$ and $\omega\sin(\omega t)$ respectively (which the mixing signals are the integrals of) resulted in the removal of the second high pass filter and an overall simplified averaging analysis.

1.3 Stabilizing by Minimization

Stabilization and control Lyapunov functions (clf) have been seminal accomplishments in the control field since the introduction of Sontag's formula in 1989 [142] and followed by constructive developments of clf's throughout the 1990s for systems with known models [73, 139], unknown parameters [73, 74, 150], uncertain nonlinearities [36], and stochastic and deterministic disturbances [74].

In the clf theory, a central place is occupied by "L_gV controllers" (damping controllers) [74, 139], which are capable of ensuring not only stability but also inverse optimality, and of which a representative example is Sontag's universal controller [142].

In developing stabilizing controllers for uncertain systems, the most challenging class of uncertainties is the unknown control direction, also referred to as the case with an unknown sign of the high frequency gain. This problem has a history that precedes clf's and goes to the early period of development of robust adaptive control. Posed in the early 1980s by Morse and first solved by Nussbaum [111], the problem of stabilization in the presence of unknown control direction has recently received increased attention in adaptive control of nonlinear systems but the classical parameter-adaptive solutions suffer from poor transient performance and fail to achieve exponential stability even in the absence of other uncertainties.

This book builds on the connection between extremum seeking (ES), Lyapunov functions, and averaging, to develop a general framework for stabilization of systems with unknown models using clf's and L_gV-like controllers. Since our approach does not require the knowledge of the control direction (for systems affine in control, the input vector field g is allowed to be unknown), as a byproduct of our effort in designing ES-based L_gV-like controllers we provide a new solution to the problem of stabilization of systems with unknown direction. The new solution guarantees exponential convergence and does not suffer from poor transients that are characteristic of solutions that employ Nussbaum gain techniques.

Consider, for example, the n-dimensional, linear time varying system

$$\dot{x} = A(t)x + B(t)u, \tag{1.19}$$

and the scalar controller

$$u = \sqrt{\alpha\omega}\cos\left(\omega t + kV(x)\right). \tag{1.20}$$

In all of our ES-feedback stabilization designs, the first step is the construction (or a guess) of a clf $V(x)$, the second step is a choice of sufficiently high gains k and α of the ES algorithm, such that the product $k\alpha$ is large enough to stabilize the average system

$$\dot{\bar{x}} = A(t)\bar{x} - \frac{k\alpha}{2} B(t) B^T(t) \frac{dV}{d\bar{x}}, \tag{1.21}$$

and the third step is the choice of a sufficiently high ω to satisfy the requirements of the averaging theorem, Theorem 2.3, an extension of the work of Kurzweil, Jarnik, Sussmann, Liu, Gurvits, and Li [53–55, 79, 145, 146] and of the semiglobal practical stability theorem of Moreau and Aeyels [105]. In the time-varying case, intuitively speaking, relative to the system dynamics, we must choose ω large enough such that the control oscillations are on a separate time-scale from the time-varying dynamics, $\omega \gg |\dot{A}(t)|, |\dot{B}(t)|$. The choice of average gain $k\alpha$ and of the dithering frequency, ω, are related to the region of attraction of our closed loop systems, with larger $k\alpha$ providing stability for larger initial conditions, but requiring larger values of ω to retain the averaging results.

Although the averaging analysis leads to a sufficiently condition for the product $k\alpha$ to be high enough, the individual terms k and α play significantly different roles in the ES algorithm. We think of k as a control gain that increases the convergence rate as well as decreases the size of the residual convergence set. The value of α is related to the size of our dithering term. Choosing a small value of α results in a smaller perturbing term which is, near $V(x) = 0$, after integration, proportional to $\frac{\alpha}{\sqrt{\omega}} \sin(\omega t)$, thereby reaching a steady state closer to the origin while decreasing the rate of convergence. If the value of α is increased, the feedback searches over a larger space, allowing the system to escape local minimums in the case of optimization applications.

Clearly, our approach is of a high-gain type in requiring that both $k\alpha$ and ω be large, furthermore we introduce fast oscillations into the system, which may become impractical, due to actuator capabilities, for very large choices of ω. When considering problems with an unknown control direction, unlike the approach by Nussbaum [111] and Mudgett and Morse [106] (which we refer to as the "MMN approach"), our approach is neither global nor asymptotic—it guarantees semiglobal exponential practical stability. As such, our results are robust to disturbances. One of the major benefits of this approach is that noisy measurement of the cost function, $V(x)$, is not problematic. On average, as long as the noise is truly random and does not happen to perfectly match the frequency of the controller's oscillations, it cannot destroy the overall system's stability. Furthermore, unlike the MMN approach, we can not only handle unknown signs of the high frequency gains, but also signs that change with time. In particular, unlike other unknown control direction approaches [39, 152, 153, 156, 160], we can allow $B(t)$ to go through zero. The price we pay, besides the lack of globality and of perfect regulation to the origin, is that our high-gain choice of $k\alpha$ requires that we know a lower bound on a mean value of $B(t)B^T(t)$ and upper bounds on mean-square values of $A(t)$ and $B(t)$.

The MMN controller is designed for the case of constant plant parameters. When it is applied to a system that is time-varying, and when the control coefficients are quickly varying with time, passing through zero, and alternating signs, such as when $B(t)$ contains sinusoids, then the MMN type controllers simply cannot keep up and repeatedly overshoot with greater and greater error magnitude. The controllers developed in this work do not suffer from any such overshoots because the ES control scheme is by design operating on a faster time scale than the dynamics in the system's coefficients. Recently the ESS method has been studied for use on submanifolds [32], a singular perturbation-based method has been studied [33], as well as new schemes for GPS-denied source localization [40].

Chapter 2
Weak Limit Averaging for Studying the Dynamics of Extremum Seeking-Stabilized Systems

2.1 Mathematical Notation

We start by reviewing a few results from functional analysis which are used throughout the book, especially in the proof of the main result, Theorem 2.3. See, for example, Conway's *A Course in Functional Analysis* [24], for a more thorough review.

Definition 2.1 For a compact set $K \subset \mathbb{R}^n$, the space of continuous functions is denoted as

$$C(K) = \{u : K \to \mathbb{R} \,|u \text{ is continuous}\}.$$

Definition 2.2 For a compact set $K \subset \mathbb{R}^n$, for $1 \leq p < \infty$,

$$L^p(K) = \left\{ u : K \to \mathbb{R} \,\middle|\, \left(\int_\Omega |u(t)|^p dt \right)^{\frac{1}{p}} < \infty \right\},$$
$$L^\infty(K) = \left\{ u : K \to \mathbb{R} \,\middle|\, \sup_{t \in \Omega} |u(t)| < \infty \right\}.$$

Definition 2.3 A sequence of functions $\{u_n\} \subset L^1(K)$ is uniformly equicontinuous if for every $\varepsilon > 0$, there exists a $\delta > 0$, such that:

$$|u_n(x) - u_m(y)| < \varepsilon, \ \forall x, y \in K, \ \text{s.t.} \ \|x - y\| < \delta.$$

Riemann-Lebesgue Lemma: If $f \in L^1(K)$, then

$$\lim_{\omega \to \infty} \int_K f(x) e^{-i\omega x} dx = 0. \tag{2.1}$$

Definition 2.4 A sequence of functions $\{f_k\} \subset L^2[0, 1]$ is said to converge weakly to f in $L^2[0, 1]$, denoted $f_k \rightharpoonup f$, if

A. Scheinker and M. Krstić, *Model-Free Stabilization by Extremum Seeking*,
SpringerBriefs in Control, Automation and Robotics,
DOI 10.1007/978-3-319-50790-3_2

$$\lim_{k\to\infty}\int_0^1 f_k(\tau)g(\tau)d\tau = \int_0^1 f(\tau)g(\tau)d\tau, \quad \forall g \in L^2[0,1].$$

For example, by application of the Riemann-Lebesgue Lemma,

$$\cos(\omega t)\sin(\omega t) \rightharpoonup 0, \tag{2.2}$$

$$\cos^2(\omega t) \rightharpoonup \frac{1}{2}, \quad \sin^2(\omega t) \rightharpoonup \frac{1}{2}, \tag{2.3}$$

$$\cos(\omega_1 t)\cos(\omega_2 t) \rightharpoonup 0, \quad \forall\, \omega_1 \neq \omega_2, \tag{2.4}$$

$$\sin(\omega_1 t)\sin(\omega_2 t) \rightharpoonup 0, \quad \forall\, \omega_1 \neq \omega_2. \tag{2.5}$$

Arzelà-Ascoli Theorem: If a sequence $\{u_n\} \subset C(K)$ is bounded and equicontinuous, then it has a uniformly convergent subsequence $\{u_{n_k}\}$.

2.2 Convergence of Trajectories and Practical Stability

In this section we review some results of Moreau and Aeyels [105], which we later apply in order to relate the stability of our weak-limit averaged systems to the stability of the original ES-controlled systems. In what follows, given a system

$$\dot{x} = f(t,x), \tag{2.6}$$

$\psi(t,t_0,x_0)$ denotes the solution of (2.6) which passes through the point x_0 at time t_0.

Definition 2.5 *Global Uniform Asymptotic Stability* (*GUAS*): An equilibrium point of (2.6) is said to be GUAS if it satisfies the following three conditions:

- *Uniform Stability*: For every $c_2 \in (0,\infty)$ there exists $c_1 \in (0,\infty)$ such that for all $t_0 \in \mathbb{R}$ and for all $x_0 \in \mathbb{R}^n$ with $\|x_0\| < c_1$,

$$\|\psi(t,t_0,x_0)\| < c_2 \ \ \forall t \in [t_0,\infty). \tag{2.7}$$

- *Uniform Boundedness*: For every $c_1 \in (0,\infty)$ there exists $c_2 \in (0,\infty)$ such that for all $t_0 \in \mathbb{R}$ and for all $x_0 \in \mathbb{R}^n$ with $\|x_0\| < c_1$,

$$\|\psi(t,t_0,x_0)\| < c_2 \ \ \forall t \in [t_0,\infty). \tag{2.8}$$

- *Global Uniform Attractivity*: For all $c_1, c_2 \in (0,\infty)$ there exists $\bar{T} \in (0,\infty)$ such that for all $t_0 \in \mathbb{R}$ and for all $x_0 \in \mathbb{R}^n$ with $\|x_0\| < c_1$,

$$\|\psi(t,t_0,x_0)\| < c_2 \ \ \forall t \in [t_0+\bar{T},\infty). \tag{2.9}$$

In conjunction with (2.6), we consider systems of the form

$$\dot{x} = f^{\varepsilon}(t, x) \tag{2.10}$$

whose trajectories are denoted as $\phi^{\varepsilon}(t, t_0, x_0)$.

Definition 2.6 *Converging Trajectories Property*: The systems (2.6) and (2.10) are said to satisfy the converging trajectories property if for every $\hat{T} \in (0, \infty)$ and compact set $K \subset \mathbb{R}^n$ satisfying $\{(t, t_0, x_0) \in \mathbb{R} \times \mathbb{R} \times \mathbb{R}^n : t \in [t_0, t_0 + \hat{T}], x_0 \in K\} \subset \text{Dom}\psi$, for every $d \in (0, \infty)$ there exists $\varepsilon^{\star}$ such that for all $t_0 \in \mathbb{R}$, for all $x_0 \in K$ and for all $\varepsilon \in (0, \varepsilon^{\star})$,

$$\|\phi^{\varepsilon}(t, t_0, x_0) - \psi(t, t_0, x_0)\| < d, \quad \forall t \in [t_0, t_0 + \hat{T}]. \tag{2.11}$$

We then define the following form of stability for system (2.10).

Definition 2.7 *ε-Semiglobal Practical Uniform Asymptotic Stability (ε-SPUAS)*: An equilibrium point of (2.10) is said to be ε-SPUAS if it satisfies the following three conditions:

- *Uniform Stability*: For every $c_2 \in (0, \infty)$ there exists $c_1 \in (0, \infty)$ and $\hat{\varepsilon} \in (0, \infty)$ such that for all $t_0 \in \mathbb{R}$ and for all $x_0 \in \mathbb{R}^n$ with $\|x_0\| < c_1$ and for all $\varepsilon \in (0, \hat{\varepsilon})$,

$$\|\phi^{\varepsilon}(t, t_0, x_0)\| < c_2 \ \ \forall t \in [t_0, \infty). \tag{2.12}$$

- *Uniform Boundedness*: For every $c_1 \in (0, \infty)$ there exists $c_2 \in (0, \infty)$ and $\hat{\varepsilon} \in (0, \infty)$ such that for all $t_0 \in \mathbb{R}$ and for all $x_0 \in \mathbb{R}^n$ with $\|x_0\| < c_1$ and for all $\varepsilon \in (0, \hat{\varepsilon})$,

$$\|\phi^{\varepsilon}(t, t_0, x_0)\| < c_2 \ \ \forall t \in [t_0, \infty). \tag{2.13}$$

- *Global Uniform Attractivity*: For all $c_1, c_2 \in (0, \infty)$ there exists $\bar{T} \in (0, \infty)$ and $\hat{\varepsilon} \in (0, \infty)$ such that for all $t_0 \in \mathbb{R}$ and for all $x_0 \in \mathbb{R}^n$ with $\|x_0\| < c_1$ and for all $\varepsilon \in (0, \hat{\varepsilon})$,

$$\|\phi^{\varepsilon}(t, t_0, x_0)\| < c_2 \ \ \forall t \in [t_0 + \bar{T}, \infty). \tag{2.14}$$

With these definitions the following result of Moreau and Aeyels [105] is used in the analysis that follows.

Theorem 2.1 ([105]) *If systems (2.10) and (2.6) satisfy the converging trajectories property and if the origin is a GUAS equilibrium point of (2.6), then the origin of (2.10) is ε-SPUAS.*

For systems which perform trajectory tracking, it is usually assumed that even the averaged system itself does not exactly reach the target, $r(t)$, thereby driving the error $e(t) = x(t) - r(t)$ to zero, but instead we design the controllers, such that for any chosen $\delta > 0$, we can guarantee bounds of the form $\lim_{t \to \infty} |e(t)| < \delta$. Towards studying such systems in this ES framework, we make the following definitions.

Definition 2.8 *Global Uniform Ultimate Boundedness with ultimate bound δ (δ-GUUB)*: For $\delta \geq 0$ an equilibrium point of (2.6) is said to be δ-GUUB if it satisfies the following three conditions:

- *δ-Uniform Stability*: For every $c_2 \in (\delta, \infty)$ there exists $c_1 \in (0, \infty)$ such that for all $t_0 \in \mathbb{R}$ and for all $x_0 \in \mathbb{R}^n$ with $\|x_0\| < c_1$,

$$\|\psi(t, t_0, x_0)\| < c_2 \ \ \forall t \in [t_0, \infty). \tag{2.15}$$

- *δ-Uniform Ultimate Boundedness*: For every $c_1 \in (0, \infty)$ there exists $c_2 \in (\delta, \infty)$ such that for all $t_0 \in \mathbb{R}$ and for all $x_0 \in \mathbb{R}^n$ with $\|x_0\| < c_1$,

$$\|\psi(t, t_0, x_0)\| < c_2 \ \ \forall t \in [t_0, \infty). \tag{2.16}$$

- *δ-Global Uniform Attractivity*: For all $c_1, c_2 \in (\delta, \infty)$ there exists $T \in (0, \infty)$ such that for all $t_0 \in \mathbb{R}$ and for all $x_0 \in \mathbb{R}^n$ with $\|x_0\| < c_1$,

$$\|\psi(t, t_0, x_0)\| < c_2 \ \ \forall t \in [t_0 + T, \infty). \tag{2.17}$$

Definition 2.9 *ε-Semiglobal Practical Uniform Ultimate Boundedness with Ultimate Bound δ ((ε, δ)-SPUUB)*: The origin of (2.10) is said to be (ε, δ)-SPUUB if it satisfies the following three conditions:

- *(ε, δ)-Uniform Stability*: For every $c_2 \in (\delta, \infty)$ there exists $c_1 \in (0, \infty)$ and $\hat{\varepsilon} \in (0, \infty)$ such that for all $t_0 \in \mathbb{R}$ and for all $x_0 \in \mathbb{R}^n$ with $\|x_0\| < c_1$ and for all $\varepsilon \in (0, \hat{\varepsilon})$,

$$\|\phi^{\varepsilon}(t, t_0, x_0)\| < c_2 \ \ \forall t \in [t_0, \infty). \tag{2.18}$$

- *(ε, δ)-Uniform Ultimate Boundedness*: For every $c_1 \in (0, \infty)$ there exists $c_2 \in (\delta, \infty)$ and $\hat{\varepsilon} \in (0, \infty)$ such that for all $t_0 \in \mathbb{R}$ and for all $x_0 \in \mathbb{R}^n$ with $\|x_0\| < c_1$ and for all $\varepsilon \in (0, \hat{\varepsilon})$,

$$\|\phi^{\varepsilon}(t, t_0, x_0)\| < c_2 \ \ \forall t \in [t_0, \infty). \tag{2.19}$$

- *(ε, δ)-Global Uniform Attractivity*: For all $c_1, c_2 \in (\delta, \infty)$ there exists $T \in (0, \infty)$ and $\hat{\varepsilon} \in (0, \infty)$ such that for all $t_0 \in \mathbb{R}$ and for all $x_0 \in \mathbb{R}^n$ with $\|x_0\| < c_1$ and for all $\varepsilon \in (0, \hat{\varepsilon})$,

$$\|\phi^{\varepsilon}(t, t_0, x_0)\| < c_2 \ \ \forall t \in [t_0 + T, \infty). \tag{2.20}$$

Theorem 2.2 ([105]) *If systems (2.10) and (2.6) satisfy the converging trajectories property and if the origin is a δ-GUUB point of (2.6), then the origin of (2.10) is (ε, δ)-SPUUB.*

Remark 2.1 In all of the analysis that follows, the trajectories of our systems are required to be confined to compact sets. In each case to be considered in this and the following chapters we first choose $R > 0$, $\delta > 0$ and consider the compact set

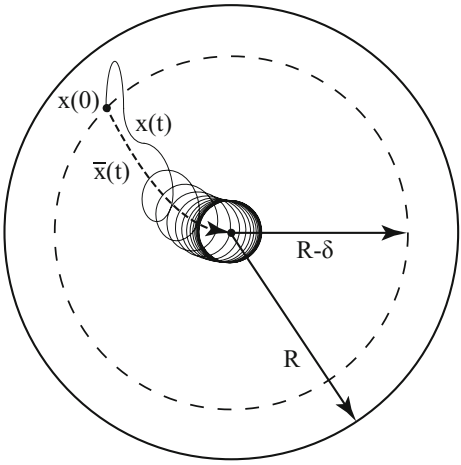

Fig. 2.1 Trajectories with initial conditions $x(0) \in B(0, R-\delta)$ are guaranteed to remain within the compact set $\bar{B}(0, R)$

$\bar{B}(0, R) = \{x \in \mathbb{R}^n : |x| \leq R\}$. Over this compact set we can apply the averaging results and therefore, for any fixed time length $\hat{T} > 0$, there exists $\varepsilon^\star$ such that for all $\varepsilon \in (0, \varepsilon^\star)$, for all $x(t), \bar{x}(t) \in \bar{B}(0, R)$,

$$\max_{t\in[0,\hat{T}]} |x(t) - \bar{x}(t)| < \delta. \tag{2.21}$$

Now we restrict our analysis to the ball of initial conditions $B(0, R-\delta) = \{x \in \mathbb{R}^n : |x| < R-\delta\}$. We also take into account that in what follows, all of the average systems are shown to be exponentially stable, and therefore

$$\max_{t\in[0,\hat{T}]} |\bar{x}(t)| < |\bar{x}(0)| = |x(0)| < R - \delta. \tag{2.22}$$

Combining conditions (2.21) and (2.22), we then have, for all $x(0) \in B(0, R-\delta)$,

$$\begin{aligned}\max_{t\in[0,\hat{T}]} |x(t)| &= \max_{t\in[0,\hat{T}]} |x(t) - \bar{x}(t) + \bar{x}(t)| \\ &\leq \max_{t\in[0,\hat{T}]} |x(t) - \bar{x}(t)| + \max_{t\in[0,\hat{T}]} |\bar{x}(t)| < \delta + R - \delta = R.\end{aligned}$$

Therefore considering $x(0) \in B(0, R-\delta)$ we are guaranteed that all trajectories are confined to the compact set $\bar{B}(0, R)$, where the choices of R and δ can be made arbitrarily large and small respectively. A graphic representation of this simple result of the triangle inequality is shown in Fig. 2.1.

2.3 Weak Limit Averaging

We establish our main results by combining a novel idea for oscillatory control with an extension of functional analytic techniques originally utilized by Kurzweil, Jarnik, Sussmann, and Liu in the late 80s and early 90s.

A proof of Sussmann and Liu's results was given by Sussmann (1992) [146, Sect. 5]. We note that Sussmann and Liu mentioned that their work is an extension of the results of Kurzweil and Jarnik [79]. Such systems were also recently studied, with an ES application in mind, by Durr et al. [31].

Our main result, Theorem 2.3, developed in [134], extends the study of ES from smoothly varying sinusoidal functions, to a much larger useful class of not necessarily continuous functions, e.g., a perturbing signal common in digital systems, a square wave with dead time between pulses. Theorem 2.3 has three useful properties. It establishes feedback control that is, on average, immune to additive, state-independent measurement noise. It establishes the on-average equivalence of variety of control choices that may be used with a range of different types of hardware. The proof is simpler and more general than the related work in [72, 145, 146].

In what follows, we use the notation $u(y,t) = u(\psi(x,t),t)$ to emphasize that the controller u is a function of t and of, a potentially unknown, function $\psi(x,t)$, i.e. that $u(y,t)$ need not have direct access to x.

Theorem 2.3 [134] *Consider the vector-valued system*

$$\dot{x} = f(x,t) + g(x,t)u(y,t), \qquad y = \psi(x,t), \tag{2.23}$$

where $x \in \mathbb{R}^n$, and the functions $f : \mathbb{R}^n \times \mathbb{R} \to \mathbb{R}^n$, $g : \mathbb{R}^n \times \mathbb{R} \to \mathbb{R}^{n\times n}$, $\psi : \mathbb{R}^n \times \mathbb{R} \to \mathbb{R}$ are unknown. Assume that f and g are twice continuously differentiable with respect to x and assume that the value y of $\psi(x,t)$ is available for measurement. Consider a controller u given by

$$u(y,t) = \sum_{i=1}^{m} k_i(y,t)h_{i,\omega}(t), \quad k_i : \mathbb{R}\times\mathbb{R} \to \mathbb{R}^n, \tag{2.24}$$

where the functions $k_i(y,t)$ are continuously differentiable and the functions $h_{i,\omega}(t)$ are piece-wise continuous. System (2.23), (2.24) has the following equivalent closed-loop form

$$\dot{x}(t) = f(x,t) + \sum_{i=1}^{m} b_i(x,t)h_{i,\omega}(t), \tag{2.25}$$

$$b_i(x,t) = g(x,t)k_i\left(\psi(x,t),t\right). \tag{2.26}$$

Suppose that the functions defined as

$$H_{i,\omega}(t) = \int_{t_0}^{t} h_{i,\omega}(\tau)d\tau \tag{2.27}$$

satisfy the uniform limits and weak limits

$$\lim_{\omega\to\infty} H_{i,\omega}(t) = 0, \qquad h_{i,\omega}(t)H_{j,\omega}(t) \rightharpoonup \lambda_{i,j}(t). \tag{2.28}$$

Consider also the average system related to (2.25) as follows

$$\dot{\bar{x}} = f(\bar{x}, t) - \sum_{i\neq j=1}^{m} \lambda_{i,j}(t)\frac{\partial b_i(\bar{x}, t)}{\partial \bar{x}} b_j(\bar{x}, t), \quad \bar{x}(0) = x(0). \tag{2.29}$$

For any compact set $K \subset \mathbb{R}^n$, any t_0, $T \in \mathbb{R}_{\geq 0}$, and any $\delta > 0$, there exists $\omega^\star$ such that for each $\omega > \omega^\star$, the trajectories of (2.25) and (2.29), satisfy $\|x(t) - \bar{x}(t)\| < \delta$ for all $t \in [t_0, t_0 + T]$. Therefore, by [105], uniform asymptotic stability of (2.29) over K implies that (2.25) is $\frac{1}{\omega}$-SPUAS.

Towards a proof of Theorem 2.3 we start with the following lemma.

Lemma 2.1 *As $\omega \to \infty$*

$$\begin{aligned} I_1 &= \int_{t_0}^{t} b_i(x_\omega, \tau)h_{i,\omega}(\tau)d\tau \\ &\to \sum_{j=1}^{m} \int_{t_0}^{t} \frac{\partial b_i(\bar{x}, \tau)}{\partial x} b_j(\bar{x}, \tau)\lambda_{j,i}(t)d\tau. \end{aligned} \tag{2.30}$$

Proof Integrating I_1 by parts gives

$$I_1 = b_i(x(\tau), \tau)H_{i,\omega}(\tau)\Big|_{t_0}^{t} - \int_{t_0}^{t} \frac{db_i(x, \tau)}{d\tau} H_{i,\omega}(\tau)d\tau.$$

As $\omega \to \infty$ the first term of I_1 converges uniformly to zero. The second term can be expanded as

$$\begin{aligned} &\underbrace{\int_{t_0}^{t} \frac{\partial b_i(x, \tau)}{\partial \tau} H_{i,\omega}(\tau)d\tau}_{I_{2,1}} + \underbrace{\int_{t_0}^{t} \frac{\partial b_i(x, \tau)}{\partial x} f(x, \tau)H_{i,\omega}(\tau)d\tau}_{I_{2,2}} \\ &+ \sum_{j=1}^{m} \underbrace{\int_{t_0}^{t} \frac{\partial b_i(x, \tau)}{\partial x} b_j(x, \tau)h_{j,\omega}(\tau)H_{i,\omega}(\tau)d\tau}_{I_{2,3}}. \end{aligned}$$

Since the functions $b_i(x, t)$ are continuously differentiable, and x is in a compact set, the functions $\{H_\omega\}$ converge uniformly to zero, the terms $I_{2,1}$ and $I_{2,2}$ vanish

as $\omega \to \infty$. The weak convergence assumption applied to $I_{2,3}$ give the desired conclusion.

We now establish Theorem 2.3.

Proof Assume the hypothesis of Theorem 2.3, fix a compact set $K \subset \mathbb{R}^n$ and consider the following sequence of differential equations on K

$$\dot{x}_\omega = f(x_\omega, t) + \sum_{i=1}^{m} b_i(x_\omega, t) h_{i,\omega}(t), \quad x_\omega(t_0) = x_0. \tag{2.31}$$

Because the functions f, b are differentiable and $h_{i,\omega}(t)$ are piece-wise continuous, a unique solution of (2.31) exists [68]. For each fixed ω and for any $t \geq t_0$, the solution of (2.31) is

$$x_\omega(t) = x_0 + \int_{t_0}^{t} f(x_\omega, \tau) d\tau + \sum_{i=1}^{m} \underbrace{\int_{t_0}^{t} b_i(x_\omega, \tau) h_{i,\omega}(\tau) d\tau}_{I_1}. \tag{2.32}$$

For any sequence $\{\omega\}$, since we are on a compact set, the functions $\{x_\omega\}$ are equicontinuous and point wise bounded, therefore the Arzelà-Ascoli Theorem implies that there exists a subsequence x_{ω_i} that converges to $\bar{x}$ uniformly. To find $\bar{x}$ we apply Lemma 2.1 to I_1 see that the sequence $\{x_{\omega_i}\}$ converges to

$$x_0 + \int_{t_0}^{t} f(\bar{x}, \tau) d\tau + \sum_{i=1}^{m} \sum_{j=1}^{m} \int_{t_0}^{t} \frac{\partial b_i(\bar{x}, \tau)}{\partial \bar{x}} b_j(\bar{x}, t) \lambda_{j,i}(t). \tag{2.33}$$

This is the solution to

$$\dot{\bar{x}} = f(\bar{x}, t) + \sum_{i,j=1}^{m} \lambda_{i,j}(t) \frac{\partial b_i(\bar{x}, t)}{\partial \bar{x}} b_j(\bar{x}, t), \quad \bar{x}(0) = x_0. \tag{2.34}$$

Because the solution is unique, these results are true for each subsequence $\{\omega_i\}$. Because the convergence guaranteed by Arzela-Ascoli is uniform, and because this is true for any sequence $\{\omega \to \infty\}$, we have shown that for any $t_0 \in \mathbb{R}$, and any $\delta > 0$, there exists $\omega^\star$ such that for all $\omega > \omega^\star$, the trajectories $x_\omega(t)$ and $\bar{x}(t)$ of (2.31) and (2.34), respectively satisfy

$$\max_{t \in [t_0, t_0+T]} \|x(t) - \bar{x}(t)\| < \delta. \tag{2.35}$$

Therefore, the solutions of (2.29) and (2.25) satisfy the converging trajectories property for any $T \in [0, \infty)$. Therefore, if the origin of (2.29) is GUAS, by Theorem 2.1, the origin of (2.25) is $\frac{1}{\omega}$-SPUAS. Thus, standard bootstrapping methods imply that, on K, if $\lim_{t\to\infty} \|\bar{x}(t)\| = 0$, then $\lim_{t\to\infty} \|x_\omega(t)\| < \delta$.

A simple example of a system of form (2.23)–(2.24) will illustrate the consequences of the theorem. The controller presented in this example has some interesting and useful properties, we will be return to it in more detail in the following chapters.

Example 2.1 Consider the system

$$\dot{x} + ax + bu, \quad u = \sqrt{\alpha\omega}\cos\left(\omega t + kx^2\right) \tag{2.36}$$

noting that when the sign of b is unknown, one cannot design a classical PID type stabilizing controller. Theorem 2.3 implies that the closed loop average system related to (2.36) is given by

$$\dot{\bar{x}} = \left(a - k\alpha b^2\right)\bar{x}, \tag{2.37}$$

which is stabilized by a sufficiently large choice of $k\alpha > \frac{a}{b^2}$, regardless of the sign of b. We now provide the details of how Theorem 2.3 is applied, carrying out weak limit calculations which we will routinely omit in the remainder of the book. In the notation used in Theorem 2.3, system (2.36) may be written as

$$\dot{x} = \underbrace{ax}_{f(x)} + \underbrace{b}_{g(x)}u, \quad y = \underbrace{x}_{\psi(x)} \tag{2.38}$$

$$\begin{aligned} u &= \sqrt{\alpha\omega}\cos\left(\omega t + kx^2\right) \\ &= \underbrace{\sqrt{\alpha\omega}\cos(\omega t)}_{h_{1,\omega}(t)}\underbrace{\cos\left(kx^2\right)}_{k_1(x)}\underbrace{-\sqrt{\alpha\omega}\sin(\omega t)}_{h_{2,\omega}(t)}\underbrace{\sin\left(kx^2\right)}_{k_2(x)}, \end{aligned} \tag{2.39}$$

which has closed loop form

$$\dot{x} = ax + \underbrace{\sqrt{\alpha\omega}\cos(\omega t)}_{h_{1,\omega}(t)}\underbrace{b\cos\left(kx^2\right)}_{b_1(x)}\underbrace{-\sqrt{\alpha\omega}\sin(\omega t)}_{h_{2,\omega}(t)}\underbrace{b\sin\left(kx^2\right)}_{b_2(x)}.$$

Consider the sequence of functions $\{h_{1,\omega}(t)\} = \{\sqrt{\alpha\omega}\cos(\omega t)\}$ and $\{h_{2,\omega}(t)\} = \{-\sqrt{\alpha\omega}\sin(\omega t)\}$ where $\omega \to \infty$. Consider corresponding sequences $\{H_{i,\omega}(t) = \int_0^t h_{i,\omega}(\tau)d\tau\}$ where

$$H_{1,\omega}(t) = \sqrt{\frac{\alpha}{\omega}}\sin(\omega(t)), \quad H_{2,\omega}(t) = \sqrt{\frac{\alpha}{\omega}}\cos(\omega(t))$$

and notice that for each i, the functions $H_{i,\omega}(t)$ converge uniformly to 0 as $\omega \to \infty$. In the present example, according the Riemann-Lebesgue Lemma [24],

$$\begin{aligned} h_{1,\omega}(t)H_{1,\omega}(t) &= \alpha\cos(\omega t)\sin(\omega t) \rightharpoonup \lambda_{1,1} = 0 \\ h_{1,\omega}(t)H_{2,\omega}(t) &= \alpha\cos^2(\omega t) \rightharpoonup \lambda_{1,2} = \frac{\alpha}{2} \end{aligned}$$

$$h_{2,\omega}(t)H_{1,\omega}(t) = -\alpha \sin^2(\omega t) \rightharpoonup \lambda_{2,1} = -\frac{\alpha}{2}$$
$$h_{2,\omega}(t)H_{1,\omega}(t) = -\alpha \sin(\omega t)\cos(\omega t) \rightharpoonup \lambda_{2,2} = 0.$$

Therefore, according to Theorem 2.3, the average system is given by

$$\begin{aligned}\dot{\bar{x}} &= a\bar{x} + \frac{1}{2}\left(\frac{\partial b_1}{\partial \bar{x}} b_2 \lambda_{1,2} + \frac{\partial b_2}{\partial \bar{x}} b_1 \lambda_{2,1}\right) \\ &= \left(a - k\alpha b^2\right)\bar{x}. \end{aligned} \tag{2.40}$$

The stability of this system over compact sets implies the $\frac{1}{\omega}$—semiglobal practical uniform asymptotic stability of the original system (2.36).

For illustrative purposes, we partially carry out the weak limit averaging for the simple linear system (2.36). Integrating (2.36) we get

$$x(t) = x(0) + \int_0^t ax(\tau)d\tau + \underbrace{\int_0^t b(\tau)\sqrt{\alpha\omega}\cos(\omega\tau)\cos\left(kx^2\right)d\tau}_{I_1}$$
$$\underbrace{-\int_0^t b(\tau)\sqrt{\alpha\omega}\sin(\omega\tau)\sin\left(kx^2\right)d\tau}_{I_2}.$$

We first integrate the term I_1 by parts, $\int udv = uv - \int vdu$, with

$$u = b(\tau)\cos(kx^2), \quad du = \dot{b}(\tau)\cos(kx^2)d\tau - 2kb(\tau)\dot{x}\sin(kx^2)d\tau,$$
$$dv = \sqrt{\alpha\omega}\cos(\omega t)d\tau, \quad v = \sqrt{\frac{\alpha}{\omega}}\sin(\omega t).$$

The term I_1 becomes

$$\underbrace{\sqrt{\frac{\alpha}{\omega}}\sin(\omega t)b(t)\cos(kx^2)}_{\text{uniformly converges to 0}} - \underbrace{\int_0^t \sqrt{\frac{\alpha}{\omega}}\sin(\omega t)\dot{b}(\tau)\cos(kx^2)d\tau}_{\text{uniformly converges to 0}}$$
$$+\underbrace{\int_0^t \sqrt{\frac{\alpha}{\omega}}\sin(\omega t)2kb(\tau)\sin(kx^2)ax(\tau)d\tau}_{\text{uniformly converges to 0}}$$
$$+\int_0^t \sqrt{\frac{\alpha}{\omega}}\sin(\omega t)2kb(\tau)\sin(kx^2)b(\tau)\sqrt{\alpha\omega}\cos(\omega t)\cos\left(kx^2\right)x(\tau)d\tau$$
$$-\int_0^t \sqrt{\frac{\alpha}{\omega}}\sin(\omega t)2kb(\tau)\sin(kx^2)b(\tau)\sqrt{\alpha\omega}\sin(\omega t)\sin\left(kx^2\right)x(\tau)d\tau$$

From the two surviving terms, the integral

$$2k\alpha \int_0^t b^2(\tau) \sin(kx^2) \cos\left(kx^2\right) x(\tau) \underbrace{\sin(\omega t) \cos(\omega t)}_{\rightharpoonup 0} d\tau \tag{2.41}$$

converges to 0, and the integral

$$-2k\alpha \int_0^t b^2(\tau) \sin^2\left(kx^2\right) x(\tau) \underbrace{\sin^2(\omega t)}_{\rightharpoonup \frac{1}{2}} d\tau$$

converges to

$$-k\alpha \int_0^t b^2(\tau) \sin^2\left(kx^2\right) x(\tau) d\tau.$$

A similar analysis of I_2 leaves us with the dynamics

$$\begin{aligned}\bar{x}(t) = x(0) &+ \int_0^t a\bar{x}(\tau) d\tau - k\alpha \int_0^t b^2(\tau) \sin^2\left(k\bar{x}^2\right) x(\tau) d\tau \\ &-k\alpha \int_0^t b^2(\tau) \cos^2\left(k\bar{x}^2\right) x(\tau) d\tau,\end{aligned}$$

which are the solution of the dynamic system

$$\begin{aligned}\dot{\bar{x}} &= a\bar{x} - k\alpha b^2(t) \left(\sin^2\left(k\bar{x}^2\right) + \cos^2\left(k\bar{x}^2\right)\right) \bar{x} \\ &= \left(a - k\alpha b^2(t)\right) \bar{x}.\end{aligned}$$

Chapter 3
Minimization of Lyapunov Functions

In this chapter, we focus on stabilization of the origin of systems of the form

$$\dot{x} = f(x,t) + g(x,t)u, \tag{3.1}$$

where $x \in \mathbb{R}^n$, $u \in \mathbb{R}$, and the vector fields $f(x,t)$ and $g(x,t)$ are unknown.

Consider a controller in either of the following on-average equivalent forms

$$u = \alpha\sqrt{\omega}\cos(\omega t) - k\sqrt{\omega}\sin(\omega t)V(x,t), \tag{3.2}$$
$$u = \sqrt{\alpha\omega}\cos\left(\omega t + kV(x,t)\right), \tag{3.3}$$

where $\alpha, k > 0$ and the function $V(x,t)$ is soon to be discussed. The average of the system (3.1), (3.2) is given by

$$\dot{\bar{x}} = f(\bar{x},t) - k\alpha g(\bar{x},t)\left(L_g V(\bar{x},t)\right)^T, \tag{3.4}$$

where we use the standard Lie derivative notation $L_g V = \frac{\partial V}{\partial x} g$.

Though our approach permits a time dependence in $f(x,t)$ and $g(x,t)$, to make the notation less burdensome, in this chapter, we sometimes concentrate on time-invariant f and g. The form of the system (3.4) motivates the following assumption.

Assumption 1 (strong $L_g V$*-stabilizability*) There exists a positive definite, radially unbounded, continuously differentiable function $V : \mathbb{R}^n \to \mathbb{R}_+$ and a constant $\beta > 0$ such that

$$L_f V - \beta\left(L_{gV}\right)^2 < 0, \qquad \forall x \neq 0. \tag{3.5}$$

Theorem 3.1 *For given V and β, denote by $\mathscr{S}(V,\beta)$ the class of all systems (3.1) for which Assumption 1 is satisfied. Under the control law (3.2) all the systems in $\mathscr{S}(V,\beta)$ are $\frac{1}{\omega}$-SPUAS for all $k\alpha \geq \beta$.*

A. Scheinker and M. Krstić, *Model-Free Stabilization by Extremum Seeking*,
SpringerBriefs in Control, Automation and Robotics,
DOI 10.1007/978-3-319-50790-3_3

It is relevant to explore the special case of linear systems

$$\dot{x} = Ax + bu \tag{3.6}$$

with control

$$u = \alpha\sqrt{\omega}\cos(\omega t) - k\sqrt{\omega}\sin(\omega t)x^T Px, \tag{3.7}$$

where P is a positive definite and symmetric matrix. The average of the system (3.6), (3.7) is given by

$$\dot{\bar{x}} = \left(A - k\alpha bb^T P\right)\bar{x}\,. \tag{3.8}$$

Hence, the linear analog of Assumption 1 is that there exists a positive definite and symmetric *control Lyapunov matrix* (clm) P and a positive constant β such that

$$PA + A^T P - 2\beta Pbb^T P < 0\,. \tag{3.9}$$

Corollary 3.1 *For given P and β, denote by $\Sigma(P,\beta)$ the class of all pairs (A,b) for which (3.9) is satisfied. Under the control law (3.7) all the systems (3.6) in $\Sigma(P,\beta)$ are $\frac{1}{\omega}$-SPUAS for all $k\alpha \geq \beta$.*

3.1 Is Assumption 1 Equivalent to Stabilizability?

It is well known that a system (3.1) with smooth f and g is stabilizable by feedback continuous at the origin and smooth away from the origin if and only if there exists a control Lyapunov function (clf) with a suitable "small control property" (scp) [142], namely, a positive definite radially unbounded function W with the properties that $L_gW = 0 \Rightarrow L_fW < 0$ and $L_fW + L_gW\alpha_c < 0$ whenever $x \neq 0$, for some continuous function α_c.

Assumption 1 is somewhat stronger than mere stabilizability. For example, for the system

$$\dot{x} = x^3 + x^2 u\,, \tag{3.10}$$

which is stabilizable by simple smooth feedback $u = -2x$, no function V exists that satisfies (3.5) for some $\beta > 0$, and yet $W = x^2/2$ is a clf with an scp.

However, Assumption 1 is satisfied for any stabilizable system whose clf W satisfies not only the clf condition $L_gW = 0 \Rightarrow L_fW < 0$ but also a *strong small control property* (sscp) that for $|x| = \varepsilon$

$$\lim_{\varepsilon\to 0}\ \max_{L_fW(x)>0}\ \frac{L_fW(x)}{(L_gW(x))^2} < \infty\,. \tag{3.11}$$

Under condition (3.11), it can be shown, by slightly modifying the proof in [75–80], that Assumption 1 is satisfied for any $\beta \geq 1$ by a new clf V constructed as

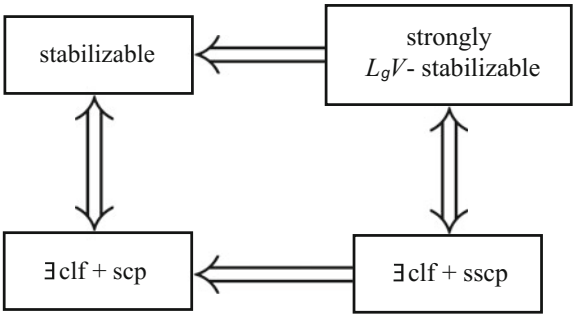

Fig. 3.1 The existence of a clf with sscp is equivalent to the system being strongly L_gV-stabilizable, which implies that the system is stabilizable, which guarantees existence of a clf with scp [142], therefore, existence of a clf with sscp implies existence of a clf with scp

$$V = \int_0^W \rho(r)dr\,, \tag{3.12}$$

where

$$\rho(r) = 1 + 2 \sup_{x:V(x)\leq r} \frac{L_fV + \sqrt{(L_fV)^2 + (L_gV)^4}}{(L_gV)^2}\,. \tag{3.13}$$

In simple terms, a system is strongly L_gV-stabilizable if it has a clf with a sscp. Though violated for the example (3.10), condition (3.11) is satisfied for many systems, including all systems in strict-feedback and strict-feedforward forms. Hence Assumption 1 is far from being overly restrictive, despite not being equivalent to stabilizability by continuous control.

Figure 3.1 shows relations between stabilizability and Assumption 1 by highlighting that both assumptions are equivalent to the existence of a clf, but with different small control properties.

In the linear case, the inequality (3.9) is simply a Riccati inequality and by no means appears to be a restrictive condition. However, when (A, b) are unknown, the designer can only guess a P, rather than solving (3.9) for a given matrix on the right-hand side of the inequality. As we shall see next, simple guesses will often violate (3.9). However, as we demonstrate in the rest of the book, good guesses for a clm are available for some non-trivial classes of systems with unknown model parameters, including unknown control direction.

3.2 Is Assumption 1 Reasonable for Systems with Unknown Models?

Given how hard it is to find a clf when f and g are known, how can the designer have V and β that satisfy (3.5) when f and g are unknown?

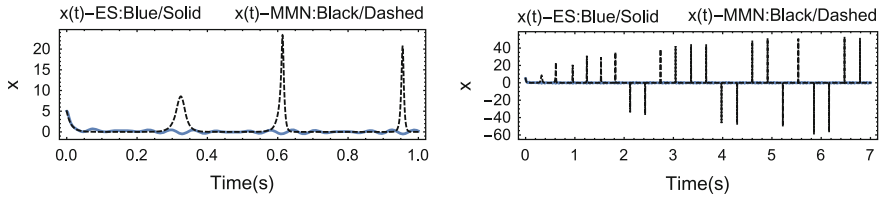

Fig. 3.2 *Left* Overshoot caused by the MMN-controller takes place whenever $\cos(10t)\cos(y(t)) > 0$. *Right* As y is always growing the overshoots grow in severity

For instance, for the scalar example $\dot{x} = f(x) + u$ with $f(x) = x^3$, the clf $V = x^2$ violates Assumption 1, though the clf $V = x^4$ verifies the assumption. In Sect. 6.5 we present an approach that allows the designer to construct a clf that verifies Assumption 1 despite not knowing f.

For the second-order linear example with $A = \begin{bmatrix} 1 & 1 \\ 0 & 0 \end{bmatrix}, b = \begin{bmatrix} 0 \\ 1 \end{bmatrix}$, which is completely controllable, a simple clm $P = I$ violates (3.9) since $PA + A^T P - 2\beta Pbb^T P = \begin{bmatrix} 2 & 1 \\ 1 & -\beta \end{bmatrix}$ cannot be made negative definite for any $\beta > 0$. Yet, as we shall see in later chapters, a more complicated, valid clm P that does not require exact knowledge of A and b can be constructed.

3.3 Comparison with Nussbaum Type Control

A clever way of dealing with control-direction uncertain systems, which is completely different from the Lyapunov approach presented above, is the approach of Mudgett, Morse, and Nussbaum (MMN). Consider the scalar example

$$\dot{x} = x + \cos(10t)u \tag{3.14}$$

and compare our static time-varying feedback

$$u = \alpha\sqrt{\omega}\cos(\omega t) - k\sqrt{\omega}\sin(\omega t)x^2 \tag{3.15}$$

to the dynamic feedback scheme of Mudgett and Morse [106],

$$u = y^2\cos(y)x, \qquad \dot{y} = x^2, \tag{3.16}$$

which admittedly was designed only for constant input coefficients. We simulate the two closed loop systems starting from $x(0) = 5$, with $\omega = 100, k = 5, \alpha = 5$ for our controller and $y(0) = 10$ for the controller of Mudgett and Morse. As shown in Fig. 3.2, the extremum-seeking method's performance is only slightly changed by

the alternating sign of the input coefficient, at most kicking the system $\frac{\alpha}{\sqrt{\omega}}$ (the size of the perturbing signal) in the wrong direction. The MMN method on the other hand suffers from overshoot each time the sign change happens as $y(t)$ cannot change fast enough to maintain $\cos(10t)\cos(y(t)) < 0$. Worse yet, the growing size of $y(t)$ causes growth of the overshoot size as well.

Chapter 4
Control Affine Systems

4.1 Scalar Linear Systems with Unknown Control Directions

Our main result for general n-th order LTV systems is given in Theorem 4.1. However, for clarity, we first present a simpler result for a scalar LTV case in Proposition 4.1, which is not a corollary to Theorem 4.1 but is proved under less restrictive conditions.

Proposition 4.1 *Consider the system*

$$\dot{x} = a(t)x + b(t)u \tag{4.1}$$
$$u = \alpha\sqrt{\omega}\cos(\omega t) - k\sqrt{\omega}\sin(\omega t)x^2, \tag{4.2}$$

and let there exist $\Delta > 0$, $\beta_0 > 0$, $\bar{a} > 0$, *and* $T > 0$ *such that* $a(t)$ *and* $b(t)$ *satisfy*

$$\frac{1}{\Delta}\int_s^{s+\Delta} b^2(\tau)d\tau \geq \beta_0, \ \forall\, s \geq T \tag{4.3}$$
$$\frac{1}{\Delta}\int_s^{s+\Delta} |a(\tau)|d\tau \leq \bar{a}, \ \forall\, s \geq T. \tag{4.4}$$

If

$$k\alpha > \frac{\bar{a}}{\beta_0}, \tag{4.5}$$

then the origin of (4.1), (4.2) is $\frac{1}{\omega}$*-SPUAS with a lower bound on the average decay rate given by*

$$\gamma_r = k\alpha\beta_0 - \bar{a} > 0. \tag{4.6}$$

Proof System (4.1), (4.2) in closed loop form is

$$\dot{x} = a(t)x + b(t)\alpha\sqrt{\omega}\cos\omega t - b(t)k\sqrt{\omega}\sin(\omega t)x^2, \tag{4.7}$$

A. Scheinker and M. Krstić, *Model-Free Stabilization by Extremum Seeking*,
SpringerBriefs in Control, Automation and Robotics,
DOI 10.1007/978-3-319-50790-3_4

which has a average dynamics

$$\dot{\bar{x}} = \left[a(t) - k\alpha b^2(t)\right]\bar{x}. \tag{4.8}$$

If $k\alpha > \frac{\bar{a}}{\beta_0}$ we have from (4.3) that

$$k\alpha \int_s^{s+\Delta} b^2(\tau)d\tau > \Delta\bar{a}. \tag{4.9}$$

Therefore, for any $s \geq T$, $N \in \mathbb{N}$ the integral

$$\begin{aligned}
&\int_s^{s+N\Delta} \left[a(\tau) - k\alpha b^2(\tau)\right] d\tau \\
&= \sum_{j=0}^{N-1} \int_{s+j\Delta}^{s+(j+1)\Delta} \left[a(\tau) - k\alpha b^2(\tau)\right] d\tau \\
&= \sum_{j=0}^{N-1} \left[\int_{s+j\Delta}^{s+(j+1)\Delta} a(\tau)d\tau - \int_{s+j\Delta}^{s+(j+1)\Delta} k\alpha b^2(\tau)d\tau\right]
\end{aligned}$$

is, by application of (4.3), (4.4) and (4.5), bounded by

$$\int_s^{s+N\Delta} \left[a(\tau) - k\alpha b^2(\tau)\right] d\tau \leq \sum_{j=0}^{N-1} [\Delta\bar{a} - \Delta k\alpha\beta_0] = \sum_{j=0}^{N-1} (-\Delta\gamma_r) = -N\Delta\gamma_r < 0, \tag{4.10}$$

where $\gamma_r > 0$ is defined in (4.6). Hence, for any $s \geq T$, $N \in \mathbb{N}$ we have

$$|\bar{x}(s + N\Delta)| = |\bar{x}(s)|e^{\int_s^{s+N\Delta}[a(\tau)-k\alpha b^2(\tau)]d\tau} < |\bar{x}(s)|e^{-N\Delta\gamma_r}. \tag{4.11}$$

Because $\gamma_r > 0$ the state $\bar{x}(t)$ converges to zero. To study the convergence rate, for any $t \geq T$ we denote $N = \left\lfloor \frac{t-T}{\Delta} \right\rfloor$, where $\lfloor\cdot\rfloor$ is the floor function. We then proceed to show that $|\bar{x}(t)| \leq M_0 e^{-\gamma_r t}\,|\bar{x}(0)|$, for all $t \geq 0$, for some $M_0 > 0$.

4.2 Vector Valued Linear Systems with Unknown Control Directions

Before we state our results we introduce the notation

$$\langle Z \rangle_\Delta(s) \triangleq \frac{1}{\Delta} \int_s^{s+\Delta} Z(\tau)d\tau \tag{4.12}$$

for $Z : \mathbb{R} \to \mathbb{R}$, and note that, for any column vector B, $BB^T \leq |B|^2 I$.

In what follows, the general n-dimensional case, is complicated by the possibility of cross talk between different components of vectors, a difficulty only possible in higher dimensions.

Theorem 4.1 *Consider the system*

$$\dot{x} = A(t)x + B(t)u, \tag{4.13}$$
$$u = \alpha\sqrt{\omega}\cos(\omega t) - k\sqrt{\omega}\sin(\omega t)|x|^2, \tag{4.14}$$

where $x \in \mathbb{R}^n$, $A \in \mathbb{R}^{n\times n}$, $B \in \mathbb{R}^n$, $u \in \mathbb{R}$, *and let there exist* $\Delta > 0$, $b_\star \geq \beta_0 > 0$, $a_\star \geq 0$, *and* $T \geq 0$ *such that* $A(t)$ *and* $B(t)$ *satisfy*

$$\frac{1}{\Delta}\int_s^{s+\Delta} B(\tau)B^T(\tau)d\tau \geq \beta_0 I, \ \forall s \geq T \tag{4.15}$$
$$\langle |B|^2\rangle_\Delta(s) \leq b_\star, \ \forall s \geq 0, \tag{4.16}$$
$$\langle < |A|^2\rangle_\Delta(s) \leq a_\star, \ \forall s \geq 0. \tag{4.17}$$

The origin of system (4.13), (4.14) is $\frac{1}{\omega}$*-SPUAS with a lower bound on the average decay rate given by*

$$R = \frac{1}{2\Delta}\left[\ln\left(\frac{1}{\gamma}\right) - \gamma_2\right] - \sqrt{a_\star} > 0, \tag{4.18}$$

where

$$\gamma = 1 - \frac{k\alpha\Delta\beta_0}{1 + 2k^2\alpha^2\Delta^2 b_\star^2} > 0 \tag{4.19}$$
$$\gamma_2 = \frac{4k\alpha\Delta^3 b_\star}{1 + 2k^2\alpha^2\Delta^2 b_\star^2}, \tag{4.20}$$

under either of the two conditions:

(i) Given $k\alpha > 0$ *and* $\Delta > 0$, $a_\star$ *is in the interval* $(0, \bar{a}_\star)$, *where*

$$\bar{a}_\star = \left(\frac{\ln\left(\frac{1}{\gamma}\right)}{\Delta + \sqrt{\Delta^2 + \gamma_2 \ln\left(\frac{1}{\gamma}\right)}}\right)^2. \tag{4.21}$$

(ii) For a given $a_\star$, *the window* Δ *satisfies* $\Delta \in (0, \bar{\Delta})$, *where*

$$\bar{\Delta} = \frac{1}{\sqrt{a_\star}}\min\left\{\bar{\Delta}_1, \ \bar{\Delta}_2\right\}, \tag{4.22}$$

where

$$\bar{\Delta}_1 = \frac{\frac{1}{2}\ln\left(\frac{2\sqrt{2}b_\star}{2\sqrt{2}b_\star - \beta_0}\right)}{1 + \frac{\sqrt{a_\star}}{b_\star}}, \tag{4.23}$$

$$\bar{\Delta}_2 = \frac{-1 + \sqrt{1 + \sqrt{2}\ln\left(\frac{2\sqrt{2}b_\star}{2\sqrt{2}b_\star - \beta_0}\right)}}{\sqrt{2}}, \tag{4.24}$$

and $k\alpha > 1$ *is selected such that*

$$k\alpha \in \left(\frac{1}{2\sqrt{2}\Delta b_\star}, \frac{1}{2\sqrt{2}\Delta b_\star} + M(a_\star, b_\star, \beta_0, \Delta)\right), \tag{4.25}$$

where

$$M = \frac{\sqrt{\beta_0^2 - 8b_\star^2\left[1 - e^{-2\Delta\left(\sqrt{a_\star} + \frac{a_\star}{b_\star}\right)}\right]^2}}{8\Delta b_\star^2\left[1 - e^{-2\Delta\left(\sqrt{a_\star} + \frac{a_\star}{b_\star}\right)}\right]} > 0. \tag{4.26}$$

Remark 4.1 Theorem 4.1(i) is a robustness result. For any $k\alpha > 0$, the controller (4.14) allows some perturbation $A(t)x$ in the system (4.13), as long as the mean of $A(t)$ is sufficiently small, as quantified by (4.21). Theorem 4.1(ii) is a design result. If the window Δ is small enough, as quantified by (4.22) and known (it is reasonable to assume that Δ is known because otherwise the a priori bounds (4.15)–(4.17) would have no meaning for the user), then $k\alpha$ can be chosen in the interval (4.25) to guarantee stability. In summary, the controller (4.14) cannot dominate an arbitrarily large $A(t)$, but if $B(t)$ is persistently exciting (PE) over Δ that is sufficiently small in relation to the size of $A(t)$, then the controller (4.14) can stabilize the system (4.13). Furthermore the allowable $k\alpha$ is not arbitrarily large but is within an interval. Overly large $k\alpha$ results in instability despite $B(t)$ being PE because, for a given Δ, an overly large $k\alpha$ forces $x(t)$ to evolve within the time-varying null space of $B^T(t)$, rather than forcing $x(t)$ to converge to zero. The proof that follows was inspired by the approach in [63].

Proof The closed-loop system (4.13), (4.14) is given by

$$\dot{x} = A(t)x + B(t)\alpha\sqrt{\omega}\cos(\omega t) - B(t)k\sqrt{\omega}\sin(\omega t)|x|^2, \tag{4.27}$$

which we decompose as

$$\dot{x} = \sum_{j=1}^{n}\sum_{i=1}^{n} b_{a,i,j}(x)\bar{u}_{a,i,j}(t) + \sum_{j=1}^{n} b_{c,j}(x)\sqrt{\omega}\hat{u}_{c,j}(t,\theta) + \sum_{j=1}^{n} b_{s,j}(x)\sqrt{\omega}\hat{u}_{s,j}(t,\theta), \tag{4.28}$$

where

$$\begin{aligned} \bar{u}_{a,i,j}(t) &= a_{ji}(t), \quad \hat{u}_{c,j}(t,\theta) = b_j(t)\cos(\omega t) \\ \hat{u}_{s,j}(t,\theta) &= b_j(t)\sin(\omega t) \end{aligned}$$

and

$$b_{a,i,j}(x) = x_i e_j,\ b_{c,j}(x) = \alpha e_j,\ b_{s,j}(x) = -k|x|^2 e_j$$

where e_j is the standard j-th basis vector of $\mathbb{R}^n$. The average dynamics are

$$\dot{\bar{x}} = A(t)\bar{x} - k\alpha B(t)B^T(t)\bar{x}. \tag{4.29}$$

Parts of this proof use steps developed in the proof of Theorem 4.3.2 (iii) in the second half of Sect. 4.8.3 in [63]. With the following Lyapunov function candidate

$$V(\bar{x}) = \frac{|\bar{x}|^2}{2} \tag{4.30}$$

we get

$$\dot{V}(\bar{x}) = \bar{x}^T\dot{\bar{x}} = \bar{x}^T A(t)\bar{x} - k\alpha\bar{x}^T B(t)B^T(t)\bar{x}. \tag{4.31}$$

Therefore, for any $s \geq T$ we have

$$V(s+\Delta) = V(s) - \underbrace{k\alpha\int_s^{s+\Delta}\left|\bar{x}^T(\tau)B(\tau)\right|^2 d\tau}_{I_1} + \underbrace{\int_s^{s+\Delta}\bar{x}^T(\tau)A(\tau)\bar{x}(\tau)d\tau}_{I_2}. \tag{4.32}$$

We first consider the term I_1 and rewrite

$$\bar{x}^T(\tau)B(\tau) = \bar{x}^T(s)B(\tau) + [\bar{x}(\tau) - \bar{x}(s)]^T B(\tau). \tag{4.33}$$

We can apply the inequality $(x+y)^2 \geq \frac{1}{2}x^2 - y^2$, obtaining

$$\left[\bar{x}^T(\tau)B(\tau)\right]^2 \geq \frac{1}{2}\left[\bar{x}^T(s)B(\tau)\right]^2 - \left[[\bar{x}(\tau) - \bar{x}(s)]^T B(\tau)\right]^2. \tag{4.34}$$

Thus, with (4.32) and (4.34) we get

$$I_1 \leq \underbrace{-k\alpha \frac{\bar{x}(s)^T}{2} \int_s^{s+\Delta} B(\tau)B^T(\tau)d\tau \bar{x}(s)}_{I_{11}} + \underbrace{k\alpha \int_s^{s+\Delta} \left[[\bar{x}(\tau) - \bar{x}(s)]^T B(\tau)\right]^2 d\tau}_{I_{12}}. \tag{4.35}$$

With (4.15) and (4.32) it readily follows that

$$I_{11} \leq -\frac{\bar{x}(s)^T}{2} k\alpha \Delta I \beta_0 \bar{x}(s) = -k\alpha\Delta\beta_0 V(\bar{x}). \tag{4.36}$$

Next we address I_{12}. Using (4.27) we get

$$\bar{x}(\tau) - \bar{x}(s) = \int_s^\tau \dot{\bar{x}}(\sigma)d\sigma = \int_s^\tau A(\sigma)\bar{x}(\sigma)d\sigma - k\alpha \int_s^\tau B(\sigma)B^T(\sigma)\bar{x}(\sigma)d\sigma. \tag{4.37}$$

Transposing (4.37) and multiplying by $B(\tau)$ we get

$$[\bar{x}(\tau) - \bar{x}(s)]^T B(\tau) = \int_s^\tau \bar{x}^T(\sigma)A^T(\sigma)d\sigma B(\tau) - k\alpha \int_s^\tau \bar{x}^T(\sigma)B(\sigma)B^T(\sigma)B(\tau)d\sigma. \tag{4.38}$$

By using the representation in (4.38) together with the inequality $(x-y)^2 \leq 2x^2+2y^2$ we get

$$I_{12} \leq \underbrace{2k\alpha \int_s^{s+\Delta} \left[\int_s^\tau \bar{x}^T(\sigma)A^T(\sigma)d\sigma B(\tau)\right]^2 d\tau}_{I_{13}} + \underbrace{2k\alpha \int_s^{s+\Delta} \left[k\alpha \int_s^\tau \bar{x}^T(\sigma)B(\sigma)B^T(\sigma)B(\tau)d\sigma\right]^2 d\tau}_{I_{14}}.$$

Next we consider the term I_{14}, to which we apply the Cauchy-Schwartz inequality followed by a change in the order of integration and obtain

$$I_{14} \leq 2k^3\alpha^3\Delta^2\langle|B|^2\rangle_\Delta^2 \int_s^{s+\Delta} \left(\bar{x}^T(\sigma)B(\sigma)\right)^2 d\sigma. \tag{4.39}$$

Now we consider the term I_{13}, whose bound is given by

$$\begin{aligned} I_{13} &\leq 2k\alpha \int_s^{s+\Delta} |B(\tau)|^2 \left[\int_s^\tau |A(\sigma)|\,|x(\sigma)|\,d\sigma\right]^2 d\tau \\ &\leq 4k\alpha \int_s^{s+\Delta} |B(\tau)|^2 \int_s^\tau |A(\zeta)|^2 d\zeta \int_s^\tau V(\sigma)d\sigma d\tau \end{aligned} \tag{4.40}$$

and, changing the order of integration, we get

$$I_{13} \leq 4k\alpha\Delta^2\langle|B|^2\rangle_\Delta\langle|A|^2\rangle_\Delta\int_s^{s+\Delta} V(\sigma)d\sigma. \tag{4.41}$$

Combining results (4.35), (4.36), and the bounds on I_{13} and I_{14} we arrive at

$$I_1 \leq -k\alpha\Delta\beta_0 V(\bar{x}) + 2k^3\alpha^3\Delta^2 b_\star^2\int_s^{s+\Delta}\left[\bar{x}^T(\sigma)B(\sigma)\right]^2 d\sigma + 4k\alpha\Delta^2 b_\star a_\star\int_s^{s+\Delta} V(\sigma)d\sigma. \tag{4.42}$$

Moving the second term on the right hand side of (4.42) to the left, we obtain

$$I_1 \leq \frac{-k\alpha\Delta\beta_0 V(\bar{x}) + 4k\alpha\Delta^2 b_\star a_\star\int_s^{s+\Delta} V(\sigma)d\sigma}{1+2k^2\alpha^2\Delta^2 b_\star^2}. \tag{4.43}$$

Now we turn our attention to the term I_2 in (4.32). Noting that

$$\bar{x}^T(\tau)A(\tau)\bar{x}(\tau) \leq |A(\tau)|\,\bar{x}^T\bar{x} = 2\,|A(\tau)|\,V(\tau), \tag{4.44}$$

we get

$$I_2 \leq 2\int_s^{s+\Delta}|A(\tau)|\,V(\tau)d\tau. \tag{4.45}$$

Combining (4.32), (4.43) and (4.45) we obtain

$$V(s+\Delta) \leq \gamma V(s) + 2\int_s^{s+\Delta}|A(\tau)|\,V(\tau)d\tau + \frac{4k\alpha\Delta^2 b_\star a_\star\int_s^{s+\Delta} V(\sigma)d\sigma}{1+2k^2\alpha^2\Delta^2 b_\star^2}$$

which can be rewritten as

$$\gamma V(s) + \int_s^{s+\Delta}\left(2\,|A(\tau)| + \frac{4k\alpha\Delta^2 b_\star a_\star}{1+2k^2\alpha^2\Delta^2 b_\star^2}\right)V(\tau)d\tau, \tag{4.46}$$

where γ is defined in (4.19). Noting that

$$\frac{k\alpha\Delta\beta_0}{1+2k^2\alpha^2\Delta^2 b_\star^2} \leq \frac{\beta_0}{2\sqrt{2}b_\star} \tag{4.47}$$

and that $\beta_0 \leq b_\star$, we get that $\gamma \in \left(\frac{2\sqrt{2}-1}{2\sqrt{2}}, 1\right)$, which implies that γ is positive. We now apply the Bellman-Gronwall lemma, and get that for all $s \geq T$,

$$V(s+\Delta) \leq \gamma e^{\left(2\int_s^{s+\Delta}|A(\tau)|d\tau + \frac{4k\alpha\Delta^3 b_\star a_\star}{1+2k^2\alpha^2\Delta^2 b_\star^2}\right)}V(s). \tag{4.48}$$

We note that the Cauchy-Schwartz inequality yields $\int_s^{s+\Delta} |A(\tau)|\, d\tau \leq \Delta\sqrt{a_\star}$, so we get, for all $s \geq T$,

$$V(s+\Delta) \leq \gamma e^{\left(2\Delta\sqrt{a_\star}+\frac{4k\alpha\Delta^3 b_\star a_\star}{1+2k^2\alpha^2\Delta^2 b_\star^2}\right)} V(s). \tag{4.49}$$

Evidently for convergence we require that

$$\gamma e^{\left(2\Delta\sqrt{a_\star}+\frac{4k\alpha\Delta^3 b_\star a_\star}{1+2k^2\alpha^2\Delta^2 b_\star^2}\right)} = \left(1-\frac{k\alpha\Delta\beta_0}{1+2k^2\alpha^2\Delta^2 b_\star^2}\right) e^{\left(2\Delta\sqrt{a_\star}+\frac{4k\alpha\Delta^3 b_\star a_\star}{1+2k^2\alpha^2\Delta^2 b_\star^2}\right)} < 1 \tag{4.50}$$

or equivalently

$$1-\frac{k\alpha\Delta\beta_0}{1+2k^2\alpha^2\Delta^2 b_\star^2} < e^{-\left(2\Delta\sqrt{a_\star}+\frac{4k\alpha\Delta^3 b_\star a_\star}{1+2k^2\alpha^2\Delta^2 b_\star^2}\right)}. \tag{4.51}$$

To prove the theorem under condition (i), we now calculate the requirement on $a_\star$ for (4.51) to hold. We take ln of both sides of (4.51) which gives us

$$a_\star \frac{4k\alpha\Delta^3 b_\star}{1+2k^2\alpha^2\Delta^2 b_\star^2} + 2\Delta\sqrt{a_\star} + \ln\left(1-\frac{k\alpha\Delta\beta_0}{1+2k^2\alpha^2\Delta^2 b_\star^2}\right) < 0. \tag{4.52}$$

We define γ_2 as in (4.20) and set the left side of (4.52) equal to zero, obtaining

$$a_\star\gamma_2 + 2\Delta\sqrt{a_\star} + \ln(\gamma) = 0 \tag{4.53}$$

with roots

$$\sqrt{a_\star} = \frac{-2\Delta \pm \sqrt{4\Delta^2 - 4\gamma_2 \ln(\gamma)}}{2\gamma_2}. \tag{4.54}$$

Since $\sqrt{a_\star}$ must be positive, we only consider the positive root

$$\sqrt{a_\star} = \frac{-\Delta + \sqrt{\Delta^2 + \gamma_2 \ln\left(\frac{1}{\gamma}\right)}}{\gamma_2}, \tag{4.55}$$

which is positive because $\gamma_2 > 0$ and $\gamma \in \left(\frac{2\sqrt{2}-1}{2\sqrt{2}}\right)$ implies that $\gamma_2 \ln\left(\frac{1}{\gamma}\right) > 0$. So we have

$$\bar{a}_\star = \left(\frac{\ln\left(\frac{1}{\gamma}\right)}{\sqrt{\Delta^2 + \gamma_2 \ln\left(\frac{1}{\gamma}\right)} + \Delta}\right)^2. \tag{4.56}$$

Since the left side of (4.52) is increasing as a function of $a_\star > 0$, for all $a_\star \in (0, \bar{a}_\star)$ we satisfy (4.50). To study the convergence rate of our system we denote (4.50) as

$$\gamma_r = \gamma e^{\left(2\Delta\sqrt{a_\star} + \frac{4k\alpha\Delta^3 b_\star a_\star}{1+2k^2\alpha^2\Delta^2 b_\star^2}\right)} < 1. \tag{4.57}$$

For any $t \geq T$ we denote $N = \left\lfloor \frac{t-T}{\Delta} \right\rfloor$, where $\lfloor \cdot \rfloor$ is the floor function. Then for $t \geq T$ we have

$$t = T + \Delta\left(\frac{t-T}{\Delta} - \left\lfloor \frac{t-T}{\Delta} \right\rfloor\right) + N\Delta \tag{4.58}$$

and from (4.49) we have the bound

$$V(t) \leq \gamma_r^N V\left(T + \Delta\left(\frac{t-T}{\Delta} - \left\lfloor \frac{t-T}{\Delta} \right\rfloor\right)\right). \tag{4.59}$$

This bound is obtained by noting from (4.49) and (4.57) that $V(s + N\Delta) \leq \gamma_r^N V(s)$ and by substituting $s = T + \Delta\left(\frac{t-T}{\Delta} - \left\lfloor \frac{t-T}{\Delta} \right\rfloor\right)$. Recalling that

$$\dot{V} = \bar{x}^T\left[A(t) - k\alpha B(t)B^T(t)\right]\bar{x} \leq 2\left|A(t) - k\alpha B(t)B^T(t)\right| V, \tag{4.60}$$

for

$$\Delta\left(\frac{t-T}{\Delta} - \left\lfloor \frac{t-T}{\Delta} \right\rfloor\right) \leq \Delta \tag{4.61}$$

we get the bound

$$V\left(T + \Delta\left(\frac{t-T}{\Delta} - \left\lfloor \frac{t-T}{\Delta} \right\rfloor\right)\right) \leq e^{2\int_0^{T+\Delta}\left|A(\tau) - k\alpha B(\tau)B^T(\tau)\right|d\tau} V(0), \tag{4.62}$$

and therefore

$$V(t) \leq e^{2\int_0^{T+\Delta}\left|A(\tau) - k\alpha B(\tau)B^T(\tau)\right|d\tau} \gamma_r^N V(0). \tag{4.63}$$

We now consider the term γ_r^N. Since $N = \frac{t-T-\Delta\left(\frac{t-T}{\Delta} - \left\lfloor \frac{t-T}{\Delta} \right\rfloor\right)}{\Delta} \geq \frac{t-T-\Delta}{\Delta}$, and $\gamma_r \in (0, 1)$ it follows that

$$\gamma_r^N \leq \gamma_r^{\frac{t-T-\Delta}{\Delta}}. \tag{4.64}$$

With (4.63) and (4.64) we obtain

$$V(t) \leq e^{2\int_0^{T+\Delta}\left|A(\tau) - k\alpha B(\tau)B^T(\tau)\right|d\tau} \gamma_r^{-\frac{T+\Delta}{\Delta}} \gamma_r^{\frac{t}{\Delta}} V(0). \tag{4.65}$$

We now define

$$M_0 = \sqrt{e^{2\int_0^{T+\Delta}\left|A(\tau) - k\alpha B(\tau)B^T(\tau)\right|d\tau} \gamma_r^{-\frac{T+\Delta}{\Delta}}} \tag{4.66}$$

and rewrite

$$\gamma_r^{\frac{t}{\Delta}} = \left(\frac{1}{\gamma_r}\right)^{\frac{-t}{\Delta}} = e^{-\frac{\ln\left(\frac{1}{\gamma_r}\right)}{\Delta}t}. \tag{4.67}$$

Recalling that $\gamma_r \in (0, 1)$ we define

$$R(k\alpha, \Delta, \beta_0, b_\star, a_\star) = \frac{\ln\left(\frac{1}{\gamma_r}\right)}{2\Delta} > 0, \tag{4.68}$$

and write the exponential decay of V as

$$V(t) \leq M_0^2 e^{-2Rt} V(0). \tag{4.69}$$

Substituting (4.57) into (4.68), we obtain (4.18). Finally recalling the definition of $V(t)$ we write the exponential decay of $|\bar{x}(t)|$ as

$$|\bar{x}(t)| \leq M_0 e^{-Rt} |\bar{x}(0)|. \tag{4.70}$$

Therefore, the origin of system (4.13), (4.14) is $\frac{1}{\omega}$-SPUAS, which proves the result under condition (i). Proceeding to the proof of the theorem under condition (ii), for any given $a_\star$ we want to find a range of stabilizing values of $k\alpha$ as a function of Δ. For a given β_0, $b_\star$, $a_\star$ we first consider over what range of $\Delta \in (0, \infty)$ it is possible to satisfy the convergence condition (4.51). We define the function

$$F(k\alpha, \Delta) = \frac{k\alpha\Delta\beta_0}{1 + 2k^2\alpha^2\Delta^2 b_\star^2} + e^{-\left(2\Delta\sqrt{a_\star} + \frac{4k\alpha\Delta^3 b_\star a_\star}{1+2k^2\alpha^2\Delta^2 b_\star^2}\right)} \tag{4.71}$$

which must achieve a value larger than 1 for (4.51) to be satisfied. In order to consider the maximum possible value of (4.71) we first fix Δ and set the derivative, with respect to $k\alpha$, of $F(k\alpha, \Delta)$ equal to zero, to find that $F(k\alpha, \Delta)$ has its maximum value at

$$(k\alpha)_{\mathrm{m}} = \frac{1}{\sqrt{2}\Delta b_\star} \tag{4.72}$$

and the maximum value is

$$F\left((k\alpha)_{\mathrm{m}}, \Delta\right) = \frac{\beta_0}{2\sqrt{2}b_\star} + e^{-\left(2\Delta\sqrt{a_\star} + \sqrt{2}\Delta^2 a_\star\right)}. \tag{4.73}$$

The convergence condition requires this maximum value (4.73) to be greater than 1. We note that $F\left((k\alpha)_{\mathrm{m}}, \Delta\right)$ is strictly decreasing as a function of $\Delta \in (0, \infty)$. Therefore if $F\left((k\alpha)_{\mathrm{m}}, \Delta^\star\right) = 1$, it follows that $F\left((k\alpha)_{\mathrm{m}}, \Delta\right) > 1$ for all $\Delta \in (0, \Delta^\star)$. The condition $F\left((k\alpha)_{\mathrm{m}}, \Delta^\star\right) = 1$ implies that

$$2\Delta\sqrt{a_\star} + \sqrt{2}\Delta^2 a_\star - \ln\left(\frac{2\sqrt{2}b_\star}{2\sqrt{2}b_\star - \beta_0}\right) = 0 \tag{4.74}$$

from which we obtain the positive root

$$\Delta^\star = \frac{-1 + \sqrt{1 + \sqrt{2}\ln\left(\frac{2\sqrt{2}b_\star}{2\sqrt{2}b_\star - \beta_0}\right)}}{\sqrt{2a_\star}}. \tag{4.75}$$

Therefore it is possible to stabilize the system when $0 < \Delta < \Delta^\star$ by choosing $k\alpha = (k\alpha)_{\mathrm{m}}$ as in (4.72). By continuity, for any $0 < \Delta < \Delta^\star$ there must be an interval containing $(k\alpha)_{\mathrm{m}}$ such that all values of $k\alpha$ within that interval satisfy condition (4.51). For $\Delta \in (0, \Delta^\star)$ we consider all values of $k\alpha$ that achieve $F(k\alpha, \Delta) > 1$. Recalling the definition of $F(k\alpha, \Delta)$,

$$F(k\alpha, \Delta) = \frac{k\alpha\Delta\beta_0}{1 + 2k^2\alpha^2\Delta^2 b_\star^2} + e^{-\left(2\Delta\sqrt{a_\star} + \frac{4k\alpha\Delta^3 b_\star a_\star}{1+2k^2\alpha^2\Delta^2 b_\star^2}\right)}, \tag{4.76}$$

to remove the $k\alpha$ dependence from the exponential in (4.76) we restrict our attention to $k\alpha > 1$, in which case

$$e^{-\left(2\Delta\sqrt{a_\star} + \frac{4k\alpha\Delta^3 b_\star a_\star}{1+2k^2\alpha^2\Delta^2 b_\star^2}\right)} > e^{-2\Delta\left(\sqrt{a_\star} + \frac{a_\star}{b_\star}\right)}. \tag{4.77}$$

We satisfy (4.76) by restricting $k\alpha$ to satisfy

$$\frac{k\alpha\Delta\beta_0}{1 + 2k^2\alpha^2\Delta^2 b_\star^2} + e^{-2\Delta\left(\sqrt{a_\star} + \frac{a_\star}{b_\star}\right)} > 1. \tag{4.78}$$

Setting (4.78) equal to 1, we solve for $k\alpha$ as

$$k\alpha = \frac{\beta_0 \pm \sqrt{\beta_0^2 - 8b_\star^2\left[1 - e^{-2\Delta\left(\sqrt{a_\star} + \frac{a_\star}{b_\star}\right)}\right]^2}}{4\Delta b_\star^2\left[1 - e^{-2\Delta\left(\sqrt{a_\star} + \frac{a_\star}{b_\star}\right)}\right]}. \tag{4.79}$$

To ensure $k\alpha$ is real valued we impose the condition

$$\beta_0^2 \geq 8b_\star^2\left[1 - e^{-2\Delta\left(\sqrt{a_\star} + \frac{a_\star}{b_\star}\right)}\right]^2 \tag{4.80}$$

which implies

$$e^{-2\Delta\left(\sqrt{a_\star} + \frac{a_\star}{b_\star}\right)} \geq 1 - \frac{\beta_0}{2\sqrt{2}b_\star}. \tag{4.81}$$

Taking ln of each side of (4.81) we obtain the condition

$$-2\Delta\left(\sqrt{a_\star}+\frac{a_\star}{b_\star}\right) > \ln\left(1-\frac{\beta_0}{2\sqrt{2}b_\star}\right) \tag{4.82}$$

which implies that the new requirement on the possible values of Δ is

$$0 < \Delta < \bar{\Delta} = \min\left\{\frac{\ln\left(\frac{1}{\sqrt{1-\frac{\beta_0}{2\sqrt{2}b_\star}}}\right)}{\left(\sqrt{a_\star}+\frac{a_\star}{b_\star}\right)},\ \Delta^\star\right\}. \tag{4.83}$$

With (4.75) and (4.83) we obtain (4.22). Returning to (4.79) and recalling the value $(k\alpha)_{\mathrm{m}} = \frac{1}{\sqrt{2}\Delta b_\star}$ we have the roots

$$k\alpha = \frac{(k\alpha)_{\mathrm{m}}}{\eta},\ k\alpha = (k\alpha)_{\mathrm{m}}\eta, \tag{4.84}$$

where

$$\eta = \frac{\beta_0 + \sqrt{\beta_0^2 - 8b_\star^2\left[1-e^{-2\Delta\left(\sqrt{a_\star}+\frac{a_\star}{b_\star}\right)}\right]^2}}{2\sqrt{2}b_\star\left[1-e^{-2\Delta\left(\sqrt{a_\star}+\frac{a_\star}{b_\star}\right)}\right]}. \tag{4.85}$$

Therefore the system is stable for

$$k\alpha \in \left(\frac{(k\alpha)_{\mathrm{m}}}{\eta},\ (k\alpha)_{\mathrm{m}}\eta\right). \tag{4.86}$$

We have thus derived sufficient conditions on Δ and $k\alpha$ to guarantee stability of our system. For each window Δ we have given an interval of stabilizing values of $k\alpha$, (4.86). However we now proceed to restrict our conditions on $k\alpha$ in order to give a more intuitive condition (4.25). We show that the interval (4.86) contains $(k\alpha)_{\mathrm{m}}$ by recalling (4.80) and calculating

$$\eta \geq 1 + \frac{\sqrt{\beta_0^2 - 8b_\star^2\left[1-e^{-2\Delta\left(\sqrt{a_\star}+\frac{a_\star}{b_\star}\right)}\right]^2}}{2\sqrt{2}b_\star\left[1-e^{-2\Delta\left(\sqrt{a_\star}+\frac{a_\star}{b_\star}\right)}\right]} \tag{4.87}$$

and

$$\frac{1}{\eta} \leq \frac{2\sqrt{2}b_\star\left[1 - e^{-2\Delta\left(\sqrt{a_\star}+\frac{a_\star}{b_\star}\right)}\right]}{\beta_0} < 1. \tag{4.88}$$

Therefore the interval (4.86) contains the more restrictive, but more illustrative interval (4.25), where we have explicitly written out the value $(k\alpha)_{\mathrm{m}} = \frac{1}{\sqrt{2}\Delta b_\star}$. From the presence of Δ in the denominator we see that this interval of stability grows unbounded in length as the window Δ decreases.

Remark 4.2 We recall from (4.22) that Δ must not exceed $\bar{\Delta}_1$. By recalling that $b_\star \geq \beta_0$, by using the fact that $\ln\left(\frac{2\sqrt{2}}{2\sqrt{2}-1}\right) < \frac{1}{\sqrt{2}}$ and by noting that

$$\frac{\ln\left(\frac{2\sqrt{2}b_\star}{2\sqrt{2}b_\star-\beta_0}\right)}{2\left(\sqrt{a_\star}+\frac{a_\star}{b_\star}\right)} < \frac{\ln\left(\frac{2\sqrt{2}b_\star}{2\sqrt{2}b_\star-b_\star}\right)}{2\sqrt{a_\star}} = \frac{\ln\left(\frac{2\sqrt{2}}{2\sqrt{2}-1}\right)}{2\sqrt{a_\star}} < \frac{1}{2\sqrt{2a_\star}}, \tag{4.89}$$

we get that $\bar{\Delta}_1 < \frac{1}{2\sqrt{2a_\star}}$. Hence, the stabilizing values of $k\alpha$ in the interval (4.25) must satisfy

$$k\alpha > \frac{1}{2\sqrt{2}\Delta b_\star} > \frac{1}{2\sqrt{2}\bar{\Delta}_1 b_\star} > \frac{\sqrt{a_\star}}{b_\star}. \tag{4.90}$$

The condition (4.90) is very similar to the stability requirement that is established in the one-dimensional case, in Proposition 4.1. As $a_\star$ increases, stability is ensured by increasing $k\alpha$.

To demonstrate the extremum seeking controller's ability to handle unknown, quickly time varying control direction we consider the system

$$\begin{bmatrix}\dot{x}_1\\ \dot{x}_2\end{bmatrix} = \begin{bmatrix}2.1 & 4.9\\ -7.5 & 3.6\end{bmatrix}\begin{bmatrix}x_1\\ x_2\end{bmatrix} + \begin{bmatrix}\cos(10t+.3)\\ \sin(10t+.3)\end{bmatrix}u\,. \tag{4.91}$$

A physical motivation for this example can be that $x = (x_1, x_2)$ is the planar coordinate of a mobile robot, with its angular velocity actuator failed and stuck at 10, and which has to be stabilized to the origin using the forward velocity input u only, in the presence of a position-dependent perturbation given by $\begin{bmatrix}2.1 & 4.9\\ -7.5 & 3.6\end{bmatrix}x$. The uncontrolled system is unstable with poles at $2.85 \pm 10.7i$. We apply ES control

$$u = \alpha\sqrt{\omega}\cos(\omega t) - k\sqrt{\omega}\sin(\omega t)\left[x_1^2(t) + x_2^2(t)\right] \tag{4.92}$$

With $\omega = 100, k = 4, \alpha = 2$ and starting from $x_1(0) = 1, x_2(0) = -1$, Fig. 4.1 shows the system's time response.

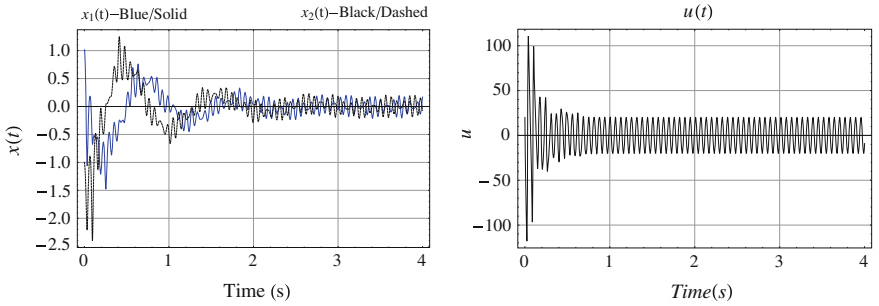

Fig. 4.1 After a transient which, in the average sense, is underdamped, the solution of (4.91)–(4.92) settles to an $O\left(\frac{\alpha}{\sqrt{\omega}}\right)$ neighborhood of the origin

4.3 Linear Systems in Strict-Feedback Form

In this section we consider linear systems in strict-feedback form and design a controller based on the backstepping approach [73, 150].

Theorem 4.2 *Consider the plant*

$$\dot{x}_i = \sum_{j=1}^{i} a_{ij}(t)x_j + x_{i+1}, \ 1 \le i \le n-1 \tag{4.93}$$

$$\dot{x}_n = \sum_{j=1}^{n} a_{nj}(t)x_j + b(t)u, \tag{4.94}$$

with the control law

$$u = \alpha\sqrt{\omega}\cos(\omega t) - k\sqrt{\omega}\sin(\omega t)\left(\sum_{i=1}^{n-1}\left(\prod_{j=i}^{n-1} c_j\right)x_i + x_n\right)^2, \tag{4.95}$$

and let $\beta_0 > 0$ and $a_{\max} > 0$ be known such that for some $T > 0$ and $\Delta > 0$, for all $s \ge T$,

$$\frac{1}{\Delta}\int_s^{s+\Delta} b^2(\tau)d\tau > \beta_0, \quad \frac{1}{\Delta}\int_s^{s+\Delta} |a_{ij}(\tau)|d\tau \le a_{\max}, \quad \forall i, j. \tag{4.96}$$

If $c_1, c_2, \ldots, c_n$ are chosen recursively so that

$$c_i > a_{\max} + \left\{C_{1i}, \max_{2\le j\le i-2} C_{2ij}, c_{i-1}\right\}, 1 \le i \le n-1, \tag{4.97}$$

where $c_0 = 0$ *and*

$$C_{1i} = \frac{(n-1)^2(1+\bar{d}_{i,i-1})^2}{4\bar{d}_{i-1,i-1}}, \quad C_{2ij} = \frac{(n-1)^2\bar{d}_{ij}^2}{4\bar{d}_{jj}}, \tag{4.98}$$

and

$$\bar{d}_{ij} = a_{\max} + a_{\max}c_j + c_{i-1}\bar{d}_{i-1,j}, 1 \le i \le n, 1 \le j \le i-2 \tag{4.99}$$

$$\bar{d}_{ii} = c_i - c_{i-1} + a_{\max}, 1 \le i \le n-1, \bar{d}_{nn} = b^2 k\alpha - c_{n-1} + a_{\max}, \tag{4.100}$$

then if

$$k\alpha > \frac{c_{n-1} + a_{\max}}{\beta_0}, \tag{4.101}$$

the origin of system (4.93)–(4.95) is $\frac{1}{\omega}$*-SPUAS.*

Proof We define

$$z_i = x_i + \sum_{k=1}^{i-1}\left(\prod_{j=k}^{i-1} c_j\right)x_k, 1 \le i \le n \tag{4.102}$$

and rewrite the controller (4.95) as

$$u = \alpha\sqrt{\omega}\cos(\omega t) - k\sqrt{\omega}\sin(\omega t)z_n^2. \tag{4.103}$$

We write the averaged system (4.93)–(4.95) as

$$\dot{\bar{z}} = D\bar{z}, \tag{4.104}$$

where

$$D = \begin{pmatrix} -d_{11} & 1 & 0 & \dots & 0 & 0 \\ d_{21} & -d_{22} & 1 & \dots & 0 & 0 \\ d_{31} & d_{32} & -d_{33} & \dots & 0 & 0 \\ \vdots & \vdots & \vdots & \vdots & \vdots & \vdots \\ d_{n-1,1} & d_{n-1,2} & d_{n-1,3} & \dots & -d_{n-1,n-1} & 1 \\ d_{n1} & d_{n2} & d_{n3} & \dots & d_{n,n-1} & -d_{nn} \end{pmatrix}, \tag{4.105}$$

with the diagonal terms of (4.105) satisfying

$$d_{ii} = c_i - c_{i-1} - a_{ii}, \ 1 \le i \le n-1$$
$$d_{nn} = b^2 k\alpha - c_{n-1} - a_{nn}.$$

The off-diagonal terms are defined as

$$d_{ij} = a_{ij} - a_{i,j+1}c_j + c_{i-1}d_{i-1,j}, \quad 1 \le i \le n, \quad 1 \le j \le i-2.$$

Considering the Lyapunov function

$$V = \frac{1}{2}\sum_{i=1}^{n} \bar{z}_i^2, \tag{4.106}$$

we get

$$\dot{V} = -\sum_{i=1}^{n} d_{ii}\bar{z}_i^2 + \sum_{i=2}^{n}(1 + d_{i,i-1})\bar{z}_i\bar{z}_{i-1} + \sum_{i=3}^{n}\sum_{j=1}^{i-2} d_{ij}\bar{z}_i\bar{z}_j$$

which we rewrite as

$$\dot{V} = \sum_{i=1}^{n-1}\sum_{j=i+1}^{n}\left[-\frac{d_{ii}}{n-1}\bar{z}_i^2 + (1 + d_{ji})\bar{z}_i\bar{z}_j - \frac{d_{jj}}{n-1}\bar{z}_j^2\right] \tag{4.107}$$

Note that $d_{ii} > 0\ \forall i$ for c_i and $k\alpha$ that satisfy

$$c_i > c_{i-1} + a_{\max},\ 1 \le i \le n-1, c_0 = 0. \tag{4.108}$$

We now rewrite (4.107) as

$$\dot{V} = \frac{-2}{n-1}\sum_{i=1}^{n-1} d_{ii}\sum_{j=i+1}^{n}\begin{bmatrix} z_i \\ z_j \end{bmatrix}^T \hat{D}_{ij}\begin{bmatrix} z_i \\ z_j \end{bmatrix}, \tag{4.109}$$

where

$$\hat{D}_{ij} = \frac{1}{2}\begin{bmatrix} 1 & \frac{(n-1)(1+d_{ij})}{d_{ii}} \\ \frac{(n-1)(1+d_{ij})}{d_{ii}} & \frac{d_{jj}}{d_{ii}} \end{bmatrix}. \tag{4.110}$$

To ensure that $\dot{V} < 0$, the matrices $\hat{D}_{ij} \ne D_{nn}$ are made positive definite by choosing

$$\sqrt{\frac{d_{ii}}{d_{i-1,i-1}}} > \frac{(n-1)(1 + d_{i,i-1})}{2d_{i-1,i-1}}, 2 \le i \le n \tag{4.111}$$

and

$$\sqrt{\frac{d_{ii}}{d_{jj}}} > \frac{(n-1)d_{ij}}{2d_{jj}}, 3 \le i \le n, 2 \le j \le i-2, \tag{4.112}$$

which is accomplished by choosing c_i such that

$$c_i = a_{ii} + d_{ii} > a_{ii} + \frac{(n-1)^2(1+d_{i,i-1})^2}{4d_{i-1,i-1}}, \quad 2 \le i \le n$$
$$c_i = a_{ii} + d_{ii} > a_{ii} + \frac{(n-1)^2 d_{ij}^2}{4d_{jj}}, \quad 3 \le i \le n, \quad 2 \le j \le i-2.$$

Finally, by choosing

$$k\alpha > \frac{c_{n-1} + a_{\max}}{\beta_0} \tag{4.113}$$

we ensure that $\int_s^{s+\Delta} D_{nn}(\tau)d\tau < 0$, and proceeding as in the proof of Proposition 4.1, we ensure that $V(s+\Delta) < V(s)$ for all $s \ge T$, and as in Theorem 1 we guarantee that the origin is an exponentially stable equilibrium point of system (4.104). Therefore by Corollary 1, the origin of system (4.93)–(4.95) is $\frac{1}{\omega}$-SPUAS.

A closer examination of the control law (4.95) and the clf (4.106), along with (4.102), shows that the control law is not exactly in the forms (3.2) and (3.7). The terms $z_1^2, \ldots, z_{n-1}^2$ are omitted because $L_g V = L_g \frac{z_n^2}{2} = z_n$.

Unknown Force Direction Simulation Example

Consider controlling the position and velocity of an object experiencing destabilizing forces proportional to its velocity and its distance from the origin, by applying a force u whose direction $b(t)$ is unknown. The dynamics are governed by Newton's law,

$$F_{\text{total}} = ma = m\ddot{x} = k_x x + k_v \dot{x} + b\sin(10t)u,$$

which may be written in strict-feedback form

$$\dot{x}_1 = x_2, \qquad \dot{x}_2 = \frac{k_x}{m}x_1 + \frac{k_v}{m}x_2 + \frac{b}{m}\sin(10t)u. \tag{4.114}$$

We implement the feedback controller

$$u = \alpha\sqrt{\omega}\cos(\omega t) - k\sqrt{\omega}\sin(\omega t)\,(2x_1 + x_2)^2\ . \tag{4.115}$$

For the case $k_x = 1, k_v = 2, m = 1$, and $b = 1$, and with controller parameters $k = 4$, $\alpha = 2$, and $\omega = 100$, the simulation, with initial condition $x_1(0) = 1, x_2(0) = -1$, is shown in Fig. 4.2.

4.4 Nonlinear MIMO Systems with Matched Uncertainties

While we have presented a general approach for nonlinear systems based on an assumed availability of a clf V that satisfies the strong $L_g V$-stabilizability condition,

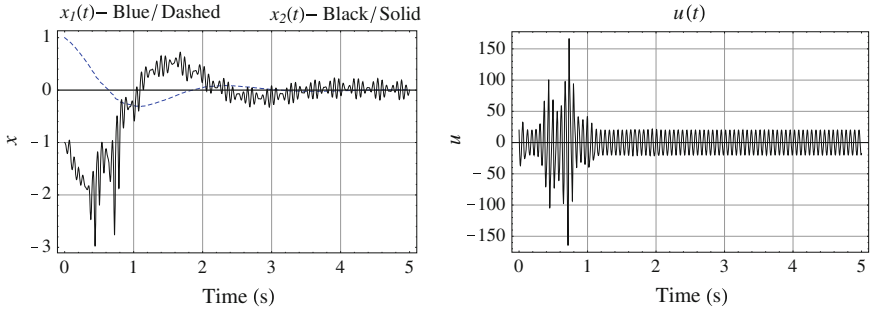

Fig. 4.2 Although the sign of the applied force is unknown to the controller the position x_1 and velocity x_2 of system (4.114)–(4.115) quickly settle to $O\left(\frac{1}{\sqrt{\omega}}\right)$ neighborhoods of the origin

in this section we turn our attention to a specific construction of such a clf for a limited but relevant class of systems that illustrates how to overcome the challenge of dealing with unknown nonlinearities.

In this section we study multi-input systems with the same number of controls and states. Admittedly, this is a class of "glorified first-order systems." However, we use this class to illustrate clearly how to deal with nonlinearities that are not only unknown but also have arbitrary growth (super-linear, exponential, or even faster than exponential). For systems with more states than controls, such as nth order systems in the strict-feedback form with one control and with only bounds on nonlinearities known, clfs satisfying Assumption 1 can be constructed using the approach introduced in [96, see Theorem 3.1, with (26) and (27) being the key steps], which we have actually used for linear strict-feedback systems in Sect. 4.3.

We consider only time-invariant nonlinear systems in this section. Time-varying systems, albeit linear, have already been dealt with in Sect. 4.2. The nonlinear systems studied in this section can be approached similarly but, for the sake of clarity, we choose not to pursue time-varying extensions here. Since the systems we consider here have the same number of controls and states, the input matrix is square. Given that the input matrix is not time-varying and thus persistency of excitation cannot be exploited in stabilization, we make an assumption that the input matrix multiplied by its transpose is positive definite for all x, which means that the system is completely controllable, though its control directions are unknown. Furthermore, the non-zero assumption on the input matrix $G(x)$ is motivated by the possible finite escape time of general nonlinear systems.

Theorem 4.3 *Consider the system*

$$\dot{x} = f(x) + G(x)u, \tag{4.116}$$

where $u,\ x \in \mathbb{R}^n$, *and* $f : \mathbb{R}^n \to \mathbb{R}^n$, $G : \mathbb{R}^n \to \mathbb{R}^{n\times n}$ *and let there exist* $\beta_0 > 0$, *and* $\eta \in \mathcal{K}_\infty$ *such that* $f(x)$ *and* $G(x)$ *satisfy the following bounds for all* $x \in \mathbb{R}^n$*:*

$$G(x)G^T(x) \geq \beta_0 I, \tag{4.117}$$

$$|f(x)| \leq \eta(|x|). \tag{4.118}$$

If k and α are chosen such that

$$k\alpha > \frac{1}{\beta_0} \tag{4.119}$$

then the controller

$$u_i = \alpha\sqrt{\omega\omega_i'}\cos(\omega\omega_i' t) - k\sqrt{\omega\omega_i'}\sin(\omega\omega_i' t)V(x), \tag{4.120}$$

where

$$V(x) = \int_0^{|x|} \eta(r)dr \tag{4.121}$$

and the frequencies ω_i' are distinct, renders the origin of (4.116), (4.120) $\frac{1}{\omega}$-SPUAS.

Proof A common period for all of the controller components is given by $T = 2\pi \text{LCM}\left\{\frac{1}{\omega_i'}\right\}$. Therefore

$$\int_0^T \cos(\omega\omega_i' t)\cos(\omega\omega_j' t)dt = \int_0^T \sin(\omega\omega_i' t)\sin(\omega\omega_j' t)dt$$
$$= \int_0^T \sin(\omega\omega_i' t)\cos(\omega\omega_j' t)dt = 0, \quad \forall\, i \neq j. \tag{4.122}$$

Consider the closed loop system

$$\dot{x} = f(x) + \sqrt{\omega}\sum_{i=1}^{n}\left[\alpha G(x)e_i\sqrt{\omega_i'}\cos(\omega_i'\theta) - kG(x)e_i V(x)\sqrt{\omega_i'}\sin(\omega_i'\theta)\right], \quad \theta = \omega t. \tag{4.123}$$

System (4.123) is in a form which we can average. Considering property (4.122), terms of different frequency combinations integrate to zero. Therefore the terms we are left with are

$$[G(\bar{x})e_i, G(\bar{x})e_i V(\bar{x})] = G(\bar{x})e_i e_i^T G^T(\bar{x})\left(\frac{\partial V(\bar{x})}{\partial \bar{x}}\right)^T. \tag{4.124}$$

Combining all terms of the form (4.124) we get

$$\sum_{i=1}^{n} Ge_i e_i^T G^T\left(\frac{\partial V}{\partial \bar{x}}\right)^T = GG^T\left(\frac{\partial V}{\partial \bar{x}}\right)^T, \tag{4.125}$$

resulting in the averaged system

$$\dot{\bar{x}} = f(\bar{x}) - \frac{k\alpha}{2} G(\bar{x}) G^T(\bar{x}) \eta(|\bar{x}|) \frac{\bar{x}}{|\bar{x}|}, \tag{4.126}$$

where we have used the fact that

$$\frac{\partial V(\bar{x})}{\partial \bar{x}} = \eta(|\bar{x}|) \frac{\bar{x}^T}{|\bar{x}|}. \tag{4.127}$$

With another Lyapunov function candidate

$$W(\bar{x}) = \frac{|\bar{x}|^2}{2}, \tag{4.128}$$

we get

$$\dot{W}(\bar{x}) = \bar{x}^T \dot{\bar{x}} = \bar{x}^T f(\bar{x}) - k\alpha \frac{\eta(|\bar{x}|)}{|\bar{x}|} \bar{x}^T G(\bar{x}) G^T(\bar{x}) \bar{x}. \tag{4.129}$$

From (6.23) we have

$$\left|\bar{x}^T f\right| \leq |\bar{x}|\,|f| \leq |\bar{x}| \eta(|\bar{x}|) \tag{4.130}$$

and from (6.22) we have that

$$k\alpha \frac{\eta(|\bar{x}|)}{|\bar{x}|} \bar{x}^T G(\bar{x}) G^T(\bar{x}) \bar{x} \geq k\alpha \frac{\eta(|\bar{x}|)}{|\bar{x}|} \beta_0 |\bar{x}|^2. \tag{4.131}$$

Plugging (4.130) and (4.131) into the equation for $\dot{W}(\bar{x})$ we get

$$\dot{W}(\bar{x}) \leq |\bar{x}| \eta(|\bar{x}|) - k\alpha\beta_0 |\bar{x}| \eta(|\bar{x}|) = (1 - k\alpha\beta_0) |\bar{x}| \eta(|\bar{x}|), \tag{4.132}$$

therefore by our choice of $k\alpha > \frac{1}{\beta_0}$, we guarantee that (4.132) is negative definite and therefore the averaged system (4.126) is globally uniformly asymptotically stable and therefore system (4.116) is $\frac{1}{\omega}$-SPUAS.

Remark 4.3 Condition (6.22) can be relaxed to a functional lower bound $G(x)G^T(x) \geq \beta(|x|)I$ for some $\beta \in \mathscr{K}$. Then, for the average system, the Lyapunov inequality (4.132) is replaced by $\dot{W}(\bar{x}) \leq (1 - k\alpha\beta(|\bar{x}|))|\bar{x}|\eta(|\bar{x}|)$, which guarantees that, for $k\alpha > 1/\beta(\infty)$, the averaged system is globally ultimately bounded (GUUB) with an ultimate bound $\beta^{-1}\left(\frac{1}{k\alpha}\right)$. Though Theorem 2.2 only allows us to relate global asymptotic stability (GUAS) of the averaged system with $\frac{1}{\omega}$-SPUAS stability of the actual system, a similar relationship can be established between GUUB and what we refer to as $\frac{1}{\omega}$-Semiglobal Practical Uniform Ultimate Boundedness ($\frac{1}{\omega}$-SPUUB) of a system. The $\frac{1}{\omega}$-SPUUB property and its applications in tracking for unknown systems are presented in later chapters.

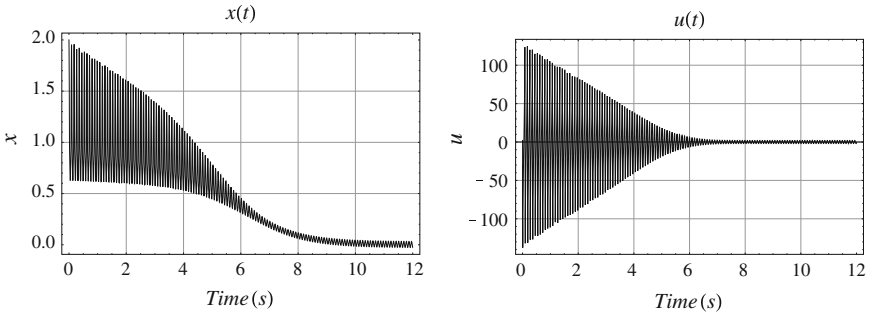

Fig. 4.3 As system (4.133) settles to within a $O\left(\frac{1}{\sqrt{\omega}}\right)$ neighborhood of the origin. The control effort, initially large, settles to a steady state magnitude of $\alpha\sqrt{\omega}$

We demonstrate the controller's ability to stabilize nonlinear systems with the following example:

$$\dot{x} = f(x) + \left(1 - \frac{1}{2}\sin(x)\right)u\,, \qquad f(x) = x^2\,. \tag{4.133}$$

Assuming that we know that the nonlinearity $f(x)$ is polynomial, we know that $f(x)$ satisfies a bound of the form

$$|f(x)| < \gamma|x|e^{|x|}\,. \tag{4.134}$$

For $f(x) = x^2, \gamma = 1$. Assuming γ to be known, and noting that $\int re^r dr = (r-1)e^r$, we choose the controller

$$u = \alpha\sqrt{\omega}\cos(\omega t) - k\sqrt{\omega}\sin(\omega t)\left[1 + (|x| - 1)e^{|x|}\right]\,. \tag{4.135}$$

With $k = 7.5,\ \alpha = 0.25$ and $\omega = 70$, simulation results starting from $x(0) = 2$ are shown in Fig. 4.3.

4.5 Trajectory Tracking

We consider tracking for a trajectory $r(t)$ satisfying the bounds $|r(s)| < r_\star$ and $|\dot{r}(s)| < \rho_\star\ \forall\ s \geq T$, where we define $e(t) = x(t) - r(t)$, choose any $\delta > 0$ and perform our analysis for $|e| \geq \delta$.

Lemma 4.1 *Consider the system*

$$\dot{x} = a(t)x + b(t)u, \tag{4.136}$$

and let there exist $\triangle > 0$, $\beta_0 > 0$, $a_\star > 0$, *and* $T > 0$ *such that* $\forall\, s \geq T$, $a(t)$ *and* $b(t)$ *satisfy*

$$\frac{1}{\triangle}\int_s^{s+\triangle} b^2(\tau)d\tau \geq \beta_0,\ |a(s)| < a_\star. \tag{4.137}$$

Given the error system

$$\dot{e} = a(t)e + b(t)u + a(t)r - \dot{r} \tag{4.138}$$
$$u = \alpha\sqrt{\omega}\cos(\omega t) - k\sqrt{\omega}\sin(\omega t)|e|^2, \tag{4.139}$$

if

$$k\alpha > \frac{a_\star(r_\star + \delta) + \rho_\star}{\delta\beta_0} \tag{4.140}$$

then the origin of system (4.138), (4.139) is $\left(\frac{1}{\omega}, \delta\right)$*-SPUUB, with average convergence rate*

$$\gamma_r = 2\left[k\alpha\beta_0 - a_\star - \frac{a_\star r_\star + \rho_\star}{\delta}\right] > 0. \tag{4.141}$$

To study convergence, we consider the Lyapunov function $V(t) = \bar{e}^2(t)/2$ and proceed in a similar manner to the proof of Theorem 4.1 to get the convergence rate. Therefore the averaged system is exponentially converging to within a δ-ball of the origin. Therefore the origin of system (4.138), (4.139) is $\left(\frac{1}{\omega}, \delta\right)$-SPUUB.

The results also extend to time-varying systems, consider the system

$$\dot{x} = A(t)x + B(t)u, \tag{4.142}$$

where $x \in \mathbb{R}^n$, $A \in \mathbb{R}^{n\times n}$, $B \in \mathbb{R}^n$, $u \in \mathbb{R}$, and let there exist $\Delta > 0$, $b_\star \geq \beta_0 > 0$, $a_\star \geq 0$, and $T \geq 0$ such that $A(t)$ and $B(t)$ satisfy

$$\frac{1}{\Delta}\int_s^{s+\Delta} B(\tau)B^T(\tau)d\tau \geq \beta_0 I,\ \forall s \geq T \tag{4.143}$$
$$\langle |B|^2\rangle_\Delta(s) \leq b_\star,\ \forall s \geq 0, \quad \langle |A|^2\rangle_\Delta(s) \leq a_\star,\ \forall s \geq 0. \tag{4.144}$$

We consider the error system

$$\dot{e} = A(t)e + B(t)u + A(t)r - \dot{r}, \tag{4.145}$$
$$u = \alpha\sqrt{\omega}\cos(\omega t) - k\sqrt{\omega}\sin(\omega t)|e|^2, \tag{4.146}$$

and proceed in a manner analogous to the approach in the proof of Theorem 4.1, see [128] for details. The tracking results are also easily extended to nonlinear systems.

Theorem 4.4 *Consider the nonlinear system*

$$\dot{x} = f(x,t) + G(x,t)u,$$

where $f, u : \mathbb{R}^n \times \mathbb{R} \to \mathbb{R}^n$, $G : \mathbb{R}^{n\times n} \times \mathbb{R} \to \mathbb{R}^{n\times n}$, *with* f *and* G *each having separable dependence on* x *and* t. *Let there exist* $\eta \in \mathscr{K}_\infty$ *and* $\beta_0 > 0$ *such that* f *and* G *satisfy the following bounds for all* $t \in \mathbb{R}^+$, $x \in \mathbb{R}^n$:

$$G(x,\tau)G^T(x,\tau) \geq \beta_0 I, \ |f(x,t)| \leq \eta(|x|). \tag{4.147}$$

Consider the error system

$$\dot{e} = f(e,t) + G(e,t)u - \dot{r}, \tag{4.148}$$

under the influence of the controller

$$u_i = \alpha\sqrt{\omega\omega_i'}\cos(\omega\omega_i' t) - k\sqrt{\omega\omega_i'}\sin(\omega\omega_i' t)\int_0^{|e|}\eta(r)dr, \tag{4.149}$$

where the frequencies ω_i' *are rational and distinct. If* $k\alpha$ *is chosen such that*

$$k\alpha > \frac{1}{\beta_0} + \frac{\rho_\star}{\beta_0\eta(\delta)} \tag{4.150}$$

then origin of (4.148), (4.149) is $\left(\frac{1}{\omega}, \delta\right)$*-SPUUB.*

To demonstrate the extremum seeking controller's ability to handle unknown, quickly time varying control direction we consider the system

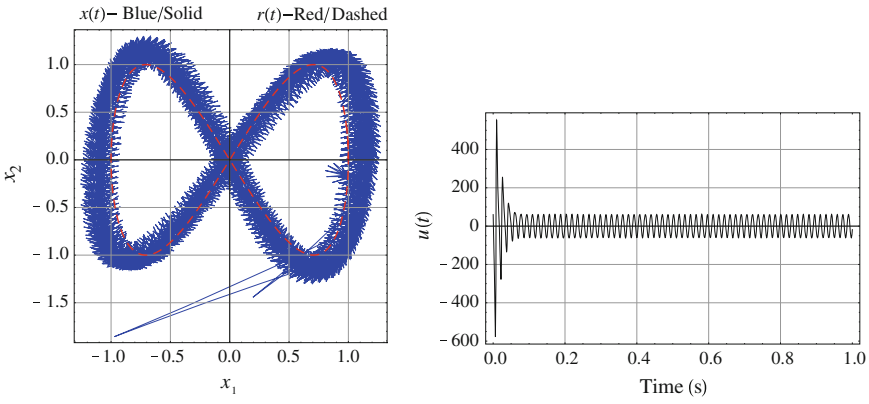

Fig. 4.4 As the system trajectory approaches $r(t)$ the control effort quickly settles to an almost periodic waveform with amplitude modulation which is due to the fact that the disturbing term Ax has magnitude which depends on position

$$\begin{bmatrix} \dot{x}_1 \\ \dot{x}_2 \end{bmatrix} = \begin{bmatrix} 1.1 & 1.2 \\ -1.1 & 1 \end{bmatrix} \begin{bmatrix} x_1 \\ x_2 \end{bmatrix} + \begin{bmatrix} \cos(20t + .3) \\ \sin(20t + .3) \end{bmatrix} u, \tag{4.151}$$

which we want to follow the trajectory

$$r(t) = [\cos(t/4), \sin(t/2)]^T. \tag{4.152}$$

The uncontrolled system is unstable with poles at $1.05 \pm 1.15i$. We apply ES control

$$u = \alpha\sqrt{\omega}\cos(\omega t) - k\sqrt{\omega}\sin(\omega t)|e(t)|^2, \tag{4.153}$$

with parameters $\omega = 400$, $k = 10$, and $\alpha = 3$ and start from $x_1(0) = 1$, $x_2(0) = -1$. Figure 4.4 shows the system's trajectory over 26 seconds. Following an initial transient the control effort settles to a periodic slightly amplitude modulated waveform whose magnitude depends on $|e|$, also shown in Fig. 4.4.

Chapter 5
Non-C^2 ES

5.1 Introduction

One of the main limitations faced by all extremum seeking schemes is the presence of a persistent controller-induced perturbation term which prevents even stable systems from settling at their equilibrium points. In this chapter, by introducing a non-smooth ES scheme we are able to reduce the introduced perturbations as the system settles towards equilibrium.

In extending the results of Moreau and Aeyels [105], in Theorem 5.1 we consider systems of the form:

$$\dot{x} = f(t, x), \tag{5.1}$$
$$\dot{x} = f^{\varepsilon}(t, x), \tag{5.2}$$

where the original system $f^{\varepsilon}(t, x) : \mathbb{R} \times \mathbb{R}^n \to \mathbb{R}$, for a fixed time s is only assumed to satisfy $f^{\varepsilon}(s, x) \in C^2(\mathbb{R}^n \setminus B)$, for some subset $B \subset \mathbb{R}^n$, while the averaged system satisfies $f(s, x) \in C^2(\mathbb{R}^n)$. We first establish a practical stability result relating the stability of the averaged system (5.1) to that of system (5.2). Our stability result is based on the two systems satisfying a closeness of trajectories property, that is if for any given distance Δ and time length T there exists some $\hat{\varepsilon}$ such that for all $\varepsilon \in (0, \hat{\varepsilon})$ whenever the trajectory of system (5.2) is outside of the set B, it is within Δ of the trajectory of its averaged system (5.1). We show that if the two systems (5.1) and (5.2) satisfy such a closeness property then the convergence of (5.1) to the set B implies the practical convergence of (5.2) to the same set.

Having extended practical stability results for non-differentiable systems we consider, for $1 \neq r \in \mathbb{R}$, systems and controllers of the form:

$$\dot{x} = A(t)x + B(t)u, \tag{5.3}$$
$$u = \alpha\sqrt{\omega}\cos(\omega t)|x|^r - \frac{k}{1-r}\sqrt{\omega}\sin(\omega t)|x|^{2-r}, \tag{5.4}$$

A. Scheinker and M. Krstić, *Model-Free Stabilization by Extremum Seeking*,
SpringerBriefs in Control, Automation and Robotics,
DOI 10.1007/978-3-319-50790-3_5

which give us the exact same C^2 averaged systems as already discussed:

$$\dot{\bar{x}} = A(t)\bar{x} - k\alpha B(t)B^T(t)\bar{x}, \qquad \bar{x}(t_0) = x(t_0), \tag{5.5}$$

for which we have proven practical stability results.

Remark 5.1 For any choice of $1 \neq r \in \mathbb{R}$, a controller of the form (5.4) results in the same averaged closed loop system (5.5). This is interesting considering that by choosing different values of r we get vastly different controllers, two of which ($r = 0$ and $r = 2$) are smooth on $\mathbb{R}^n$, with all others non-smooth and even undefined at the origin. In general, we would like to choose $r \in (0, 1)$ so that control effort is zero at the origin. In particular, we choose $r = \frac{1}{2}$ because through simulation it has shown the greatest balance in the magnitude of the perturbing term $\alpha\sqrt{\omega}\cos(\omega t)|x|^{\frac{1}{2}}$, the control gain term $2k\sqrt{\omega}\sin(\omega t)|x|^{\frac{3}{2}}$, and their decay as $|x|$ approaches zero. Therefore throughout the simulations we have chosen $r = \frac{1}{2}$ and used the controller

$$u = \alpha\sqrt{\omega}\cos(\omega t)|x|^{\frac{1}{2}} - 2k\sqrt{\omega}\sin(\omega t)|x|^{\frac{3}{2}}. \tag{5.6}$$

Recognizing that these new controllers, (5.4), for almost always all values of r, are not differentiable at the origin, we are motivated to extend the averaging results to non-C^2 functions in order to prove a closeness of trajectories property, with which we establish the extended practical stability results of Moreau and Aeyels [105].

In what follows we consider systems of the form

$$\dot{x} = \sum_{i=1}^{m_1} b_i(x)\bar{u}_i(t) + \sum_{i=1}^{m_2} \hat{b}_i(x)\frac{1}{\sqrt{\varepsilon}}\hat{u}_i(t,\theta), \tag{5.7}$$

over compact sets $D \subset \mathbb{R}^n$, such that $b_i(x) \in C^2(\mathbb{R}^n)$ for all $i \in \{1, \ldots, m_1\}$ and $\hat{b}_i(x) \in C^2(D)$ for all $i \in \{1, \ldots, m_2\}$. We show that for $x(t), \bar{x}(t) \in D$ we can relate to (5.7) the averaged system

$$\dot{\bar{x}} = \sum_i b_i(\bar{x})\bar{u}_i(t) + \frac{1}{T}\sum_{i<j}\left[\hat{b}_i, \hat{b}_j\right](\bar{x})\nu_{i,j}(t), \quad \bar{x}(t_0) = x(t_0), \tag{5.8}$$

where

$$\nu_{i,j}(t) = \int_0^T \int_0^\theta \hat{u}_i(t,\tau)\hat{u}_j(t,\theta)d\tau d\theta \quad \left[\hat{b}_i, \hat{b}_j\right] = \frac{\partial \hat{b}_j}{\partial \bar{x}}\hat{b}_i - \frac{\partial \hat{b}_i}{\partial \bar{x}}\hat{b}_j,$$

and the function $\left[\hat{b}_i, \hat{b}_j\right]$ are in $C^2(\mathbb{R}^n)$. We show, as above, that the two systems satisfy the property that for any $\hat{T} > 0$ and $\delta > 0$, there exists $\varepsilon^\star$ such that for all $\varepsilon \in (0, \varepsilon^\star)$, $\forall t \in \left[t_0, t_0 + \hat{T}\right]$ for all $x(t) \in D$,

$$|x(t) - \bar{x}(t)| < \delta. \tag{5.9}$$

5.2 Averaging for Systems Not Differentiable at a Point

We start with a definition relating the trajectory of one system with another on a given set. The motivation for this definition is in order to perform analysis on a system which is only well defined on a subset of $\mathbb{R}^n$. We want to prove stability results about the original system by relating it to an averaged system, which is well defined on all of $\mathbb{R}^n$.

Definition 5.1 *Δ-Convergence of Trajectories on a set B (Δ-CT on B):* For any $\Delta > 0$ and any set $B \subset \mathbb{R}^n$, the trajectory $\psi(t, t_0, x_0)$ of systems (2.6) is Δ-CT relative to the trajectory $\psi^\varepsilon(t, t_0, x_0)$ of system (2.10) on B if for any $\hat{T} > 0$ there exists $\varepsilon^\star$ such that for all $\varepsilon \in (0, \varepsilon^\star)$, for all $t \in \left[t_0, t_0 + \hat{T}\right]$ for which $\psi^\varepsilon(t, t_0, x_0) \in B$,

$$|\psi(t, t_0, x_0) - \psi^\varepsilon(t, t_0, x_0)| < \Delta. \tag{5.10}$$

Theorem 5.1 *Consider the systems*

$$\dot{x} = f(t, x), \tag{5.11}$$
$$\dot{x} = f^\varepsilon(t, x), \tag{5.12}$$

whose trajectories, passing through the common point x_0 at time t_0 are denoted respectively as $\psi(t, t_0, x_0)$ and $\psi^\varepsilon(t, t_0, x_0)$. Consider functions f and f^ε such that for every fixed $s \in \mathbb{R}$, $f(s, x) \in C^2(\mathbb{R}^n)$ and $f^\varepsilon(s, x) \in C^2(\mathbb{R}^n \setminus \{0\})$. If for some $\delta > 0$, $\psi(t)$ is Δ-CT relative to $\psi^\varepsilon(t)$ on $D = \mathbb{R}^n \setminus B(0, \delta) = \{x \in \mathbb{R}^n : |x| \geq \delta\}$, then if the origin is a GUAS equilibrium point of system (5.11) it is also a (ε, δ)-SPUUB equilibrium point of system (5.12).

We now introduce a Lemma which we will use in the analysis that follows, which shows that if for a given system a point is (ε, δ)-SPUUB for all $\delta > 0$ then it is in fact ε-SPUAS.

Lemma 5.1 *If the origin of the system*

$$\dot{x} = f^\varepsilon(x, t), \tag{5.13}$$

is (ε, δ)-SPUUB for all $\delta > 0$, then the origin is ε-SPUAS.

Proof If the origin of (5.13) is (ε, δ)-SPUUB for all $\delta > 0$, then for every $c_2 \in (0, \infty)$, for any $\delta \in (0, c_2)$, there exists $\hat{\varepsilon}$ such that the conditions of ε-SPUAS stability hold for all $\varepsilon \in (0, \hat{\varepsilon})$.

Corollary 5.1 *Consider the systems*

$$\dot{x} = f(t, x), \tag{5.14}$$

$$\dot{x} = f^{\varepsilon}(t, x), \tag{5.15}$$

whose trajectories, passing through the common point x_0 at time t_0 are denoted respectively as $\psi(t, t_0, x_0)$ and $\psi^{\varepsilon}(t, t_0, x_0)$. Consider functions f and f^{ε} such that for every fixed $s \in \mathbb{R}$, $f(s, x) \in C^2(\mathbb{R}^n)$ and $f^{\varepsilon}(s, x) \in C^2(\mathbb{R}^n \setminus \{0\})$. If for all $\delta > 0$, $\psi(t)$ is Δ-CT relative to $\psi^{\varepsilon}(t)$ on $D = \mathbb{R}^n \setminus B(0, \delta) = \{x \in \mathbb{R}^n : |x| \geq \delta\}$, then if the origin is a GUAS equilibrium point of system (5.14) it is also a ε-SPUAS equilibrium point of system (5.15).

Proof Because the origin of (5.15) is (ε, δ)-SPUUB for all $\delta > 0$, by Lemma 5.1 the origin of (5.15) is ε-SPUAS.

Remark 5.2 Corollary 5.1 extends to a non-differentiable point the results of Moreau and Aeyels, [105, Theorem 1] which state that if p is a GUAS equilibrium point of (5.15) then p is also an ε-SPUAS equilibrium point of (5.14).

We have established a stability relationship between two general systems (5.11) and (5.12), we now apply these results to a more specific class of systems.

We start by establishing the convergent trajectories property between a possibly not well defined system and its averaged version.

Theorem 5.2 *Given functions $b_i(x) \in C^2(\mathbb{R}^n)$ and $\hat{b}_i(x) \in C^2(\mathbb{R}^n \setminus \{0\})$, consider for $x \neq 0$ the system*

$$\dot{x} = \sum_{i=1}^{m_1} b_i(x)\bar{u}_i(t) + \sum_{i=1}^{m_2} \hat{b}_i(x)\frac{1}{\sqrt{\varepsilon}}\hat{u}_i(t, \theta), \tag{5.16}$$

where each $\hat{u}_i(t, \theta)$ is T-periodic in $\theta = \frac{t}{\varepsilon}$ and has zero average, $\int_{\tau}^{\tau+T} \hat{u}_i(t, \theta)d\theta = 0$. Consider also the averaged system

$$\dot{\bar{x}} = \sum_{i} b_i(\bar{x})\bar{u}_i(t) + \frac{1}{T}\sum_{i<j}\left[\hat{b}_i, \hat{b}_j\right](\bar{x})v_{i,j}(t), \quad \bar{x}(t_0) = x(t_0), \tag{5.17}$$

such that the average system is smooth, satisfying $\left[\hat{b}_i, \hat{b}_j\right](\bar{x}) \in C^2(\mathbb{R}^n)$. For any $R > r > 0$ and $\Delta > 0$, the trajectory of system (5.17) is Δ-CT relative to the trajectory of system (5.16) on the closed annulus ann $(0; r, R) = \{x \in \mathbb{R}^n : r \leq |x| \leq R\}$.

Having established the convergent trajectories property we now present our main result regarding averaged systems.

Theorem 5.3 *Given functions $b_i(x) \in C^2(\mathbb{R}^n)$ and $\hat{b}_i(x) \in C^2(\mathbb{R}^n \setminus \{0\})$, consider for $x \neq 0$ the system*

$$\dot{x} = \sum_{i=1}^{m_1} b_i(x)\bar{u}_i(t) + \frac{1}{\sqrt{\varepsilon}} \sum_{i=1}^{m_2} \hat{b}_i(x)\hat{u}_i(t,\theta), \tag{5.18}$$

where each $\bar{u}_i(t)$ and $\hat{u}_i(t,\theta)$ are bounded as functions of t and $\hat{u}_i(t,\theta)$ is T-periodic in $\theta = \frac{t}{\varepsilon}$ and has zero average, $\int_\tau^{\tau+T} \hat{u}_i(t,\theta)d\theta = 0$. Consider also the averaged system

$$\dot{\bar{x}} = \sum_i b_i(\bar{x})\bar{u}_i(t) + \frac{1}{T} \sum_{i<j} \left[\hat{b}_i, \hat{b}_j\right](\bar{x})v_{i,j}(t), \ \bar{x}(t_0) = x(t_0). \tag{5.19}$$

Assume that $\left[\hat{b}_i, \hat{b}_j\right](\bar{x}) \in C^2(\mathbb{R}^n)$, namely, assume that the average system (5.19) is smooth despite $\hat{b}_i(x)$ being possibly non-differentiable at the origin. If the origin of (5.19) is GUAS then the origin of system (5.18) is ε-SPUAS.

Proof By Theorem 5.2, we have that for any $R, \delta > 0$ the trajectory of system (5.19) is Δ-CT relative to the trajectory of (5.18) on $\bar{B}_{R+\delta}(0) \setminus B_\delta(0) = \{x \in \mathbb{R}^n : \delta \leq |x| \leq R + \delta\}$. Therefore, for the given R and δ, for any $\hat{T} > 0$, there exists $\varepsilon^\star$ such that for all $\varepsilon \in (0, \varepsilon^\star)$ and any $x(0) \in \bar{B}_R(0) \setminus B_\delta(0)$,

$$\max_{t\in\left[0,\hat{T}\right]} |x(t)| = \max_{t\in\left[0,\hat{T}\right]} |x(t) - \bar{x}(t) + \bar{x}(t)| \leq \max_{t\in\left[0,\hat{T}\right]} |x(t) - \bar{x}(t)| + \max_{t\in\left[0,\hat{T}\right]} |\bar{x}(t)| \leq \delta + R,$$

where the last inequality holds due to the origin of (5.19) being GUAS. Therefore trajectories $x(t)$ starting in $\bar{B}_R(0) \setminus B_\delta(0)$ can only leave the set $\bar{B}_{R+\delta}(0) \setminus B_\delta(0)$ through the inner boundary $|x| = \delta$. Because the values R and δ may be chosen arbitrarily large and small respectively, by Theorem 5.1 the origin of system (5.18) is (ε, δ)-SPUUB and by Corollary 5.1 it is in fact ε-SPUAS.

5.3 Non-C^2 Control for Time-Varying Systems

Proposition 5.1 *For $1 \neq r \in \mathbb{R}$, consider the system*

$$\dot{x} = a(t)x + b(t)u \tag{5.20}$$

$$u = \alpha\sqrt{\omega}\cos(\omega t)|x|^r - \frac{k\sqrt{\omega}}{1-r}\sin(\omega t)|x|^{2-r}, \tag{5.21}$$

and let there exist $\Delta > 0$, $\beta_0 > 0$, $a_\star > 0$, *and* $T > 0$ *such that* $a(t)$ *and* $b(t)$ *satisfy*

$$\frac{1}{\Delta}\int_s^{s+\Delta} b^2(\tau)d\tau \geq \beta_0, \forall s \geq T \tag{5.22}$$

$$\langle |a| \rangle_\Delta(s) \leq a_\star, \forall s \geq T. \tag{5.23}$$

If

$$k\alpha > \frac{a_\star}{\beta_0}, \tag{5.24}$$

then the origin of (5.20), (5.21) is $\frac{1}{\omega}$*-SPUAS with a lower bound on the average decay rate given by:*

$$\gamma_r = k\alpha\beta_0 - a_\star > 0. \tag{5.25}$$

Proof System (5.20), (5.21) in closed loop form is

$$\dot{x} = a(t)x + b(t)\alpha\sqrt{\omega}\cos\omega t|x|^r - \frac{b(t)k\sqrt{\omega}}{1-r}\sin(\omega t)|x|^{2-r}, \tag{5.26}$$

which is C^2 on $\mathbb{R}^n \setminus \{0\}$ and has an average

$$\dot{\bar{x}} = \left[a(t) - k\alpha b^2(t)\right]\bar{x}, \tag{5.27}$$

which in Proposition (4.1) was shown to exponentially converge to the origin. Therefore, by Theorem 5.3 we conclude that the origin of (5.20), (5.21) is $\frac{1}{\omega}$-SPUAS. The decay rate is calculated as in [126].

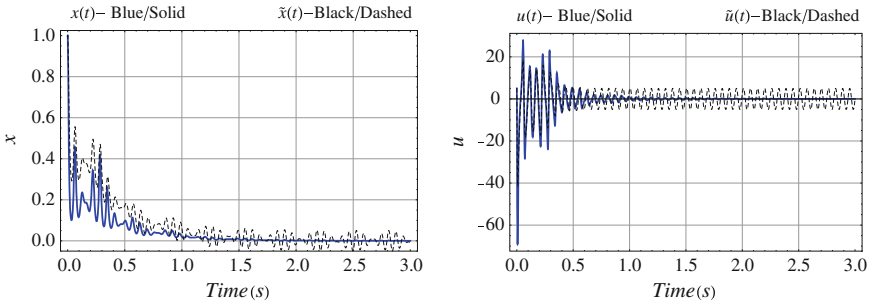

Fig. 5.1 As the trajectories approach the origin the $\alpha\sqrt{\omega}\cos(\omega t)$ term of $\tilde{u}(t)$ persists which shows up in both the persistent control effort and the trajectory $\tilde{x}(t)$, which for $|\tilde{x}(t)| \ll 1$ settles to a steady state of $\tilde{x}(t) \approx \frac{\alpha}{\sqrt{\omega}}\sin(\omega t)$

5.4 Comparison with C^2 Controllers

We simulate and compare the performance of the system

$$\dot{x} = \sin(10t)x + \cos(10t)u,\ x(0) = 1 \tag{5.28}$$

under the influence of the controllers

$$u = \alpha\sqrt{\omega}\cos(\omega t)|x|^{\frac{1}{2}} - 2k\sqrt{\omega}\sin(\omega t)|x|^{\frac{3}{2}},\quad \tilde{u} = \alpha\sqrt{\omega}\cos(\omega t) - k\sqrt{\omega}\sin(\omega t)|x|^2,$$
$$k = 10,\ \alpha = 0.5,\ \omega = 100.$$

We denote the trajectories of (5.28) with controllers $u(t)$ and $\tilde{u}(t)$ as $x(t)$ and $\tilde{x}(t)$ respectively, where we have chosen $r = \frac{1}{2}$ and $r = 0$ respectively. The first 3 s of the simulation results are shown in Fig. 5.1. In Fig. 5.2 the last second of simulation

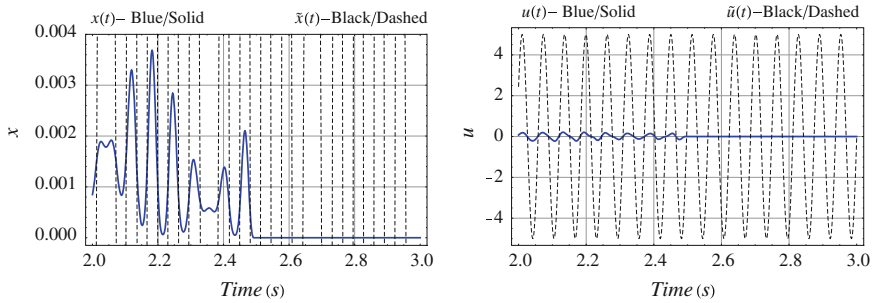

Fig. 5.2 As the trajectory of system (5.28) with controller u approaches the origin the control effort also approaches zero. Once $x(t)$ reaches the origin, the system and control effort remain at that equilibrium point

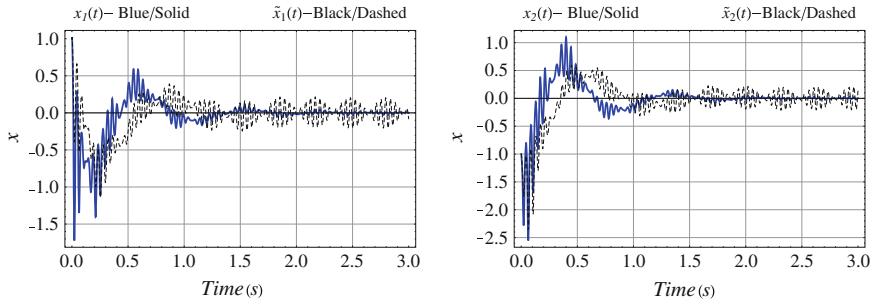

Fig. 5.3 Near the origin the steady state oscillations of $x_i(t)$ due to the controller's input are greatly reduced relative to those of $\tilde{x}_i(t)$ which, for $|\tilde{x}| \ll 1$ reach a steady state proportional to $\frac{\alpha}{\sqrt{\omega}}$

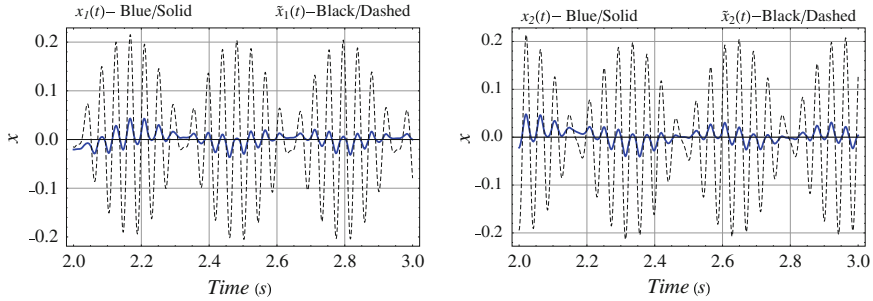

Fig. 5.4 In the 2-dimensional case, even with the non-smooth controllers, the system may never settle to equilibrium at the origin, this would only be achieved if $x_1(t)$ and $x_2(t)$ reached the origin simultaneously

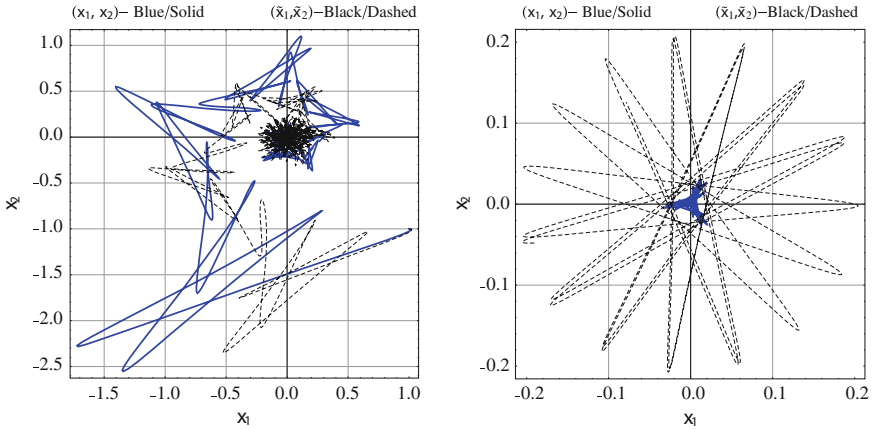

Fig. 5.5 This figure shows the parametric view of the simulation of system (4.91) under both control laws. A zoom in on the last half second of the simulation clearly shows the benefit of the new controller

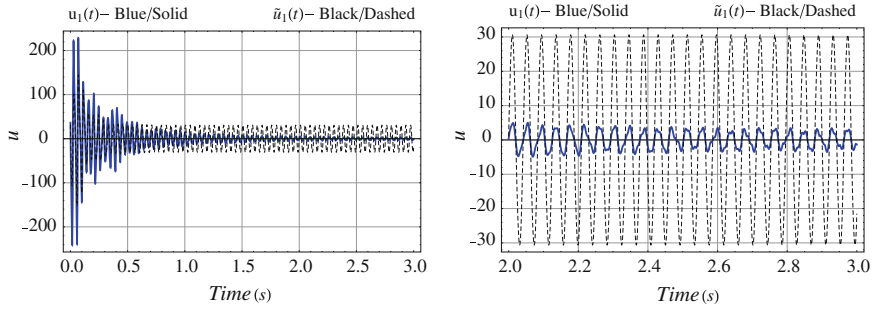

Fig. 5.6 The initial effort of controller u is greater than that of $\tilde{u}$ due to the $2k$ term, which dominates for large values of $|x|$. The advantages of controller u are seen in the great reduction of control effort once the system has reached a neighborhood of the origin

is shown where both the state and control effort for system (5.28) with controller u have converged to zero.

To compare the C^2 and non-C^2 controllers' performances for a 2-dimensional system we recall the system (4.91):

$$\begin{bmatrix} \dot{x}_1 \\ \dot{x}_2 \end{bmatrix} = \begin{bmatrix} 2.1 & 4.9 \\ -7.5 & 3.6 \end{bmatrix} \begin{bmatrix} x_1 \\ x_2 \end{bmatrix} + \begin{bmatrix} \cos(10t + .3) \\ \sin(10t + .3) \end{bmatrix} u.$$

A physical motivation for this example can be that $x = (x_1, x_2)$ is the planar coordinate of a mobile robot, with its angular velocity actuator failed and stuck at 10, and which has to be stabilized to the origin using the forward velocity input u only, in the presence of a position-dependent perturbation given by $\begin{bmatrix} 2.1 & 4.9 \\ -7.5 & 3.6 \end{bmatrix} x$. The uncontrolled system is unstable with poles at $2.85 \pm 10.7i$. Noting that $\beta_0 = 1$ and $a_\star = 8.325$, we apply ES controllers

$$u = \alpha\sqrt{\omega}\cos(\omega t)|x|^{\frac{1}{2}} - 2k\sqrt{\omega}\sin(\omega t)|x|^{\frac{3}{2}}, \quad \tilde{u} = \alpha\sqrt{\omega}\cos(\omega t) - k\sqrt{\omega}\sin(\omega t)|x|^2$$

with $\omega = 150$, $k = 4$, $\alpha = 2.5$, and start from $x_1(0) = 1$, $x_2(0) = -1$. We denote the trajectories of system (4.91) with controllers u and $\tilde{u}$ as $x = (x_1, x_2)^T$ and $\tilde{x} = (\tilde{x}_1, \tilde{x}_2)^T$ respectively, where we have chosen $r = \frac{1}{2}$ and $r = 0$ respectively. Figure 5.3 compares the systems' behavior over 3 s. Figures 5.4 and 5.5 zoom in on the last second of simulation time. Figure 5.6 compares the systems' control efforts.

Chapter 6
Bounded ES

6.1 Introduction

Because ES is designed to perform with unknown systems, one of the most promising applications is for the control of autonomous vehicles, and has been demonstrated as a powerful tool for steering vehicles toward a source in GPS-denied environments [22, 23, 157].

Despite the mentioned theoretical advancements and applications, one limitation which remains in all ES schemes is the uncertainty of convergence rate and control effort. This is due to the fact that an unknown function, whether it is the unknown output of a system which is being minimized, or a Lyapunov candidate for a system which is being stabilized, enters the control scheme in an affine way.

In this chapter we present a new ES scheme, in which the uncertainty is confined to the argument of a sine/cosine function, resulting in guaranteed bounds on update rate in minimum seeking and control effort in stabilization.

The controller that we develop, in the case of minimization of a measurable, but unknown output function $J(\theta)$ of a dynamic system, is given by

$$\dot{\theta}_i = u_i = \sqrt{\alpha_i \omega_i} \cos\left(\omega_i t + k_i J\right). \tag{6.1}$$

In this scheme, a high frequency (ω_i) dither is applied to parameter θ_i, whose magnitude is proportional to (after averaging) α_i, k_i can be thought of as the controller gain. These parameters are discussed in more detail below.

In the case of stabilization of a system of the form

$$\dot{x} = f(x,t) + g(x,t)u, \tag{6.2}$$

the controller's components are chosen as

$$u_i = \sqrt{\alpha_i \omega_i} \cos\left(\omega_i t + k_i V(x)\right), \tag{6.3}$$

A. Scheinker and M. Krstić, *Model-Free Stabilization by Extremum Seeking*,
SpringerBriefs in Control, Automation and Robotics,
DOI 10.1007/978-3-319-50790-3_6

where V is a Lyapunov function candidate. In these two cases, the closed loop systems, on average, satisfy the dynamics:

$$\dot{\bar{\theta}}_i = -\frac{k\alpha}{2}\frac{\partial J}{\partial \bar{\theta}_i}, \tag{6.4}$$

$$\dot{\bar{x}} = f(\bar{x}, t) - \frac{k\alpha}{2} g(\bar{x}, t) g^T(\bar{x}, t) \frac{\partial V(\bar{x})}{\partial \bar{x}}. \tag{6.5}$$

Note that both the update rate (6.1) and control effort (6.3) have bounds of the form $\sqrt{\alpha\omega}$, independent of $J(\theta)$ or $V(x)$.

Next, we consider the particular case of 2D vehicle control, in which an unknown, but measurable function $J(x, y)$, whose value depends on vehicle position (x, y) is to be minimized or maximized, in a GPS denied environment. The controller that we develop towards this goal is given by:

$$\dot{x} = \sqrt{\alpha\omega}\cos\left(\omega t + kJ(x, y) + \theta_0\right) \tag{6.6}$$

$$\dot{y} = \sqrt{\alpha\omega}\sin\left(\omega t + kJ(x, y) + \theta_0\right) \tag{6.7}$$

where θ_0 is an arbitrary initial vehicle orientation. The resulting closed loop system, on average, has dynamics

$$[\dot{x}, \dot{y}]^T = -\frac{k\alpha}{2}\left(\nabla J\right)^T, \tag{6.8}$$

and performs gradient descent towards a local minimum of $J(x, y)$. Note that in this case, the vehicle velocity $v = \sqrt{\dot{x}^2 + \dot{y}^2} = \sqrt{\alpha\omega}$, is constant, and the vehicle performs smooth, unicycle-type motion in circular trajectories.

6.2 Immunity to Measurement Noise

An important noise-rejecting feature of the controllers (6.1) and (6.3) is buried in the partial derivatives $\frac{\partial b_i(\bar{x}, t)}{\partial \bar{x}}$ which take place during the averaging analysis. It turns out that these controllers are inherently robust to measurement noise, a fact which we illustrate below.

Consider the problem of minimizing the unknown function $\psi(x, t)$ based only on a noise corrupted measurement, in a system of the form,

$$\dot{x} = b(t)u(y), \quad y = \hat{\psi}(x, t) = \psi(x, t) + n(t), \tag{6.9}$$

where $b(t)$ is an unknown, time-varying control direction. Consider a controller of the form,

$$u = h_{1,\omega}(t) + h_{2,\omega}(t)\hat{\psi}(x, t), \tag{6.10}$$

such that the functions $h_{i,\omega}(t)$ satisfy the assumptions of Theorem 2.3, with $\lambda_{1,2} = \lambda_{2,1} = 1$. In this case, relative to (2.29), $b_1(y,t) = b(t)$ and $b_2(y,t) = b(t)y$, and the average system dynamics are

$$\begin{aligned}\dot{\bar{x}} &= -b_2 \frac{\partial b_1}{\partial \bar{x}} - b_1 \frac{\partial b_2}{\partial \bar{x}}, \\ &= -b^2(t)\hat{\psi}(\bar{x},t)\frac{\partial}{\partial \bar{x}}(1) - b^2(t)\frac{\partial}{\partial \bar{x}}(\psi(\bar{x},t) + n(t)) = -b^2(t)\frac{\partial \psi(\bar{x},t)}{\partial \bar{x}}. \end{aligned} \tag{6.11}$$

Therefore, when $b(t)$ is not identically zero, the system, on average, converges towards a minimum of the actual function $\psi(x,t)$ despite having access only to its noise-corrupted measurement $\hat{\psi}(x,t)$.

Remark 6.1 In practice, if there is any large noise in the system, $n(t)$, at a given frequency, ω_0, then the dithering frequency, ω, should be chosen such that $\omega \neq \omega_0$, this can always be done by choosing $\omega > \omega_0$.

6.3 Physical Motivation

It is well known that by adding a fast, small oscillation into a system's dynamics, unexpected stability properties may be achieved. The classic example is of the inverted pendulum, whose vertical equilibrium point may be stabilized by rapidly vertically oscillating the pendulum's pivot point. The dynamics of this process were first analytically described in the 1950s by Kapitza [65]. The ES scheme has some similarities to this approach, in that we introduce high frequency oscillations into a system in order to force certain points of the state space to become stable equilibrium points towards which the system's trajectory converges. By abstracting this to a general state space and choosing such a point to be the minimum of a cost function, we are able to tune a wide range of systems towards various performance goals.

We start with a simple example, we do not introduce any destabilizing terms in (6.12), (6.13). To give a simple 2D overview of this method, we consider finding the minimum of a measurable function $C(x,y)$, for which we cannot simply implement a gradient descent for the trajectory of $(x(t), y(t))$ because we are unaware of its analytic form. We propose the following adaptive scheme:

$$\frac{dx}{dt} = \sqrt{\alpha\omega}\cos(\omega t + kC(x,y)) \tag{6.12}$$

$$\frac{dy}{dt} = \sqrt{\alpha\omega}\sin(\omega t + kC(x,y)). \tag{6.13}$$

Note that although $C(x,y)$ enters the argument of the adaptive scheme, we do not rely on any knowledge of the analytic form of $C(x,y)$, we simply assume that it's value is available for measurement at different locations (x,y).

The velocity vector,

$$\mathbf{v} = \left(\frac{dx}{dt}, \frac{dy}{dt}\right) = \sqrt{\alpha\omega}\left[\cos\left(\theta(t)\right), \sin\left(\theta(t)\right)\right], \quad \theta(t) = \omega t + kC(x(t), y(t)), \tag{6.14}$$

has constant magnitude, $\|\mathbf{v}\| = \sqrt{\alpha\omega}$, and therefore the trajectory $(x(t), y(t))$ moves at a constant speed. However, the rate at which the direction of the trajectories' heading changes is a function of ω, k, and $C(x(t), y(t))$ expressed as:

$$\frac{d\theta}{dt} = \omega + k\frac{dC}{dt}. \tag{6.15}$$

Therefore, when the trajectory is heading in the correct direction, towards a decreasing value of $C(x(t), y(t))$, the term $k\frac{\partial C}{\partial t}$ is negative so the overall turning rate $\frac{\partial\theta}{\partial t}$ (6.15), is decreased. On the other hand, when the trajectory is heading in the wrong direction, towards an increasing value of $C(x(t), y(t))$, the term $k\frac{\partial C}{\partial t}$ is positive, and the turning rate is increased. On average, the system ends up approaching the minimizing location of $C(x(t), y(t))$ because it spends more time moving towards it than away.

6.4 Extremum Seeking for Unknown Map

Consider the problem of locating an extremum point of the function $J(\theta) : \mathbb{R}^n \to \mathbb{R}$, for $\theta = (\theta_1, \ldots, \theta_n) \in \mathbb{R}^n$. We assume that $J(\theta)$ has a global extremum such that there exists a unique $\theta^\star$ for which:

$$\nabla J|_{\theta^\star} = 0 \quad \text{and} \quad \nabla J \neq 0, \quad \forall\theta \neq \theta^\star. \tag{6.16}$$

Theorem 6.1 *Consider the ES scheme shown in Fig. 6.1 (for maximum seeking we replace k_i with $-k_i$):*

$$\dot{\theta}_i = \sqrt{\alpha_i\omega_i}\cos\left(\omega_i t + k_i J(\theta)\right), \tag{6.17}$$

where $\omega_i = \omega\hat{\omega}_i$ such that $\hat{\omega}_i \neq \hat{\omega}_j$ $\forall i \neq j$ and J satisfies (6.16). The point $\theta^\star$ is $\frac{1}{\omega}$-SPUAS.

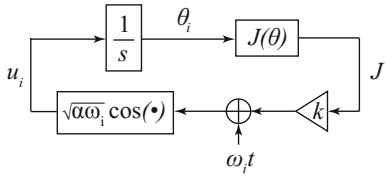

Fig. 6.1 ES scheme for the ith component θ_i of θ

The proof is carried out by expanding $\cos(\cdot)$, rewriting the θ_i dynamics as

$$\dot{\theta}_i = \sqrt{\omega_i}\cos(\omega_i t)\sqrt{\alpha_i}\cos\left(k_i J\right) - \sqrt{\omega_i}\sin(\omega_i t)\sqrt{\alpha_i}\sin\left(k_i J\right), \tag{6.18}$$

and applying Theorem 2.3. The trajectory of system (6.17) then uniformly converges to the trajectory of

$$\dot{\bar{\theta}}_i = -\frac{k_i\alpha_i}{2}\frac{\partial J\left(\bar{\theta}\right)}{\partial\bar{\theta}_i}, \tag{6.19}$$

where we have used the fact that mismatched terms of the form $\cos(\omega_i t)\sin(\omega_j t)$, $\forall i \neq j$, and terms of the form $\cos(\omega_i t)\cos(\omega_j t)$, and $\sin(\omega_i t)\sin(\omega_j t)$, $\forall i, j$ have averaged to zero. Combining all the θ_i components we then get:

$$\dot{\bar{\theta}} = -\frac{k\alpha}{2}\left(\nabla J\right)^T, \tag{6.20}$$

where $k\alpha$ is the diagonal matrix with entries $k_i\alpha_i$.

6.5 Nonlinear MIMO Systems with Matched Uncertainties

We study multi-input systems with the same number of controls and states. We use this class to illustrate clearly how to deal with nonlinearities that are not only unknown but also have arbitrary growth (super-linear, exponential, or even faster than exponential).

Theorem 6.2 *Consider the following system over a compact set $K \subset \mathbb{R}^n$:*

$$\dot{x} = f(x,t) + G(x,t)u(x,t), \tag{6.21}$$

where $x(t) : \mathbb{R}^+ \to \mathbb{R}^n$, and $u(x,t), f(x,t) : \mathbb{R}^n \times \mathbb{R}^+ \to \mathbb{R}^n$, $G(x,t) : \mathbb{R}^n \times \mathbb{R}^+ \to \mathbb{R}^{n\times n}$ and let there exist $\zeta \in \mathcal{K}$, and $\eta \in \mathcal{K}_\infty$ such that $f(x,t)$ and $G(x,t)$ satisfy the following bounds for all $(x,t) \in \mathbb{R}^n \times \mathbb{R}^+$:

$$G(x,t)G^T(x,t) \geq \zeta(|x|)I, \ \forall x \in K \tag{6.22}$$

$$\sup_{x\in K}|f(x,t)| \leq \eta(|x|). \tag{6.23}$$

If k and α are chosen such that

$$k\alpha > \sup_{x\in K}\frac{1}{\zeta(|x|)}, \tag{6.24}$$

then the vector-valued controller with components

$$u_i = \sqrt{\alpha\omega_i}\cos\left(\omega_i t + kV(x)\right), \tag{6.25}$$

where $\omega_i = \omega\hat{\omega}_i$ *such that* $\hat{\omega}_i \neq \hat{\omega}_j\ \forall i \neq j$, *and*

$$V(x) = \int_0^{|x|} \eta(r)dr, \tag{6.26}$$

renders the origin of (6.21), (6.25) $\left(\frac{1}{\omega}, \zeta^{-1}\left(\frac{1}{k\alpha}\right)\right)$*-SPUUB.*

Remark 6.2 The proof is based on an existence result regarding a large enough value of ω for our desired result to hold. Clearly, from the form of (6.21), (6.25), in order for stabilization to be possible, we must choose ω large enough such that $\zeta(|x|)\sqrt{\alpha\omega} > |f|$. Although this detail is glossed over in our existence result, exactly such a requirement can be found if one writes out the proof of Theorem 2.3 for this particular system, in which, after integration by parts, terms of the form $\frac{|f|}{\sqrt{\omega}}$ will appear, which approach zero as $\omega \to \infty$.

6.6 2D Vehicle Control

In this section we consider a vehicle in a GPS-denied environment, unaware of its own orientation, whose goal it is to reach the location of the minimum of $J(x, y)$, where $J(x, y)$ is a detectable value, whose analytic form is unknown.

Theorem 6.3 *If the function* $J(x, y)$ *has a global minimum at* $(x^\star, y^\star)$, *such that*

$$\nabla J|_{(x^\star, y^\star)} = 0, \quad \nabla J \neq 0,\ \forall (x, y) \neq (x^\star, y^\star), \tag{6.27}$$

then for any $\delta > 0$, *by a sufficiently large choice of* $k\alpha$ *the point* $(x^\star, y^\star)$ *is* $\left(\frac{1}{\omega}, \delta\right)$*-SPUUB relative to the system* $(x(t), y(t))$, *as shown in Fig. 6.2:*

$$\dot{x} = \sqrt{\alpha\omega}\cos\left(\omega t + kJ(x, y) + \theta_0\right) \tag{6.28}$$

$$\dot{y} = \sqrt{\alpha\omega}\sin\left(\omega t + kJ(x, y) + \theta_0\right) \tag{6.29}$$

where θ_0 *is an unknown initial orientation.*

Remark 6.3 In the analysis that follows, it becomes apparent that the value of the arbitrary initial orientation, θ_0, is irrelevant, when we make the simplification:

$$\sin^2(kJ + \theta_0) + \cos^2(kJ + \theta_0) = 1,$$

therefore for notational convenience, and without loss of generality, from now on we set $\theta_0 = 0$.

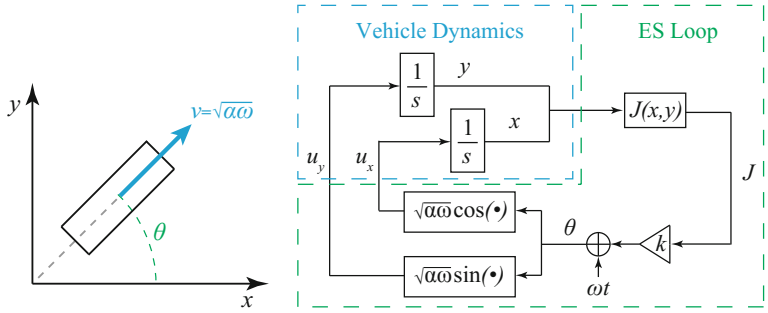

Fig. 6.2 Velocity actuated ES control scheme

Proof We expand

$$\cos(\omega t + kJ) = \cos(\omega t)\cos(kJ) - \sin(\omega t)\sin(kJ) \tag{6.30}$$

and

$$\sin(\omega t + kJ) = \cos(\omega t)\sin(kJ) + \sin(\omega t)\cos(kJ) \tag{6.31}$$

and rewrite (6.28), (6.29) as

$$\begin{bmatrix} \dot{x} \\ \dot{y} \end{bmatrix} = \sqrt{\omega}\cos(\omega t)\begin{bmatrix} \sqrt{\alpha}\cos(kJ) \\ \sqrt{\alpha}\sin(kJ) \end{bmatrix} + \sqrt{\omega}\sin(\omega t)\begin{bmatrix} -\sqrt{\alpha}\sin(kJ) \\ \sqrt{\alpha}\cos(kJ) \end{bmatrix}. \tag{6.32}$$

By Theorem 2.3, the trajectory of (6.32) uniformly converges to the trajectory of

$$\begin{bmatrix} \dot{\bar{x}} \\ \dot{\bar{y}} \end{bmatrix} = \frac{\alpha}{2} D\left(\begin{bmatrix} -\sin(kJ) \\ \cos(kJ) \end{bmatrix}\right)\begin{bmatrix} \cos(kJ) \\ \sin(kJ) \end{bmatrix} - \frac{\alpha}{2} D\left(\begin{bmatrix} \cos(kJ) \\ \sin(kJ) \end{bmatrix}\right)\begin{bmatrix} -\sin(kJ) \\ \cos(kJ) \end{bmatrix}. \tag{6.33}$$

Performing derivatives, Eq. (6.33) simplifies to

$$\dot{\bar{x}} = -\frac{k\alpha}{2}\left(\frac{\partial J}{\partial \bar{x}}\cos^2(kJ) + \frac{\partial J}{\partial \bar{x}}\sin^2(kJ)\right), \tag{6.34}$$

$$\dot{\bar{y}} = -\frac{k\alpha}{2}\left(\frac{\partial J}{\partial \bar{y}}\sin^2(kJ) + \frac{\partial J}{\partial \bar{y}}\cos^2(kJ)\right). \tag{6.35}$$

Applying the identity $\cos^2(\cdot) + \sin^2(\cdot) = 1$, we arrive at the average system dynamics

$$\begin{bmatrix} \dot{\bar{x}} \\ \dot{\bar{y}} \end{bmatrix} = -\frac{k\alpha}{2}\left(\nabla J(\bar{x}, \bar{y})\right)^T. \tag{6.36}$$

Therefore, by Theorem 2.3 the trajectory $(x(t), y(t))$ of system (6.28)–(6.29) uniformly converges to the trajectory $(\bar{x}(t), \bar{y}(t))$, of the system

$$\dot{\bar{x}} = -\frac{k\alpha}{2}\frac{\partial J}{\partial \bar{x}}, \quad \bar{x}(0) = x(0), \quad \dot{\bar{y}} = -\frac{k\alpha}{2}\frac{\partial J}{\partial \bar{y}}, \quad \bar{y}(0) = y(0), \tag{6.37}$$

and therefore, for any $\delta > 0$, by choosing arbitrarily large values of $k\alpha$ we may ultimately bound $(\bar{x}, \bar{y})$ within a δ neighborhood of $(x^\star, y^\star)$.

Remark 6.4 Although the results presented above are for functions having a stationary extremum, they are easily extended to systems where the extremum point varies with time, such as the case of trajectory tracking, in which the cost is the distance between a mobile agent and its target.

Corollary 6.1 *Consider a function* $f(x, y, t) = \left(f_x(x, y, t), f_y(x, y, t)\right)^T$, *over a compact set* $(x, y) \in K \subset \mathbb{R}^2$, *which is continuous with respect to* t *and Lipschitz continuous with respect to* (x, y). *If the function* $J(x, y, t)$ *has a global minimum at* $(x^\star(t), y^\star(t)) \in K \ \forall t$, *such that the location of the minimum point has bounded velocity* $|\dot{x}^\star|, |\dot{y}^\star| < M$, *and*

$$\nabla J|_{(x^\star(t), y^\star(t))} = 0, \quad \nabla J \neq 0, \ \forall (x(t), y(t)) \neq (x^\star(t), y^\star(t)), \tag{6.38}$$

then for any $\delta > 0$, *by a sufficiently large choice of* $k\alpha$, $(x^\star(t), y^\star(t))$ *is* $\left(\frac{1}{\omega}, \delta\right)$-*SPUUB relative to the system:*

$$\dot{x} = f_x(x, y, t) + \sqrt{\alpha\omega}\cos\left(\omega t + kJ(x, y, t)\right) \tag{6.39}$$

$$\dot{y} = f_y(x, y, t) + \sqrt{\alpha\omega}\sin\left(\omega t + kJ(x, y, t)\right) \tag{6.40}$$

where θ_0 *is an unknown initial orientation.*

Proof We define the error variables $e_x(t) = x(t) - x^\star(t)$ and $e_y(t) = y(t) - y^\star(t)$ and show, by the same proof as above, that the the trajectory of the error system of (6.39)–(6.40) uniformly converges to the trajectory of

$$\dot{\bar{e}}_x = f_x(\bar{e}_x + x^\star, \bar{e}_y + y^\star, t) - \frac{k\alpha}{2}\frac{\partial J}{\partial \bar{e}_x} + \dot{x}^\star(t), \tag{6.41}$$

$$\dot{\bar{e}}_y = f_y(\bar{e}_x + x^\star, \bar{e}_y + y^\star, t) - \frac{k\alpha}{2}\frac{\partial J}{\partial \bar{e}_y} + \dot{y}^\star(t). \tag{6.42}$$

Because the velocities $|\dot{x}^\star|$ and $|\dot{y}^\star|$ are bounded, and the function $f(x, y, t)$ is bounded on the compact set K, for any $\delta > 0$, by choosing arbitrarily large values of $k\alpha$ we may ultimately bound $(\bar{x}, \bar{y})$ within a δ neighborhood of $(x^\star, y^\star)$.

6.7 2D Vehicle Simulations

6.7.1 Stationary Source Seeking

In order to illustrate the behavior of the control system for a vehicle with unknown orientation we first demonstrate the scheme in an environment without external disturbance, in which the goal is to seek the stationary minimum of an unknown, but measurable function. We consider the system

$$\dot{x} = \sqrt{\alpha\omega}\cos\left(\omega t + kJ(x, y)\right), \quad x(0) = 1 \tag{6.43}$$

$$\dot{y} = \sqrt{\alpha\omega}\sin\left(\omega t + kJ(x, y)\right), \quad y(0) = -1, \tag{6.44}$$

where $J = x^2 + y^2$, $\alpha = \frac{1}{2}$, $k = 2$, $\theta(0) = 1.2$, and $\omega = 25$.

The simulation results are shown in Fig. 6.3. By showing the system's trajectory (x, y), alongside that of the averaged system, $(\bar{x}, \bar{y})$, it is easy to see that the convergence is along a gradient descent towards the minimum of $J(x, y)$.

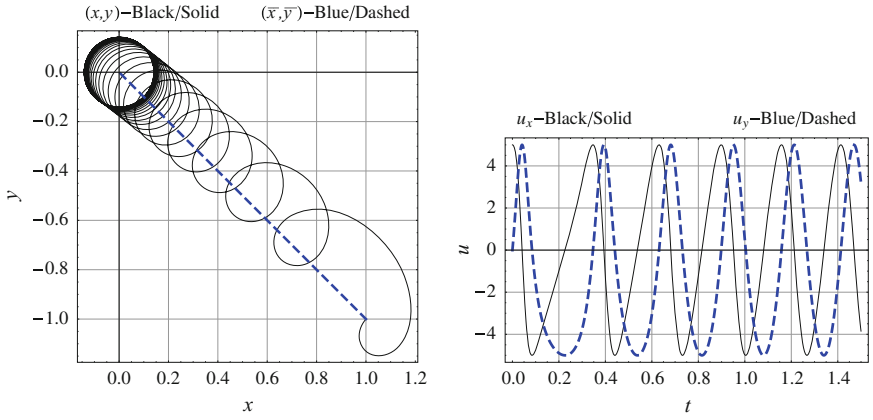

Fig. 6.3 Tracking of a stationary source is shown for 10 s, along with control effort for the first 1.5 s. The initial trajectory of $(x(t), y(t))$ is far from circular, as the system rotates slower while heading in the correct direction (towards decreasing J), which is the mechanism of convergence. This is also clearly seen in the control effort, where both the sine and cosine terms are initially asymmetric, changing faster or slower, depending on the heading direction

6.7.2 Tracking by Heading Rate Control, with Disturbances

We demonstrate the tracking and stabilizing abilities of the controller by tracking a moving source with an open loop unstable system. Furthermore, in order to demonstrate the ability to control heading angle velocity, rather than the angle value directly, we implement the following scheme, in which an additional filter (6.48) of the function $J(x, y, t)$ has been introduced. The system is:

$$\dot{x} = x + 0.75y + \sqrt{\alpha\omega}\cos(\theta), \quad x(0) = 1 \tag{6.45}$$

$$\dot{y} = 0.5x + 2y + \sqrt{\alpha\omega}\sin(\theta), \quad y(0) = -1 \tag{6.46}$$

$$\dot{\theta} = \omega + k\omega^2(J - \eta), \quad \theta(0) = 1.2 \tag{6.47}$$

$$\dot{\eta} = -\omega^2\eta + \omega^2 J, \quad \omega = 250 \tag{6.48}$$

$$r_x = \cos(t), \quad r_y = \sin(2t) \tag{6.49}$$

$$J = (x - r_x)^2 + \left(y - r_y\right)^2, \quad \alpha = 2, \quad k = 10. \tag{6.50}$$

Intuitively, if one considers the combined θ, η dynamics as in (6.47), (6.48), then $\dot{\theta} = \omega + k\dot{\eta}$ and therefore $\theta(t) = \omega t + k\eta(t)$. Considering the transfer function $\eta = \frac{\omega^2}{s+\omega^2} J$, in the limit as ω approaches infinity, η approaches J, and so $\theta(t)$ approaches $\omega t + kJ$ as before. Note that the system is open loop unstable, with eigenvalues $\lambda_i = 2.3, 0.7$. Because of the disturbance and the non-zero velocity of $(r_x(t), r_y(t))$, we must use larger values of k, α, and ω. The simulation results are shown in Fig. 6.4.

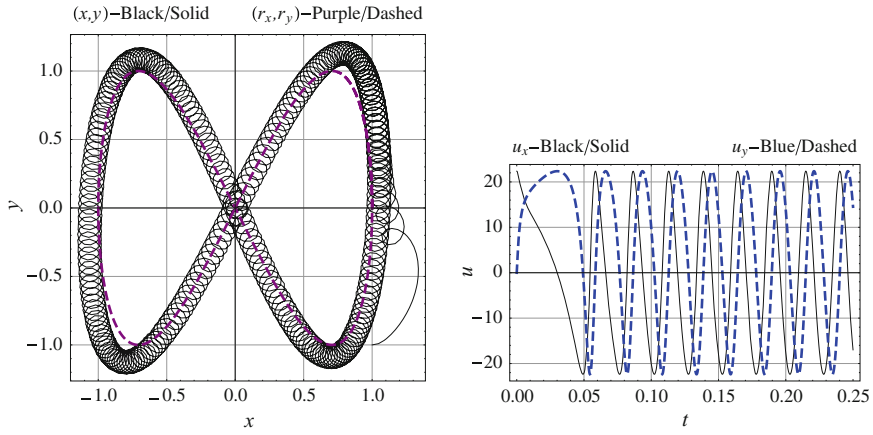

Fig. 6.4 Tracking of a moving source, despite external disturbances, is shown for 7 s, along with control effort for the first 0.25 s. The initial trajectory of $(x(t), y(t))$ is far from circular, the system rotates slower while heading in the correct direction (towards decreasing J), as it makes a large arc towards the location of the minimum of J. This is also obvious in the initial control effort, where both the sine and cosine terms are initially extremely distorted, changing faster or slower, depending on the heading direction

Chapter 7
Extremum Seeking for Stabilization of Systems Not Affine in Control

In all of the methods of ESC for stabilization described above, the unknown systems are assumed to be affine in control, namely, of the form:

$$\dot{x} = f(x,t) + g(x,t)u. \tag{7.1}$$

However, in most physical systems the control effort enters the system's dynamics through a nonlinear function, such as an input with a deadzone or saturation. Thus, it would be a major limitation if ESC applied only to systems affine in control.

In this chapter we study ESC for vector-valued systems not affine in control:

$$\dot{x} = f(x,t) + g(x,t,u),\ g(x,t,u) = \sum_{i=0}^{m} g_i(x,t)u^{2i+1} \tag{7.2}$$

where g is a control non-linearity given as an odd polynomial in u. The forthcoming Theorem 7.1 reduces controlling system (7.2) to the significantly easier problem of controlling the averaged system

$$\dot{\bar{x}} = f(\bar{x},t) - k\alpha K_g g_m(\bar{x},t) g_m^T(\bar{x},t) \left(\frac{\partial V}{\partial \bar{x}}\right)^T, \tag{7.3}$$

where K_g is a constant that depends on the function g. If there exist k, α, and V that stabilize system (7.3), then there exists $\omega^\star$ such that for all $\omega > \omega^\star$ the following feedback law stabilizes system (7.2):

$$u(x,t) = (\alpha\omega)^{\frac{1}{2(2m+1)}} \cos\left(\omega t + kV(x,t)\right). \tag{7.4}$$

In Sect. 7.2, we give sufficient conditions for Theorem 7.1 to be applicable to a broader range of systems of the form

$$\dot{x} = f(x,t) + g(x,t)v(u(x,t)), \tag{7.5}$$

A. Scheinker and M. Krstić, *Model-Free Stabilization by Extremum Seeking*,
SpringerBriefs in Control, Automation and Robotics,
DOI 10.1007/978-3-319-50790-3_7

where the $v(u)$ is an odd function of u. In Sect. 7.4, numerical experiments show that this approach is robust to un-modeled odd nonlinearities, errors in approximation, and perturbations with even exponents such as εu^{2n}, for $|\varepsilon| \ll 1$.

7.1 The Main Result

Theorem 7.1 *In the system*

$$\dot{x} = f(x,t) + \sum_{n=0}^{m} g_n(x,t) u^{2n+1}(x,t), \tag{7.6}$$

$$f : \mathbb{R}^n \times \mathbb{R} \to \mathbb{R}^n, \quad g_i : \mathbb{R}^n \times \mathbb{R} \to \mathbb{R}^{n\times n}, \quad V : \mathbb{R}^n \times \mathbb{R} \to \mathbb{R},$$

let the functions f, g_i, and V are twice continuously differentiable with respect to x and piecewise differentiable with respect to t. Consider the controller

$$u(x,t) = (\alpha\omega)^{\frac{1}{2(2m+1)}} \cos\left(\omega t + kV(x,t)\right), \tag{7.7}$$

and the related averaged system

$$\dot{\bar{x}} = f(\bar{x},t) - k\alpha A_m \left(\frac{g_m(\bar{x},t) g_m^T(\bar{x},t)}{2^{4m+1}}\right)\left(\frac{\partial V}{\partial \bar{x}}\right)^T, \quad A_m = \sum_{l=0}^{m} \binom{2m+1}{l}^2, \tag{7.8}$$

with $\bar{x}(0) = x(0)$. For any compact set $K \subset \mathbb{R}^n$, if $x^\star$ is a GUAS equilibrium point of (7.8) for all $x(0) \in K$, then $x^\star$ is a $\frac{1}{\omega}$ -SPUAS equilibrium point of (7.6), (7.7).

Proof The closed-loop form of system (7.6), (7.7) is (throughout the proof we omit the arguments of f, g_i, and V to simplify the notation)

$$\dot{x} = f(x,t) + \sum_{n=0}^{m} g_n(x,t) (\alpha\omega)^{\frac{2n+1}{2(2m+1)}} \cos^{2n+1}(\omega t + kV). \tag{7.9}$$

Let $b_n = 2n+1$ and $b_{n,l} = 2n+1-2l$, apply trigonometric power identities, and rewrite the sum as

$$\sum_{n=0}^{m} g_n \sum_{l=0}^{n} \frac{(\alpha\omega)^{\frac{b_n}{2b_m}}}{2^{2n}} \binom{b_n}{l} \cos\left(b_{n,l}(\omega t + kV)\right). \tag{7.10}$$

Apply trigonometric identities to expand (7.10) as the sum of

$$\sum_{n=0}^{m} g_n \sum_{l=0}^{n} \underbrace{\frac{(\alpha\omega)^{\frac{b_n}{2b_m}}}{2^{2n}} \binom{b_n}{l} \cos\left(b_{n,l}\omega t\right)}_{h_{c,n,l,\omega}(t)} \cos\left(b_{n,l}kV\right)$$

and

$$-\sum_{n=0}^{m} g_n \sum_{l=0}^{n} \underbrace{\frac{(\alpha\omega)^{\frac{b_n}{2b_m}}}{2^{2n}} \binom{b_n}{l} \sin\left(b_{n,l}\omega t\right)}_{h_{s,n,l,\omega}(t)} \sin\left(b_{n,l}kV\right).$$

For all $n \leq m$ and $\omega \geq \frac{1}{\alpha}$, $(\alpha\omega)^{\frac{2n+1}{2(2m+1)}} \leq \sqrt{\alpha\omega}$, the functions $h_{s,n,l,\omega}(t)$ and $h_{c,n,l,\omega}(t)$ have uniform limits

$$\lim_{\omega\to\infty} H_{c/s,n,l,\omega}(t) = \lim_{\omega\to\infty} \int_{t_0}^{t} h_{c/s,n,l,\omega}(\tau)d\tau = 0, \tag{7.11}$$

and for all $n_1, n_2 < m$, have weak limits

$$h_{c/s,n_1,i,\omega}(t) H_{c/s,n_2,j,\omega}(t) \rightharpoonup 0. \tag{7.12}$$

For $n = m$, we must consider all of the terms

$$h_{c,m,l,\omega}(t) = \binom{b_m}{l} \frac{\sqrt{\alpha\omega}\cos\left(b_{m,l}\omega t\right)}{2^{2m}}, \quad h_{s,m,l,\omega}(t) = \binom{b_m}{l} \frac{\sqrt{\alpha\omega}\sin\left(b_{m,l}\omega t\right)}{2^{2m}}. \tag{7.13}$$

The products $h_{c,m,i,\omega}(t) H_{s,m,j,\omega}(t)$ are given by

$$-\alpha\left(\frac{1}{2^{2m}}\right)^2 \binom{b_m}{l}^2 \cos^2\left(b_{m,l}\omega t\right) + \alpha\left(\frac{1}{2^{2m}}\right)^2 \binom{b_m}{l}^2 \cos\left(b_{m,l}\omega t_0\right)\cos\left(b_{m,l}\omega t\right).$$

The terms $\cos^2\left(b_{m,l}\omega t\right)$ and $\cos\left(b_{m,l}\omega t\right)$ weakly converge to 1/2 and 0, respectively, therefore

$$h_{c,m,i,\omega}(t) H_{s,m,j,\omega}(t) \rightharpoonup -\alpha\frac{1}{2^{4m+1}}\binom{b_m}{l}^2, \quad h_{s,m,i,\omega}(t) H_{c,m,j,\omega}(t) \rightharpoonup \underbrace{\alpha\frac{1}{2^{4m+1}}\binom{b_m}{l}^2}_{a_{m,l}}. \tag{7.14}$$

Therefore, by application of Theorem 2.3, the $b_{m,l}\omega$ frequency component's contribution to the average dynamics are

$$-\alpha a_{m,l} g_m \cos(k b_{m,l} V) \frac{\partial}{\partial \bar{x}} \left(g_m \sin(k b_{m,l} V) \right) \tag{7.15}$$

$$+\alpha a_{m,l} g_m \sin(k b_{m,l} V) \frac{\partial}{\partial \bar{x}} \left(g_m \cos(k b_{m,l} V) \right). \tag{7.16}$$

The term (7.15) can be expanded as

$$-\alpha a_{m,l} g_m \cos(k b_{m,l} V) \left(\frac{\partial g_m}{\partial \bar{x}} \sin(k b_{m,l} V) - k b_{m,l} \frac{\partial V}{\partial \bar{x}} g_m \cos(k b_{m,l} V) \right), \tag{7.17}$$

and (7.16) can be expanded as

$$+\alpha a_{m,l} g_m \sin(k b_{m,l} V) \left(\frac{\partial g_m}{\partial \bar{x}} \cos(k b_{m,l} V) - k b_{m,l} \frac{\partial V}{\partial \bar{x}} g_m \sin(k b_{m,l} V) \right). \tag{7.18}$$

Adding (7.17) and (7.18) we are left with

$$-k\alpha b_{m,l} a_{m,l} g_m g_m^T \left(\frac{\partial V}{\partial \bar{x}} \right)^T. \tag{7.19}$$

Plugging in for the values of $a_{m,l}$ from (7.14), the overall average system dynamics are given by

$$\dot{\bar{x}} = f(\bar{x}, t) - k\alpha \sum_{l=0}^{m} \binom{b_m}{l}^2 \left(\frac{g_m(\bar{x}, t) g_m^T(\bar{x}, t)}{2^{4m+1}} \right) \left(\frac{\partial V}{\partial \bar{x}} \right)^T$$

and the desired convergence and the existence of the appropriate ω are guaranteed by Theorem 2.3.

Theorem 7.1 implies that to stabilize system (7.6) one must choose the gain k, dithering amplitude α, and a Lyapunov-type function $V(x, t)$ relative to upper and lower bounds on $\|f(x, t)\|$ and $\left\|g_m(x, t) g_m^T(x, t)\right\|$, respectively. Once k, α, and V are chosen, there exists a sufficiently large $\omega^\star$, such that for all $\omega > \omega^\star$, the above results hold. In practice we specify ω and design the controller to maintain the values of u within some compact set K_u. Because $g_m(x, t) g_m^T(x, t) \geq 0$ one need not know the sign of $g_m(x, t)$ which simplifies significantly the stabilization problem.

7.2 An Application of the Main Result

In this section we give sufficient conditions to use our main result to control a general nonlinear system of the form:

$$\dot{x} = f(x,t) + g(x,t)v(u(x,t)). \tag{7.20}$$

The stability of a system of the form (7.20) may be studied by considering an odd-polynomial system of the form

$$\dot{x} = f(x,t) + g(x,t)\underbrace{\sum_{n=0}^{m} u^{2n+1}(x,t)}_{p(x,t)}. \tag{7.21}$$

We assume the functions f and g are twice differentiable and the function $v : \mathbb{R} \to \mathbb{R}$ is a continuous, odd function of u, i.e., for fixed x and t, $v(-u(x,t)) = -v(u(x,t))$. Fix the system (7.20), $[t_0, t_0 + T] \subset R_{\geq 0}$, $K \subset R^n$, and $K_u \subset R$. On $[t_0, t_0 + T]$, K, and K_u. Because g is continuous and $K \times [t_0, t_0 + T]$ is compact there exists a $G > ||g||_{K\times[t_0,t_0+T]}$, where $\|\cdot\|$ denotes the uniform norm: $||f||_Y = \sup_{y\in Y} ||f(y)||$. For any $\varepsilon > 0$, the Stone-Weierstrass Theorem (see, e.g. [24]) implies there exists an odd polynomial p so that $\|v - p\|_{K_u} < \frac{\varepsilon}{G}$. Therefore, we can rewrite the system (7.20) as

$$\dot{x} = f(x,t) + g(x,t)p + \underbrace{g(x,t)(v-p)}_{l(x,t)}, \tag{7.22}$$

such that $\|l(x,t)\|_K < \varepsilon$ (Fig. 7.1).

Therefore, given a system of the form (7.20), we can always rewrite it as a system of the form (7.22) which we can think of as a perturbation of the system

$$\dot{x} = f(x,t) + g(x,t)p(u), \tag{7.23}$$

which we can stabilize by the use of Theorem 7.1. Because we can make the perturbation arbitrarily small, if we stabilize the origin of the odd polynomial system (7.41)

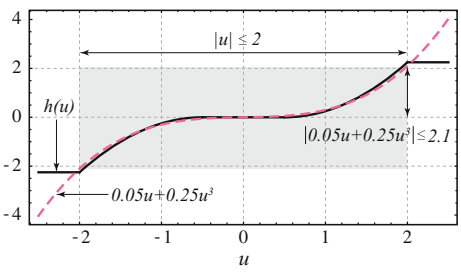

Fig. 7.1 Polynomial approximation of $h(u)$ for $|u| < 2$

such that it has a Lyapunov function satisfying Lemma 9.1 in [68], then by Lemma 9.2 of [68], the origin of system (7.20) is also stable for a set of initial conditions which can be made arbitrarily large by making ε arbitrarily small.

7.3 Example of System Not Affine in Control

Non-affine controllers, in particular non-linear controllers with dead zones, arise in a variety of practical control systems [68, 110, 122, 138]. For example, a water cooling system whose flow rate is controlled by a valve with limited maximum open surface area and digital resolution-limited minimum valve opening setting. We provide examples that demonstrate how to develop a controller for systems in which the control effort enters through an odd non-linear function $h(u)$. In what follows we take the common approach of approximating $h(u)$ with an odd polynomial $p(u)$ [62, 77].

Example 7.1 Consider the system

$$\dot{x} = f(x,t) + g(x,t)h(u), \tag{7.24}$$

and the general approximation $h(u) \approx p(u) = a_1 u + a_3 u^3$, which produces the approximate system:

$$\dot{x} = f(x,t) + g(x,t)\left(a_1 u(x,t) + a_3 u^3(x,t)\right). \tag{7.25}$$

We will design a controller of the form

$$u = (\alpha\omega)^{\frac{1}{6}} \cos\left(\omega t + kV(x)\right). \tag{7.26}$$

The reason for the choice $(\alpha\omega)^{\frac{1}{6}}$ is explained as follows. The closed loop dynamics of (7.25), (7.26) are given by

$$\begin{aligned}\dot{x} = {} & f(x,t) + a_1 g(x,t)(\alpha\omega)^{\frac{1}{6}} \cos\left(\omega t + kV(x)\right) \\ & + a_3 g(x,t)\sqrt{\alpha\omega}\cos^3\left(\omega t + kV(x)\right).\end{aligned} \tag{7.27}$$

The cos() and $\cos^3()$ terms can be expanded as

$$\begin{aligned}& a_1 g(x,t)(\alpha\omega)^{\frac{1}{6}}\Big(\cos(\omega t)\cos(kV) - \sin(\omega t)\sin(kV)\Big) \\ & + a_3 g(x,t) 0.75\sqrt{\alpha\omega}\Big(\cos(\omega t)\cos(kV) - \sin(\omega t)\sin(kV) \\ & + 0.25\cos(3\omega t)\cos(3kV) - 0.25\sin(3\omega t)\sin(3kV)\Big).\end{aligned}$$

Theorem 2.3 implies that as $\omega \to \infty$ products containing the $a_1 g(x,t)$ terms contain powers of ω of the form $1/\omega^{\frac{2}{3}}$ and $1/\omega^{\frac{1}{3}}$, which uniformly converge to zero. In the remaining terms, by choosing $(\alpha\omega)^{\frac{1}{6}}$, for u^3, we get terms with amplitudes proportional to $\sqrt{\alpha\omega}$ and by Theorem 2.3, are left with products in which the ω amplitude dependence has disappeared, only leaving terms of the form $\cos^2(\omega t)$, and $\sin^2(\omega t)$, which weakly converge to $1/2$, leaving us with the average system

$$\dot{\bar{x}} = f(\bar{x},t) - \frac{k\alpha}{2} a_3^2 g^2(\bar{x},t)\left((3/4)^2 + (1/4)^2\right)\frac{\partial V(\bar{x})}{\partial \bar{x}}, \tag{7.28}$$

where $\bar{x}(0) = x(0)$. Thus, to stabilize the origin, it suffices to choose ω, k, α, V sufficiently large with respect to $a_3^2 g^2(x,t)$ and $f(x,t)$.

We consider the special case of System (7.24), where

$$h(u) = \begin{cases} 0 & |u| < 0.5 \\ \operatorname{sgn}(u)(|u| - 0.5)^2 & 0.5 < |u| <= 2 \\ 2.25 & 2 < |u| \end{cases}. \tag{7.29}$$

Figure 7.2 shows the results of a simulation of

$$\dot{x} = \frac{\cos(2t)x^2}{2} + 2\cos(20t)\,h(u),\ u = (\alpha\omega)^{\frac{1}{6}}\cos\left(\omega t + kx^2\right) \tag{7.30}$$

with control parameters $\omega = 200$, $\alpha = 64/\omega$, $k = 50$, and $x(0) = 1.5$, where $h(u)$ is given by (7.29) and the controller was designed using the approximation (7.25) with $a_1 = 0.05$ and $a_3 = 0.25$, which has average dynamics

$$\dot{\bar{x}} = 0.5\cos(2t)\bar{x}^2 - (5/16)k\alpha\cos^2(20t)\,\bar{x}, \quad \bar{x}(0) = x(0). \tag{7.31}$$

Example 7.2 **Second Order System**: Consider an unstable mechanical or electrical second order system in which the control actuator involves $h(u)$ given above

$$\ddot{x} = 0.5x^2 + 2\cos(20t)h(u), \quad x(0) = 1.5, \quad \dot{x}(0) = 0. \tag{7.32}$$

Defining $x_1 = x$, $x_2 = \dot{x}$, we use the controller from [128] for systems in strict feedback form and rewrite the system

$$\dot{x}_1 = x_2 \tag{7.33}$$

$$\dot{x}_2 = 0.5x_1^2 + 2\cos(20t)\,h(u), \tag{7.34}$$

$$u = (\alpha\omega)^{\frac{1}{6}}\cos\left(\omega t + k\left(x_1 + 2x_2\right)^2\right), \tag{7.35}$$

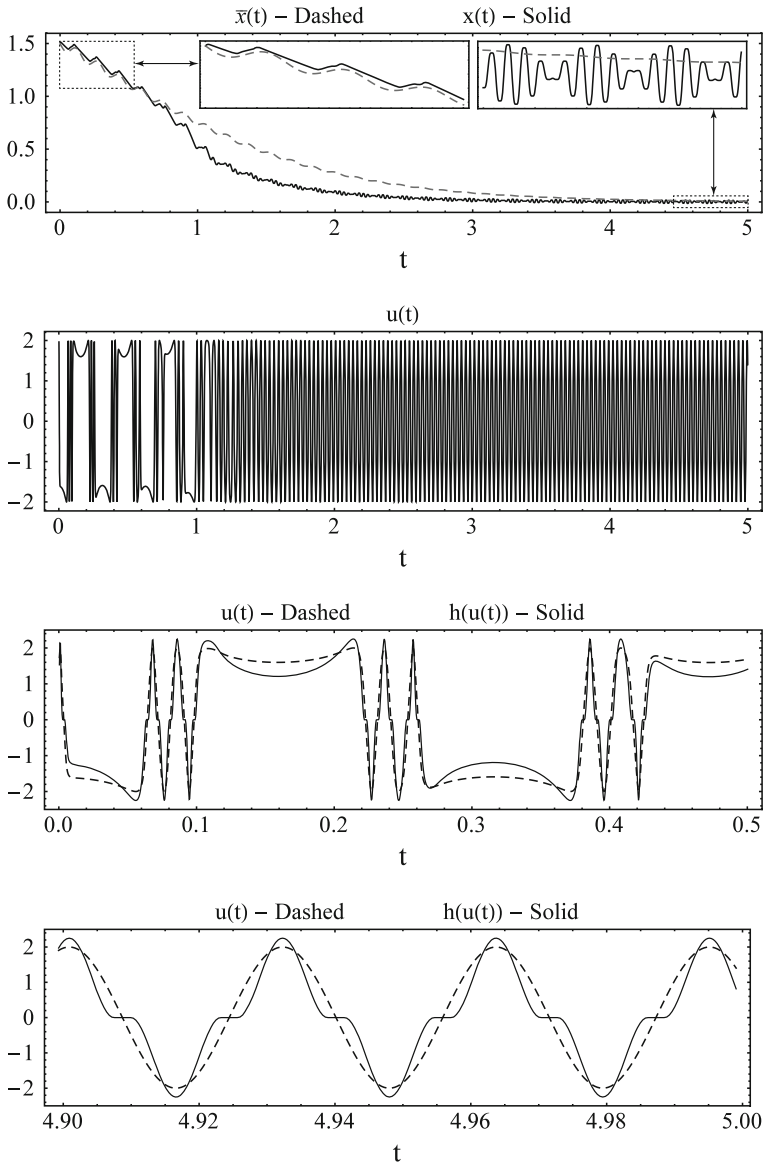

Fig. 7.2 The trajectory $x(t)$ of the system (7.30) is shown alongside the trajectory $\bar{x}(t)$ of the averaged system (7.31). It is clear that the system behaves as expected despite our controller design being based on the approximation of the nonlinearity. The control effort $u(t)$ shows strong initial phase modulation before a steady state is reached. A zoomed in view of the initial 0.5 s and final 0.1 s of control effort $u(t)$ and control signal $h(u(t))$ shows the details of the saturation, dead zone, and steady state oscillation

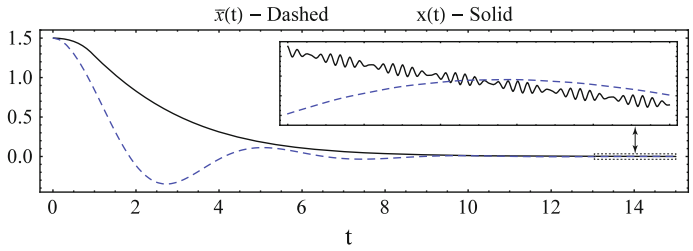

Fig. 7.3 The trajectory $x(t)$ of the system (7.33)–(7.35) is shown alongside the trajectory $\bar{x}(t)$ of the averaged system (7.36), (7.37). The trajectory of the second order system is noticeably smoother because of the filtering property of the integrator

with k, α as above and $\omega = 250$. The average dynamics are

$$\dot{\bar{x}}_1 = \bar{x}_2, \quad \bar{x}_1(0) = x_1(0), \quad \bar{x}_2(0) = x_2(0), \tag{7.36}$$

$$\dot{\bar{x}}_2 = 0.5\bar{x}^2 - \frac{5}{16}k\alpha \cos^2(20t)\,(2\bar{x}_1 + \bar{x}_2)\,, \tag{7.37}$$

the simulation is shown in Fig. 7.3.

Example 7.3 **Approximating summations of non-linear functions**: Our results allow for the stabilization of systems where $h(x, t, u)$ is a weighted sum of nonlinear control functions such as $h(, x, t, u) = g_1(x, t)\sin(u) + g_2(x, t)u^3$. To approximate such an h, we approximate each odd term and rearrange the summation.

We suppress the dependance on x, t, u and use the approximation $\sin(u) \approx u - \frac{1}{6}u^3$ for $|u| < \frac{\pi}{3}$ to approximate h as follows

$$h \approx g_1(u - \frac{1}{6}u^3) + g_2u^3 = g_1u + \left(g_2 - \frac{1}{6}g_1\right)u^3 = \tilde{g}_1u + \tilde{g}_3u^3. \tag{7.38}$$

7.4 Robustness of Nonlinear Approximation

We showed that when the control nonlinearity $h(u)$ is odd we can design a feedback controller and calculate analytically the approximate average behavior. In this section we propose a conjecture on the robustness of our controller when $h(u)$ is not odd. We use numerical simulations to demonstrate the relationship between stability and our controller's two primary inputs to the system, higher gains and higher oscillatory rates. We divide our analysis based on estimates of the dominant term of the controller, information that may be available even when the form of the controller is unknown. In Sect. 7.4.1 we demonstrate that for a system with dominant odd power terms our controller is robust with respect to different choices of the power $2m + 1$. In Sect. 7.4.2 we demonstrate, as expected, that for a system with dominant even power

terms our controller will only stabilize the system for a specific range of values of the gain α and the power $2m+1$. In Sect. 7.4.3 we demonstrate that the well chosen lower powers $2m+1$ will stabilize the system with lower gains α.

We consider a more general class of systems with even-powered perturbations and un-modeled odd nonlinearities:

$$\dot{x} = f(x,t) + \sum_{i=0}^{n_o} g_{2i+1}(x,t)u^{2i+1}(x,t) + \varepsilon \sum_{i=1}^{n_e} g_{2i}(x,t)u^{2i}(x,t). \tag{7.39}$$

If there were no even terms and we knew that $2m+1$ was the highest power odd nonlinearity of (7.39), then we would choose a controller of the form

$$u_m = (\alpha\omega)^{\frac{1}{2(2m+1)}} \cos(\omega t + kV). \tag{7.40}$$

However, for the present analysis we must address two additional issues. First, the power of our controller $2m+1$ need not equal the highest odd power of the system $2n_0+1$, and therefore the averaging analysis of Theorem 7.1 breaks down because $m < n_o$ introduces terms of the form $(\alpha\omega)^{\frac{2n_o+1}{2(2m+1)}} \cos^{2n_o+1}(\omega t + kV)$, resulting in divergent weak limits which are not independent of ω, because in this case $\frac{2n_o+1}{2(2m+1)} > \frac{1}{2}$. Second, the averaging analysis of Theorem 7.1 further breaks down since the even powers of u introduce into the system dynamics positive semi-definite terms of the form $(\alpha\omega)^{\frac{2l}{2(2m+1)}} \cos^{2l}(\omega t + kV)$ which grow without bound as ω grows. However, it turns out that we may still be able to approximate the behavior of this system.

We integrate (7.39) by parts, notice that as $\omega \to \infty$ the highest power terms of (7.39) dominate the dynamics, keep only the highest order odd and even power terms, and average the oscillatory functions to produce the approximation (7.41), which leads us to make the following conjecture:

Conjecture 7.1 Consider systems (7.39), (7.40) and:

$$\begin{aligned}
\dot{\bar{x}} &= f(\bar{x},t) + \varepsilon g_{2n_e}(\bar{x},t)(\alpha\omega)^{\frac{2n_e}{2m+1}} B_{n_e} \\
&\quad - k\alpha^{\frac{2n_o+1}{2m+1}} \omega^{(\frac{2n_o+1}{2m+1}-1)} A_{n_0} \frac{g_{n_o}(\bar{x},t) g_{n_o}^T(\bar{x},t)}{2^{4n_o+1}} \left(\frac{\partial V}{\partial \bar{x}}\right)^T, \\
A_{n_0} &= \sum_{l=0}^{n_o} \binom{2n_o+1}{l}^2, \quad B_{n_e} = \frac{1}{2^{2n_e}} \binom{2n_e}{n}.
\end{aligned} \tag{7.41}$$

For any $\delta > 0$, any compact set $K \subset \mathbb{R}^n$, and any $t_0, T \in \mathbb{R}_{\geq 0}$ there exists $\varepsilon^\star(\delta, K, T) > 0$ such that for all $|\varepsilon| < \varepsilon^\star$, there exists $\omega^\star$ such that for each $\omega > \omega^\star$, the trajectories $x(t)$ of (7.39), (7.40) and $\bar{x}(t)$ of (7.41) satisfy

$$\max_{t\in[t_0,t_0+T]} \|x(t) - \bar{x}(t)\| < \delta, \quad \lim_{t\to\infty} \|\bar{x}(t)\| = 0 \Longrightarrow \lim_{t\to\infty} \|x(t)\| < \delta.$$

Remark 7.1 When $n_o = m$ and there are no even power terms, (7.41) simplifies to (7.8).

7.4.1 Dominant Odd Power Terms

To test Conjecture 7.1 we study the system

$$\dot{x} = x + 0.1\left(u + u^3 + u^5\right) + \varepsilon\left(u^2 + u^4\right), \tag{7.42}$$

$$u = u_m = (\alpha\omega)^{\frac{1}{2(2m+1)}} \cos\left(\omega t + kx^2\right). \tag{7.43}$$

According to the conjecture, the closed loop dynamics should, for large ω, approximate

$$\dot{\bar{x}} = \bar{x} - \frac{2k}{100}\frac{1}{2^9} A_2 \alpha^{\frac{5}{2m+1}} \omega^{\left(\frac{5}{2m+1}-1\right)} \bar{x} + \varepsilon B_2 (\alpha\omega)^{\frac{4}{2(2m+1)}}. \tag{7.44}$$

Therefore, the trajectory of the system should converge to the equilibrium point $x^\star$ satisfying

$$\left(\frac{2k}{100}\frac{1}{2^9} A_2 \alpha^{\frac{5}{2m+1}} \omega^{\left(\frac{5}{2m+1}-1\right)} - 1\right) x^\star = \varepsilon B_2 (\alpha\omega)^{\frac{4}{2(2m+1)}}. \tag{7.45}$$

Thus, for each $\varepsilon > 0$ and each controller power $2m+1$, we can find $\alpha_m(\omega, \varepsilon, x^\star)$ which solves (7.45), such that for all $\alpha > \alpha_m(\omega, \varepsilon, x^\star)$ the system should converge to $|x| \leq |x^\star|$.

When $\varepsilon = 0$, the system should be stable for

$$\frac{2k}{100}\frac{1}{2^9} A_2 \alpha^{\frac{5}{2m+1}} \omega^{\left(\frac{5}{2m+1}-1\right)} > 1. \tag{7.46}$$

Thus, for any chosen control power $2m+1$, we can estimate a required $\alpha_m(\omega)$ such that the system will be stable for all $\alpha > \alpha_m(\omega)$, of the form

$$\alpha_m(\omega) = \left(\frac{100 \times 2^7}{63k\omega^{\left(\frac{5}{2m+1}-1\right)}}\right)^{\frac{2m+1}{5}}. \tag{7.47}$$

We confirm the estimates (7.45) and (7.47) by simulating system (7.42), (7.43) with $k = 100$, $m = 1, 3, 5$, $\varepsilon = 0, 0.05$, $\alpha \in [0.1, 2]$, $\omega \in [5, 200]$, $x(0) = 1$. We let the system evolve for $T = 5$ s and then record $|x(T)|$ (with a cutoff at 3), in order to determine whether the trajectory is converging towards the origin or diverging. We plot the results in Fig. 7.4 and compare to the analytically predicted boundaries of stability (7.45) and (7.47). We see that for large values of $(\alpha\omega)^{\frac{1}{2m}}$, the prediction is accurate, which happens for much smaller values of $\alpha\omega$ for the lower powers $m = 1, 3$ than for $m = 5$ because the term $(\alpha\omega)^{\frac{1}{10}}$ grows very slowly.

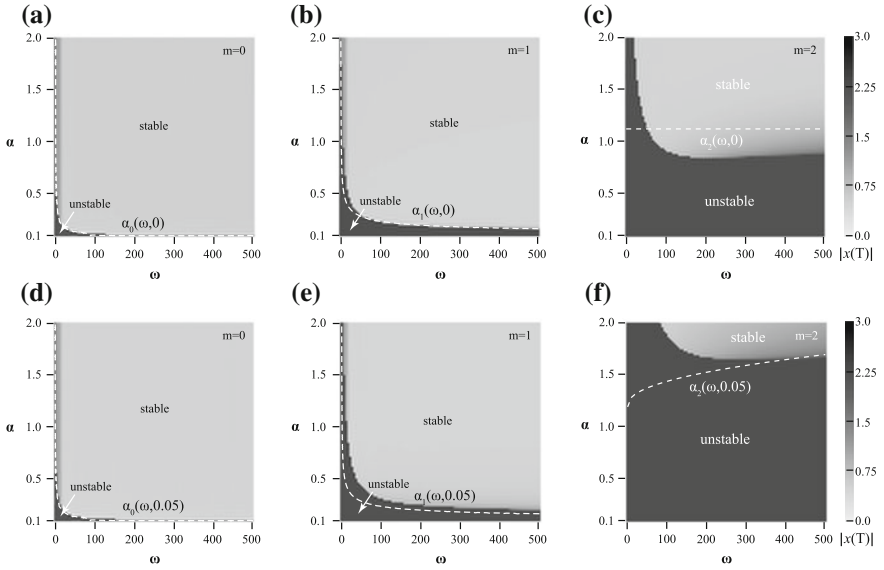

Fig. 7.4 The region of stability is shown for several choices of controller and ε for system (7.42), (7.43). For $\varepsilon = 0$, the region of stability is shown for $m = 1$ in **(a)**, $m = 3$ in **(b)** and $m = 5$ in **(c)**, relative to the predicted $\alpha_m(\omega, \varepsilon = 0)$ curve as calculated in (7.47). For $\varepsilon = 0.05$, the region of stability is shown for $m = 1$ in **(d)**, $m = 3$ in **(e)** and $m = 5$ in **(f)**, relative to the predicted $\alpha_m(\omega, \varepsilon = 0.05)$ curve as calculated in (7.45)

7.4.2 *Dominant Even Power Terms*

When the highest power of control nonlinearity is even, we have little chance of controlling the system, except in a very limited range of values of ε and ω, because the positive semi-definite destabilizing terms dominate the dynamics and grow with ω. We consider the system

$$\dot{x} = 0.1u + 0.1u^3 + \varepsilon u^4, \tag{7.48}$$

with controller $u_m = (\alpha\omega)^{\frac{1}{2(2m+1)}} \cos\left(\omega t + kx^2\right)$, $m = 0, 1$. For the case $m = 1$, applying Conjecture 7.1, we get the following estimate for a bound on ε for the stability of the average system:

$$\varepsilon < \varepsilon_1(\omega) = \frac{2k\left(0.1^2\right) A_1\alpha - 1}{(\alpha\omega)^{\frac{2}{3}} B_2}, \tag{7.49}$$

which is numerically confirmed in Fig. 7.5a. In the case $m = 0$ even the averaging estimates completely break down. The best we can do is to simply compare the dominant stabilizing $(\alpha\omega)^{\frac{3}{2}}$ and destabilizing $(\alpha\omega)^{\frac{4}{2}}$ powers and estimate a bound

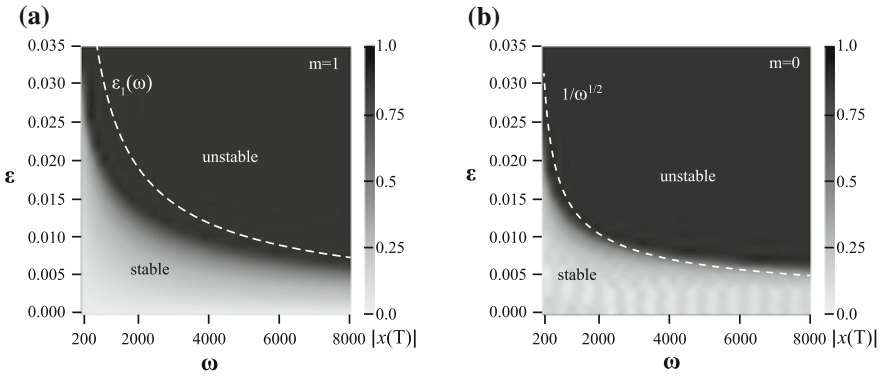

Fig. 7.5 **a** Region of stability (in terms of ε and ω) when assuming $h(u)$ to be of first order, utilizing a controller with amplitude $(\alpha\omega)^{\frac{1}{2}}$. **b** Region of stability (in terms of ε and ω) when assuming $h(u)$ to be of third order and utilizing a controller with amplitude $(\alpha\omega)^{\frac{1}{6}}$

on ε of the form $\varepsilon < \frac{1}{\sqrt{\alpha\omega}}$, which is in surprisingly good agreement with the numerical study, as shown in Fig. 7.5b.

7.4.3 *Even Nonlinearities in Bounded System*

We consider the nonlinearity from Example 7.1 with even power nonlinearities, $h_\varepsilon(u)$ which is shown in Fig. 7.6. We consider the system

$$\dot{x} = x + h_\varepsilon(u), \quad x(0) = 1, \quad u_m = (\alpha\omega)^{\frac{1}{2(2m+1)}} \cos\left(\omega t + kx^2\right), \tag{7.50}$$

with various control options $m = 0, 1, 2$. The numerically calculated regions of stability are shown in Fig. 7.7, with $k = 100$ and $\alpha = 5$. The system remains stable for a small range of $\varepsilon \neq 0$, and, as expected, is most robust with the $m = 0$ controller, which makes it least predictable as the averaging no longer holds, but highest gain. Even when $\varepsilon = 0$, as ω is increased the system loses stability because, as $\sqrt{\alpha\omega}$ grows, u leaves any fixed compact set K_u and therefore the polynomial approximation that closely approximates $h(u)$ over the growing range has increasingly higher numbers of significant high power terms whose coefficients decay. At some point, the dominant power of u in the approximation has such a small coefficient, that the given $\alpha = 5$ is no longer sufficient in order to stabilize the system.

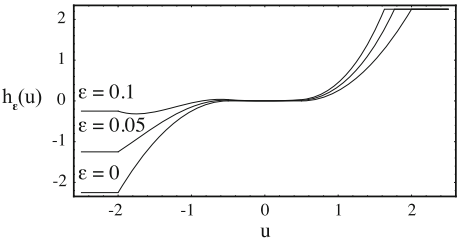

Fig. 7.6 The nonlinearity $h_\varepsilon(u)$ for $|u| < 2.5$ for various values of ε

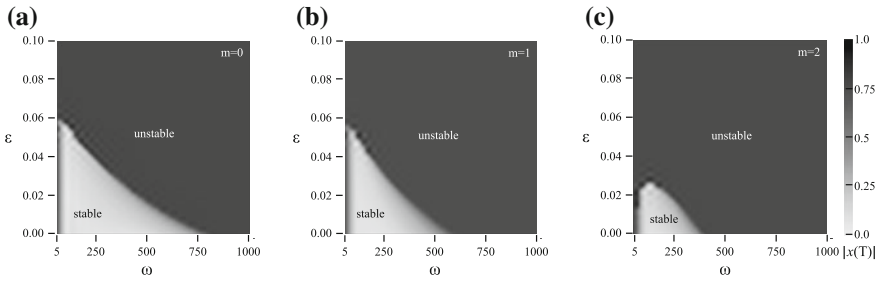

Fig. 7.7 Region of stability. **a** Assuming $h(u)$ to be of first order, utilizing a controller with amplitude $(\alpha\omega)^{\frac{1}{2}}$. **b** Assuming $h(u)$ to be of third order, utilizing a controller with amplitude $(\alpha\omega)^{\frac{1}{6}}$. **c** Assuming $h(u)$ to be of fifth order and utilizing a controller with amplitude $(\alpha\omega)^{\frac{1}{10}}$

7.4.4 Summary of Robustness Study

From the numerical studies above it is clear that the system is very robust to the degree of odd nonlinearity approximation and is even somewhat robust to the existence of even nonlinearities, expectedly much less so when the powers of the even nonlinearities are dominant. When choosing a controller for unknown nonlinearity, $h(u)$, if the actual highest order odd term is of the form u^{2n_o+1}, and the controller is chosen based on a guess, m, of n_o, of the form $(\alpha\omega)^{\frac{1}{2(2m+1)}}$, then the dominant stabilizing term of the averaged system is proportional to:

$$-k\alpha^{\frac{2n_o+1}{2m+1}}\omega^{\left(\frac{2n_o+1}{2m+1}-1\right)}. \tag{7.51}$$

If the guess is correct, and $m = n_o$, then (7.51) simplifies to

$$-k\alpha^{\frac{2n_o+1}{2m+1}}\omega^{\left(\frac{2n_o+1}{2m+1}-1\right)} = -k\alpha, \tag{7.52}$$

as calculated in Theorem 7.1.

If the guess underestimates the actual degree of $h(u)$, n_o, such that $m < n_o$, then for some $\hat{m} > 0$, $n_o = m + \hat{m}$ and

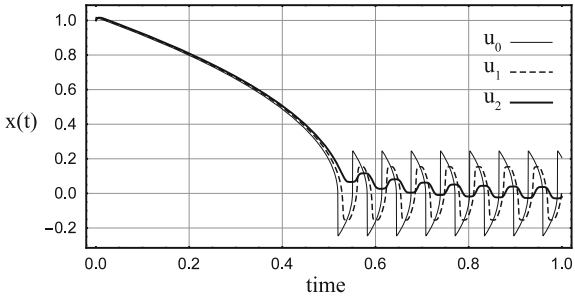

Fig. 7.8 A simulation of system (7.42), (7.43), comparing the use of controllers with $m = 0, 1, 2$. Although lower values of m result in faster convergence, the resulting steady state oscillations are increased

$$-k\alpha^{\frac{2n_o+1}{2m+1}}\omega^{\left(\frac{2n_o+1}{2m+1}-1\right)} = -k\alpha^{\left(1+\frac{\hat{m}}{2m+1}\right)}\omega^{\frac{\hat{m}}{2m+1}} = -k\alpha\,(\alpha\omega)^{\frac{\hat{m}}{2m+1}}, \tag{7.53}$$

which is effectively equivalent to increasing the gain of the controller by a factor of $(\alpha\omega)^{\frac{\hat{m}}{2m+1}}$. This is confirmed by the numerical study which shows that lower choices of m result in larger regions of stability relative to α, ω, and ε.

If the guess overestimates the actual degree of $h(u)$, n_o, such that $m > n_o$, then for some $\hat{m} > 0$, $n_o = m - \hat{m}$ and

$$-k\alpha^{\frac{2n_o+1}{2m+1}}\omega^{\left(\frac{2n_o+1}{2m+1}-1\right)} = -k\alpha^{\left(1-\frac{\hat{m}}{2m+1}\right)}\omega^{\frac{-\hat{m}}{2m+1}} = -\frac{k\alpha}{(\alpha\omega)^{\frac{\hat{m}}{2m+1}}}, \tag{7.54}$$

which is effectively equivalent to decreasing the gain of the controller by a factor of $\frac{1}{(\alpha\omega)^{\frac{\hat{m}}{2m+1}}}$, and in the weak limit the system's control effort will converge to 0, as ω is increased, rendering the system completely uncontrollable.

When the degree $2n_o + 1$ of the highest odd nonlinearity of $h(u)$ is uncertain, the best bet is to use the lowest, $m = 0$, controller of the form $\sqrt{\alpha\omega}\cos(\omega t + kV(x,t))$, in order to guarantee sufficient gain. However, one must be careful, because for large ω, if $m < n_o$, the system's approximate dynamics will begin to diverge from those predicted by the averaging analysis. Furthermore, as shown above, the use of a lower m for a higher order system n_o, is effectively equivalent to increasing the control gain. If a system's actuators can handle higher gains, it is safer to simply use a higher gain $k\alpha$, with a higher m, so that the system's dynamics will be closer to those analytically predicted. Furthermore, if the controller is based on an underestimate of the degree of the nonlinearity and has a relatively large amplitude, the dithering terms will result in the system's steady state oscillations having larger magnitude. This is shown in Fig. 7.8, a simulation of system (7.42), (7.43), comparing the use of controllers with $m = 0, 1, 2$.

Chapter 8
General Choice of ES Dithers

Different dithers are appropriate in different control designs. In an analog system based on sinusoidal oscillators, a sinusoidal dither is a natural choice. In a switching system, such as the high voltage application in Sect. 8.2, a square wave with dead time is the choice that can be implemented in hardware. In this chapter we take advantage of the generality of Theorem 2.3, which has the useful property that a variety of different controllers have, on average, identical dynamics and allows for the study of discontinuous and non-differentiable dithers.

8.1 The On-Average Equivalence of Various Dithers

Recall that Theorem 2.3 allows us to study the dynamics of vector-valued systems of the form

$$\dot{x} = f(x,t) + g(x,t)u(y,t), \tag{8.1}$$
$$y = \psi(x,t) + n(t) = \hat{\psi}(x,t), \tag{8.2}$$

where $x \in \mathbb{R}^n$, and the functions $f : \mathbb{R}^n \times \mathbb{R} \to \mathbb{R}^n$, $g : \mathbb{R}^n \times \mathbb{R} \to \mathbb{R}^{n\times n}$, $\psi : \mathbb{R}^n \times \mathbb{R} \to \mathbb{R}$, and $n(t) : \mathbb{R} \to \mathbb{R}$ are unknown and twice continuously differentiable with respect to x. Also, ψ and $\partial\psi/\partial t$ are bounded with respect to t for x in a compact set, and $n(t)$, $\dot{n}(t)$ are bounded.

For controlling such systems, we choose controllers of the form $u : \mathbb{R}\times\mathbb{R} \to \mathbb{R}^n$, given by

$$u(y,t) = \sum_{i=1}^{m} k_i(y,t)h_{i,\omega}(t), \quad k_i : \mathbb{R}\times\mathbb{R} \to \mathbb{R}^n, \tag{8.3}$$

where the functions $k_i(y,t)$ are continuously differentiable and the only requirement on the high frequency dithering functions $h_{i,\omega}(t)$ is that they are piece-wise continuous.

A. Scheinker and M. Krstić, *Model-Free Stabilization by Extremum Seeking*,
SpringerBriefs in Control, Automation and Robotics,
DOI 10.1007/978-3-319-50790-3_8

System (8.1)–(8.3) has the following equivalent closed-loop form

$$\dot{x}(t) = f(x,t) + \sum_{i=1}^{m} b_i(x,t) h_{i,\omega}(t), \tag{8.4}$$

$$b_i(x,t) = g(x,t) k_i \left(\hat{\psi}(x,t), t \right). \tag{8.5}$$

The general result of Theorem 2.3 is that if the integrals of the functions $h_{i,\omega}(t)$ satisfy the uniform limits

$$\lim_{\omega \to \infty} H_{i,\omega}(t) = \lim_{\omega \to \infty} \int_{t_0}^{t} h_{i,\omega}(\tau) d\tau = 0, \tag{8.6}$$

and the weak limits

$$h_{i,\omega}(t) H_{j,\omega}(t) \rightharpoonup \lambda_{i,j}(t), \tag{8.7}$$

then we can also consider the average system related to (8.1)–(8.3) as follows

$$\dot{\bar{x}} = f(\bar{x},t) - \sum_{i,j=1}^{n} \lambda_{i,j}(t) \frac{\partial b_i(\bar{x},t)}{\partial \bar{x}} b_j(\bar{x},t), \quad \bar{x}(0) = x(0), \tag{8.8}$$

and for any compact set $K \subset \mathbb{R}^n$, any $t_0, T \in \mathbb{R}_{\geq 0}$, and any $\delta > 0$, there exists $\omega^\star$ such that for each $\omega > \omega^\star$, the trajectories $x(t)$ and $\bar{x}(t)$ of (8.4) and (8.8), satisfy

$$\max_{t \in [t_0, t_0+T]} \| x(t) - \bar{x}(t) \| < \delta. \tag{8.9}$$

Furthermore,

$$\lim_{t \to \infty} \| \bar{x}(t) \| = 0 \Longrightarrow \lim_{t \to \infty} \| x(t) \| < \delta.$$

In other words, uniform asymptotic stability of (8.8) over K implies the semiglobal practical uniform asymptotic stability of (8.1)–(8.3).

In this chapter, we demonstrate that the generality of Theorem 2.3 allows us to analytically study a large class of dithers, once which are not differentiable or continuous, but which are naturally implemented in most discrete time digital systems.

Consider the linear system

$$\dot{x} = a_{11} x + a_{12} y + b_1 u_x(\psi(x,y), t), \tag{8.10}$$

$$\dot{y} = a_{21} x + a_{22} y + b_2 u_y(\psi(x,y), t), \tag{8.11}$$

where $\psi(x, y)$ is an analytically unknown function to be minimized. We will consider four controllers, one of which is a perturbing signal common in digital systems, a square wave with dead time between pulses. We pick gains such that the $\lambda_{i,j}$ equal $\pm\frac{1}{2}$ for all dither choices, which results in a uniform convergence rate for all controllers.

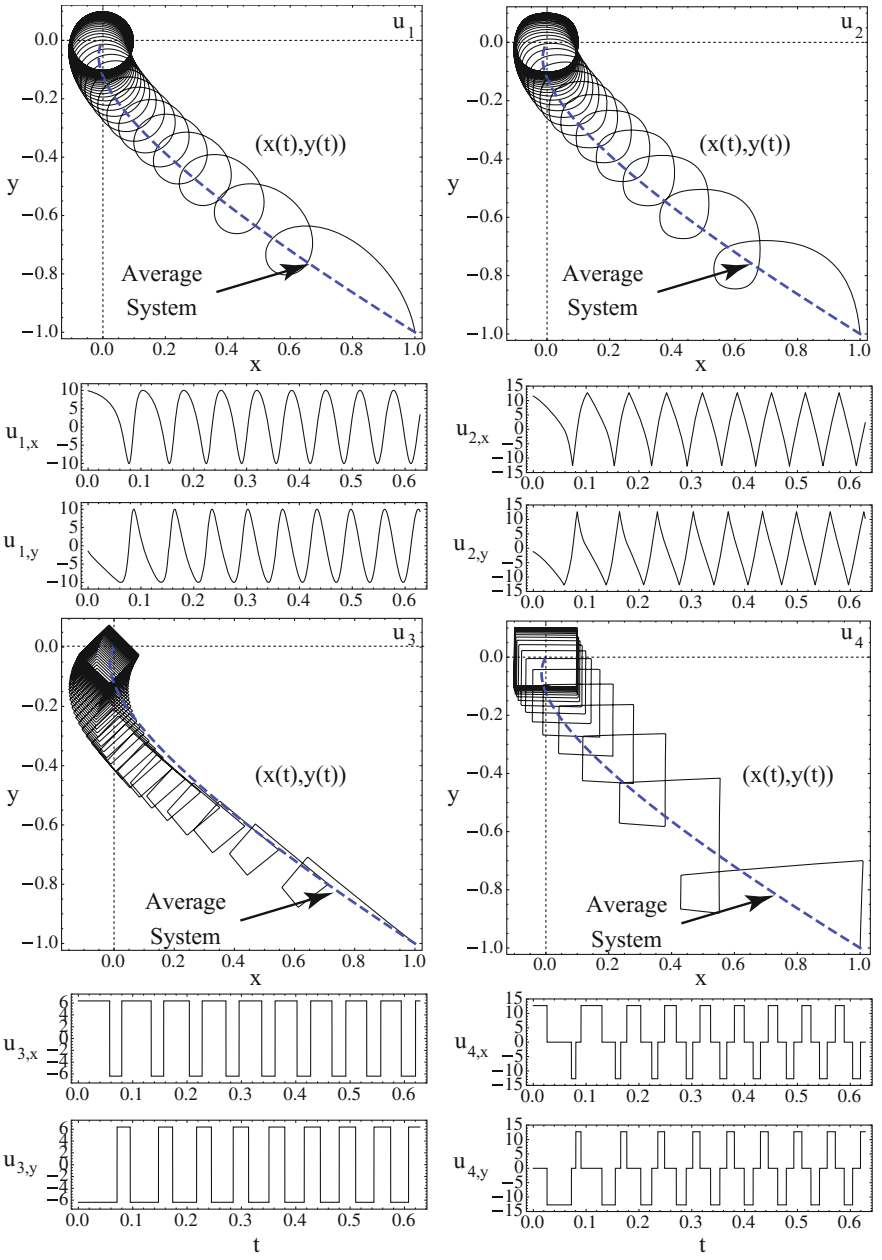

Fig. 8.1 The trajectories of system (8.10), (8.11) with controllers u_1, u_2, u_3, and u_4 are shown next to the trajectory of their common average system (8.27), (8.28). Control efforts in each case are shown for only a few of the initial oscillations in which the phase modulation is obvious

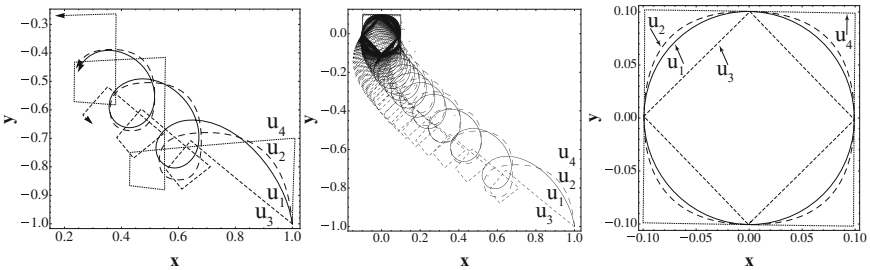

Fig. 8.2 **Left** Initial $\frac{3.5\times 2\pi}{\omega}$ seconds of the simulation of system (8.10), (8.11), shows the various trajectories evolving with similar average velocities. **Center** Evolution of the trajectories over the entire simulation time. **Right** The last $\frac{2\pi}{\omega}$ seconds of the simulation, when all trajectories have settled near the origin, but in this case are slightly tilted due to the destabilizing terms a_{ij}. The size of the oscillation about the final point of convergence is given in each case by a circle (U_1), ellipse (u_2), diamond (u_3), and square (u_4) of size $\sqrt{\frac{\alpha}{\omega}} = \frac{1}{10}$ as analytically predicted by the choice of gains

As the averaged systems for each choice of dither are equivalent, so are their domains of attraction. The amplitude of the final, steady state oscillation about the stable equilibrium of the average system, is the same $\sqrt{\frac{\alpha}{\omega}}$ for each choice of dither.

The first controller is smooth, it is given by:

$$u_{1,x} = \cos\left(\omega t + k\psi(x, y)\right)\sqrt{\alpha\omega}, \tag{8.12}$$

$$u_{1,y} = \sin\left(\omega t + k\psi(x, y)\right)\sqrt{\alpha\omega}, \tag{8.13}$$

which can be expanded via trigonometric identities as

$$u_{1,x} = \sqrt{\alpha\omega}\cos(\omega t)\cos(k\psi(x, y)) - \sqrt{\alpha\omega}\sin(\omega t)\sin(k\psi(x, y)), \tag{8.14}$$

$$u_{2,x} = \sqrt{\alpha\omega}\cos(\omega t)\sin(k\psi(x, y)) + \sqrt{\alpha\omega}\sin(\omega t)\cos(k\psi(x, y)), \tag{8.15}$$

and then the overall dynamics can be rewritten as

$$\begin{bmatrix}\dot{x}\\ \dot{y}\end{bmatrix} = \begin{bmatrix}a_{11} & a_{12}\\ a_{21} & a_{22}\end{bmatrix}\begin{bmatrix}x\\ y\end{bmatrix} + \underbrace{\sqrt{\omega}\cos(\omega t)}_{h_{1,\omega}(t)}\underbrace{\begin{bmatrix}b_1\sqrt{\alpha}\cos(k\psi(x, y))\\ b_2\sqrt{\alpha}\sin(k\psi(x, y))\end{bmatrix}}_{k_1(x,y)}$$

$$+\underbrace{\sqrt{\omega}\sin(\omega t)}_{h_{2,\omega}(t)}\underbrace{\begin{bmatrix}-b_1\sqrt{\alpha}\sin(k\psi(x, y))\\ b_2\sqrt{\alpha}\cos(k\psi(x, y))\end{bmatrix}}_{k_2(x,y)}. \tag{8.16}$$

The second controller is continuous, but not differentiable, and is implemented by the use of phase shifted triangle waves of period $\frac{2\pi}{\omega}$:

$$u_{2,x} = f_{\text{tri},1}\left(\omega t + k\psi(x, y)\right)\frac{4}{\pi}\sqrt{\alpha\omega}, \tag{8.17}$$

$$u_{2,y} = f_{\text{tri},2}\left(\omega t + k\psi(x,y)\right)\frac{4}{\pi}\sqrt{\alpha\omega}, \tag{8.18}$$

where $f_{\text{tri},1}(t)$ is in phase with $\cos(t)$ and $f_{\text{tri},2}(t)$ is in phase with $\sin(t)$. One particular, analytical form of such controllers is

$$u_{2,x} = \left(1 - 2\left\| f_{\text{tri}}\left[\cos\left(\omega\frac{t}{2} + k\frac{\psi(x,y)}{2}\right)\right]\right\|\right)\frac{4}{\pi}\sqrt{\alpha\omega}, \tag{8.19}$$

$$u_{2,y} = f_{\text{tri}}\left[\cos\left(\omega t + k\psi(x,y)\right)\right]\frac{4}{\pi}\sqrt{\alpha\omega}. \tag{8.20}$$

In this case the λ_{ij} are determined by integrals of triangle waves.

The third controller is given by the discontinuous square wave of period $\frac{2\pi}{\omega}$:

$$u_{3,x} = f_{\text{sqr},1}\left(\omega t + k\psi(x,y)\right)\frac{2}{\pi}\sqrt{\alpha\omega}, \tag{8.21}$$

$$u_{3,y} = f_{\text{sqr},2}\left(\omega t + k\psi(x,y)\right)\frac{2}{\pi}\sqrt{\alpha\omega}, \tag{8.22}$$

where $f_{\text{sqr},1}(t)$ is in phase with $\cos(t)$ and $f_{\text{sqr},2}(t)$ is in phase with $\sin(t)$. Which can be expressed as

$$u_{3,x} = \operatorname{sgn}\left[\cos\left(\omega t + k\psi(x,y)\right)\right]\frac{2}{\pi}\sqrt{\alpha\omega}, \tag{8.23}$$

$$u_{3,y} = \operatorname{sgn}\left[\sin\left(\omega t + k\psi(x,y)\right)\right]\frac{2}{\pi}\sqrt{\alpha\omega}. \tag{8.24}$$

In this case the λ_{ij} are determined by integrals of sign functions.

The last controller is the most realistic for digital implementation. Is is given by a square wave of period $\frac{2\pi}{\omega}$ with dead time:

$$u_{4,x} = f_{\text{sqrd},1}\left(\omega t + k\psi(x,y)\right)\frac{2}{\pi}\sqrt{\alpha\omega}, \tag{8.25}$$

$$u_{4,y} = f_{\text{sqrd},1}\left(\omega t + k\psi(x,y)\right)\frac{2}{\pi}\sqrt{\alpha\omega}, \tag{8.26}$$

where $f_{\text{sqrd},1}(t)$ is in phase with $\cos(t)$ and $f_{\text{sqrd},2}(t)$ is in phase with $\sin(t)$. This controller can be expressed as

$$u_{4,x} = \left(\operatorname{sgn}\left[\cos\left(\omega t + k\psi(x,y) + \frac{\pi}{4}\right)\right] + \operatorname{sgn}\left[\sin\left(\omega t + k\psi(x,y) + \frac{\pi}{4}\right)\right]\right)\frac{2}{\pi}\sqrt{\alpha\omega},$$

$$u_{4,y} = \left(\operatorname{sgn}\left[\cos\left(\omega t + k\psi(x,y) - \frac{\pi}{4}\right)\right] + \operatorname{sgn}\left[\sin\left(\omega t + k\psi(x,y) - \frac{\pi}{4}\right)\right]\right)\frac{2}{\pi}\sqrt{\alpha\omega}.$$

In this case the λ_{ij} are determined by integrals of sign functions.

For all of the controllers above, we use the same function, $\psi(x,y) = x^2 + y^2$. For each fixed i, the controllers $u_{i,x}$ and $u_{i,y}$ are orthogonal and their gains have been

chosen such that $\lambda_{i_x,i_y}(t) \equiv -\frac{1}{2}$, $\lambda_{i_y,i_x}(t) \equiv \frac{1}{2}$. Thus, the same averaged system is attained for each i:

$$\dot{\bar{x}} = a_{11}\bar{x} + a_{12}\bar{y} - b_1^2 k\alpha\bar{x}, \tag{8.27}$$
$$\dot{\bar{y}} = a_{21}\bar{x} + a_{22}\bar{y} - b_2^2 k\alpha\bar{y}. \tag{8.28}$$

We simulate how the controllers stabilize the system (8.10), (8.11) with $b_i = 1$, $a_{11} = 1$, $a_{12} = 0.75$, $a_{21} = 0.5$, and $a_{22} = 2$. With these constants, the $\{a_{ij}\}$ matrix has positive real eigenvalues 2.29 and 0.71 and the system is open loop unstable. We perform the simulation with $\omega = 100$, $k = 4$, and $\alpha = 1$. The results are in Figs. 8.1 and 8.2.

Remark 8.1 In order to apply Theorem 1 to the examples above, such as for the square wave of period $\frac{2\pi}{\omega}$, we must expand them as their Fourier series:

$$\begin{aligned} u_{\text{sqr}}(\omega t + \psi(x,t)) &= \frac{4}{\pi}\sum_{n \text{ odd}} \frac{1}{n}\sin\left(n\omega t + n\psi(x,t)\right) \\ &= \frac{4}{\pi}\sum_{n \text{ odd}} \frac{1}{n}\sin\left(n\omega t\right)\cos\left(n\psi(x,t)\right) \\ &\quad + \frac{4}{\pi}\sum_{n \text{ odd}} \frac{1}{n}\cos\left(n\omega t\right)\sin\left(n\psi(x,t)\right). \end{aligned}$$

A less elegant, but easier to study and on-average equivalent example of such a discontinuous bounded controller is

$$u = \sqrt{\alpha\omega}u_{\text{sqr},1}(\omega t)\cos(k\psi(x,t)) - \sqrt{\alpha\omega}u_{\text{sqr},2}(\omega t)\sin(k\psi(x,t)), \tag{8.29}$$

where

$$u_{\text{sqr},1}(\omega t) = \text{sgn}\left[\cos(\omega t)\right], \quad u_{\text{sqr},2}(\omega t) = \text{sgn}\left[\sin(\omega t)\right]. \tag{8.30}$$

Although we have written $u_{\text{sqr}}(\omega t) = \text{sgn}\left[\cos(\omega t)\right]$ so that it is easy for the reader to interpret the values of the function, the digital implementation of such a function does not require the calculation of $\cos(\omega t)$ and is instead accomplished by using a combination of a resetting ramp with slope $\frac{\omega}{2\pi}$ and the $\text{sgn}(\cdot)$ function, both of which are trivially implemented with minimal resources in fixed-integer length digital logic such as that used in high speed field programmable gate arrays (FPGA), such as:

$$u_{\text{sqr}}(\omega t) = \text{sgn}\left[\text{ramp}\left(\frac{\omega}{2\pi}t\right) - \frac{1}{2}\right], \tag{8.31}$$

where $\text{ramp}(t)$ ramps from 0 up to 1 in 1 s, resets to 0, and repeats.

8.2 Application to Inverter Switching Control

We consider a class of systems in which discontinuous, high frequency switching control is necessary by design and for which high frequency extremum seeking is especially well suited: DC to AC voltage inverters. Inverters are the basic building blocks of many electrical systems. Control methods for inverters include the application of classical PID, sliding mode, model predictive control methods [1, 4, 21, 26, 27], and continue to be an active area of research in power electronics. We present a simple ESCO approach which can accommodate uncertainties in the voltage input into the system and unpredictable energy use which results in time-variation of the load. This is especially important for the uncertain/time-varying characteristics of renewable energy sources such as wind and solar due to unpredictable weather.

A typical DC to AC inverter is shown in Fig. 8.3. A DC voltage source is connected to ground across an H-bridge and the load. The H-bridge functions by closing alternating pairs (A_1 and A_2 or B_1 and B_2) of metal-oxide-semiconductor field-effect transistors (MOSFETS), transistors designed for high frequency switching. As alternate pairs of MOSFETS are activated the resulting voltage across the circuit, V_{in}, switches from positive to negative and back. Currently available power electronics MOSFETS are capable of holding off tens of thousands of volts and switching within hundreds of nanoseconds. For our application, the switching is performed at ~80 kHz and 709 V. The output of the switching H-Bridge is followed by a simple LC filter and finally an uncertain, time-varying load, $R(t)$, across which the goal is to maintain a constant amplitude sinusoidal AC voltage.

The state equations of the circuit are $V_{in} = L\frac{di_L}{dt} + V_R, i_L = i_C + i_R, i_C = C\frac{dV_R}{dt}$, $i_R = \frac{V_R}{R}$, $V_{in} = u(t) \times V_{DC}(t)$, where i_L, i_C, and i_R are the currents through the inductor, capacitor, and resistor, respectively, and $u(t)$ is the controlled H-bridge switching signal. The system dynamics can be summarized as

$$\ddot{V}_R(t) = -\frac{V_R(t)}{LC} - \frac{\dot{V}_R(t)}{R(t)C} - \frac{V_{DC}(t)}{LC}u(t). \tag{8.32}$$

Defining the error variables $e_1 = V_R - V_{\text{ref}}$, $\dot{e}_1 = e_2$ and choosing the control law

$$u = \sqrt{\alpha\omega}\, f_{\text{sqrd}}\left[\omega t + k(J(e_1, e_2) + n(t))\right], \tag{8.33}$$

where $J(e_1, e_2) = (e_1 + k_2 e_2)^2$, whose minimization, is equivalent to trajectory tracking and $n(t)$ is noise. The closed loop dynamics are then

$$\dot{e}_1 = e_2, \tag{8.34}$$

$$\dot{e}_2 = -\frac{e_1}{LC} - \frac{e_2}{RC} - \frac{V_{\text{ref}}}{LC} - \frac{\dot{V}_{\text{ref}}}{RC} + \ddot{V}_{\text{ref}} - \frac{V_{DC}(t)}{LC}\sqrt{\alpha\omega}\, f_{\text{sqrd}}\left[\omega t + kJ\,(e_1, e_2) + kn(t)\right]. \tag{8.35}$$

Theorem 2.3 implies that the averaged dynamics are:

$$\dot{\bar{e}}_1 = \bar{e}_2, \tag{8.36}$$

$$\dot{\bar{e}}_2 = -\frac{\bar{e}_1}{LC} - \frac{\bar{e}_2}{RC} - \frac{V_{\text{ref}}}{LC} - \frac{\dot{V}_{\text{ref}}}{RC} + \ddot{V}_{\text{ref}} - \left(\frac{V_{DC}(t)}{LC}\right)^2 k\alpha k_2 \left(\bar{e}_1 + k_2 \bar{e}_2\right). \tag{8.37}$$

For any $M > 0$, we can guarantee the stabilization and convergence to the origin of system (8.36), (8.37) over the compact set $e_1, r, e_2, \dot{r}, \ddot{r} \in K = \{x \in \mathbb{R} \text{ s.t. } |x| < M\}$. We do so with the Lyapunov function $V_L = \frac{e_1^2}{2} + \frac{(e_1 + k_2 e_2)^2}{2}$ and gains k, k_2 and α such that for all $e_1, r, e_2, \dot{r}, \ddot{r} \in K$, $\dot{V}_L < 0$.

Remark 8.2 In this application, we have no choice on the magnitude of the input voltage, the only signal that the controller, u, can send is to alternate between ± 1, while the magnitude of the actual voltage input to the system is fixed by $V_{\text{DC}}(t)$:

$$V_{\text{in}}(t) = V_{\text{DC}}(t)u(t) = V_{\text{DC}}(t)\sqrt{\alpha\omega}\, f_{\text{sqrd}}\left(\omega t + \ldots\right). \tag{8.38}$$

Therefore we first choose $\omega > 0$ and we are then forced to choose $\alpha = \frac{1}{\omega}$, so that the input voltage of the system satisfies the constraint:

$$|V_{\text{in}}(t)| = \left|V_{\text{DC}}(t)\sqrt{\alpha\omega}\, f_{\text{sqrd}}\left(\omega t + \ldots\right)\right| = \left|V_{\text{DC}}(t)\, f_{\text{sqrd}}\left(\omega t + \ldots\right)\right| \leq |V_{\text{DC}}(t)|.$$

This type of constraint is exactly what the bounded form of extremum seeking presented above is especially well suited for since unknowns enter the controller dynamics as the arguments of a-priori chosen, known, bounded functions.

We demonstrate this controller by simulating a system with a time-varying resistance

$$R(t) = 50\left(1 + \frac{4}{5}\sin\left(2\pi \times 30t\right)\right),$$

and a two time-scale varying input voltage

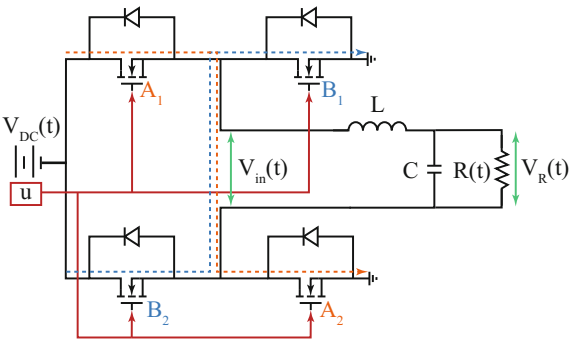

Fig. 8.3 The timing of the switching of the H-bridge is controlled by the control signal, $u(t)$, which closes the MOSFETS in alternating pairs, A_1 and A_2 or B_1 and B_2, causing the current to flow clockwise or counterclockwise through the circuit, respectively

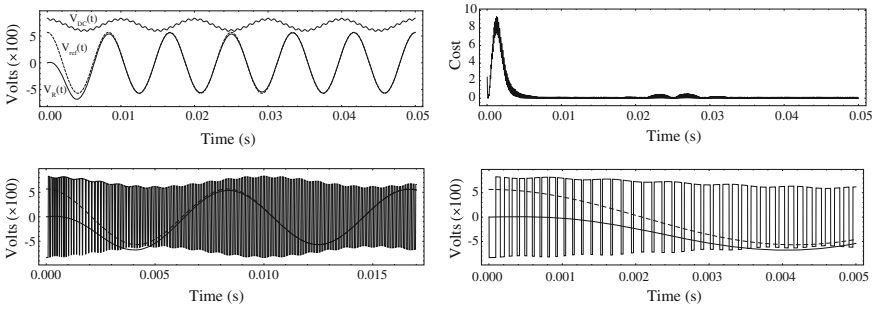

Fig. 8.4 The system is shown to closely track the desired output voltage trajectory despite time variation of both the DC voltage and the output load. The entire 0.05 s simulation as well as detailed views of certain time segments are shown

$$V_{\mathrm{DC}}(t) = 709 + 106\cos(2\pi \times 100t) + 18\cos(2\pi \times 1200t).$$

The system parameters are

$$L = 3.5\,\mathrm{mH},\ C = 500\,\mu\mathrm{F},\ V_{\mathrm{DC}} \equiv 709\,\mathrm{V},\quad V_{\mathrm{ref}}(t) = 570\cos(2\pi \times 120t)\ \mathrm{V}.$$

Simulation results with $\omega = 2\pi \times 8000, \alpha = \frac{1}{\omega}, k = 35 \times 10^{-6}$, and $k_2 = 7.5 \times 10^{-3}$ are shown in Fig. 8.4.

Chapter 9
Application Study: Particle Accelerator Tuning

It is rarely possible to build exact, deterministic input to output models for complex physical systems. It is especially difficult when the behavior of the system is influenced by many coupled parameters. Some common methods for dealing with large complex systems are genetic algorithm (GA) and multi-objective genetic algorithm (MOGA) based multidimensional, nonlinear optimization schemes. Although such methods do an exhaustive search of parameter space and can provide globally optimal designs, they are limited in being model-dependent. For example, MOGAs and GAs have been used to successfully optimize many aspects of particle accelerators, such as magnet and radio frequency (RF) cavity design [56], photoinjector design [9], damping ring design [34], storage ring dynamics [11], global optimization of a lattice [154], neutrino factory design [120], simultaneous optimization of beam emittance and dynamic aperture [38], and free electron laser linac drivers [8]. A thorough review of GA for accelerator physics applications is given in [60].

However, after any large system design has been finalized and the machine has been constructed, one often encounters time varying and nonlinear coupling effects between the imperfectly manufactured and misaligned/unknown orientation components. In theory, accelerator design takes a certain level of uncertainty into account. In practice however, most large systems, such as, for example, particle accelerators, require post-manufacture and post-installation tuning. This is especially the case for facilities with limited real-time diagnostics and noise measurement. In this case components may have to be retuned after each shutdown or change in operating conditions. Effects such as unknown hysteresis curves and time varying component thermal cycling also add to system uncertainty.

Extremum seeking, with its ability to handle open-loop unstable, time-varying, nonlinear systems, is therefore an ideal candidate for online persistent control and optimization of complex, many parameter, large systems.

In this chapter we present the results of a detailed simulation study of applying ES for the optimal tuning of a particle accelerator with time-varying components and time-varying proton beam properties. This large, nonlinear, complex system is ideal for demonstrating how powerful this ES approach is. We also provide experimental results of applying ES to actively tune the resonant frequency of an RF cavity based

A. Scheinker and M. Krstić, *Model-Free Stabilization by Extremum Seeking*,
SpringerBriefs in Control, Automation and Robotics,
DOI 10.1007/978-3-319-50790-3_9

only on reflected power measurements. We begin with a few guidelines for the digital implementation of ES.

9.1 Guidelines for Digital Implementation

9.1.1 Cost and Constraints

The first step in applying ES to an actual system is to choose tunable machine parameters, $p = (p_1, \ldots, p_m)$ and a cost function to be minimized,

$$C = C(p_1(t), \ldots, p_m(t), t).$$

Next, constraints for all parameters are chosen

$$p_{\max} = \left(p_{1,\max}, \ldots, p_{m,\max}\right), \quad p_{\min} = \left(p_{1,\min}, \ldots, p_{m,\min}\right).$$

Implementing initial parameter settings $p(1)$, which are chosen based on the physics model and numerical methods, allows one to calculate $C(p(1))$. The iterative update scheme is then:

$$p_i(n+1) = p_i(n) + \Delta\sqrt{\alpha\omega_i}\cos\left(\omega_i n\Delta + kC(p(n))\right), \tag{9.1}$$

which is based on the finite difference approximation of the derivative:

$$\frac{p_i(t+\Delta) - p_i(t)}{\Delta} \approx \frac{\partial p_i}{\partial t} = \sqrt{\alpha\omega_i}\cos\left(\omega_i t + kC(p(t), t)\right), \tag{9.2}$$

which, according the Theorem 6.1 will drive the system towards a minimum of C. The constraints are implemented by checking the updated parameters at each step and confining them to their bounds if necessary:

$$p_i(n+1) > p_{i,\max} \implies p_i(n+1) = p_{i,\max}, \; p_i(n+1) < p_{i,\min}, \implies p_i(n+1) = p_{i,\min}.$$

9.1.2 Choice of ω, and Δ

It is important that $\omega_i \gg kC$, so that the adaptive scheme is operating on a faster time scale then and able to adapt to time variation of the cost function. Because ES depends on distinguishing between different frequency components of the cost, Δ should be chosen in the range of:

$$\Delta \leq \frac{2\pi}{20 \times \max\{\omega_i\}}, \tag{9.3}$$

ensuring that at least 20 iterations ($10\times$ the Nyquist sampling rate) are required to perform one complete cosine oscillation in the iterative scheme (9.1). Choosing smaller values of Δ results in smoother parameter oscillation and more iterative steps required for convergence, larger values of Δ speed up the convergence, but may destabilize the overall scheme.

According to Theorem 6.1, the only requirement on the choices of ω_i is that they are big enough and distinct, but in practice, the more harmonically independent they are (such as $\omega_i \neq 2\omega_j$ for all $i \neq j$) the better. The sensitivity to frequency independence is different for every system and depends on the coupling between different components. One simple method is to choose a scaling factor, ω_0, and

$$\omega_i = \omega_0 r_i, \tag{9.4}$$

where the values r_i are distinct.

9.1.3 Choice of k and α

The rate of convergence is proportional to the product $k\alpha$, increasing either k or α speeds up convergence, as long as they are not too big relative to the value of ω_0, so that the finite difference is an accurate approximation of the derivative. If, after ω_0 has been chosen, the convergence is too slow, or if a local minimum is suspected, k or α may be increased, with the possible need to increase ω_0 as well. The vector $p(t)$ is moving through the parameter space $\mathbb{R}^m$ in ellipses with approximate major axes of magnitude $\sqrt{\frac{\alpha}{\omega}}$, increasing α causes larger steady state parameter oscillations, which is not a problem if the adaptation is turned off following successful convergence.

9.1.4 Digital Resolution

Although the analytic form of $C(n)$ may be unknown, at each iteration the parameters are perturbed by a quantities with known bounds:

$$0 \leq \left|\Delta\sqrt{\alpha\omega_i}\cos\left(\omega_i n\Delta + kC(p(n))\right)\right| \leq \Delta\sqrt{\alpha\omega_{\max}}. \tag{9.5}$$

For a system with n_b bits of resolution, and maximum bounds $\pm M_i$ on the parameter settings, if Δ, α, and ω_i are chosen such that $\Delta\sqrt{\alpha\omega_i} \geq N \times \frac{M_i}{2^{n_b}}$, then, as cos() varies between 0 and 1, it is possible for the parameter value to take N discrete steps of minimum resolution $\frac{M_i}{2^{n_b}}$.

9.1.5 Normalization of Parameters

Different parameters p_i may require individual values of k_i and α_i, in which case normalizing the parameters to within $[-1, 1]$ bounds may be useful. For example, at each step n, one may compute the cost $C(n)$ based on parameter settings $p(n)$, then translate into the scaled parameters $p_s(n)$:

$$p_{s,i}(n) = \frac{2\left(p_i(n) - C_{p,i}\right)}{D_{p,i}}, \tag{9.6}$$

where $C_{p,i} = \frac{p_{i,\max}+p_{i,\min}}{2}$ and $D_{p,i} = p_{i,\max} - p_{i,\min}$, bounding each parameter within $[-1, 1]$. We then perform the update

$$p_{s,i}(n+1) = p_{s,i}(n) + \Delta\sqrt{\alpha_i \omega_i}\cos\left(\omega_i n\Delta + k_i C(\mathbf{p}(n))\right), \tag{9.7}$$

force the scaled parameters to satisfy the constraints -1 and 1, and transform back into un-scaled parameter values in order to calculate the cost for the next iteration:

$$p_i(n+1) = \frac{p_{s,i}(n+1)D_{p,i}}{2} + C_{p,i}. \tag{9.8}$$

Remark 9.1 In the case of different parameters having vastly different response characteristics and sensitivities (such as when tuning both RF and magnet settings in the same scheme), the choices of k and α may be specified differently for each component p_i, as k_i and α_i, without change to the above analysis.

9.2 Automatic Particle Accelerator Tuning: 22 Quadrupole Magnets and 2 Buncher Cavities

A particular problem faced by many accelerator systems is the arbitrary phase shift of the RF systems, a time-varying uncertainty, requiring time consuming tuning such as phase scans. The method presented here is demonstrated to automatically adapt for time varying properties, such as phase shift.

In this section we present simulation results of using the ES scheme to tune up the twenty two quadrupole magnets and two buncher cavities in the Los Alamos linear accelerator H^+ transport region, a simplified schematic of which is shown in Fig. 9.1. The simulations were done using a GPU-accelerated online beam dynamics simulator, which is being developed to predict beam properties along the linac using real time machine parameters. It can serve as a virtual beam experiment environment and contribute to the cost being minimized by the ES optimizer, by providing pseudo realtime estimates of beam sizes and current information in parts of the machine where diagnostics are not available. Currently being demonstrated on the LANSCE

low energy beam transport (LEBT) and drift tube linac (DTL), simulating a bunch of 32 K macro particles through the LEBT or DTL takes fractions of a second, which is 40 times faster than the simple CPU version of the code.

9.2.1 Magnet Tuning for Beam Transport

In a first, simple demonstration of the technique, we perform a simulation of only the LEBT, with all initial magnet current set points set to 0 A, and allowed to tune up based purely on the ES scheme as described above, in which the four costs (j = 1,2,3,4) being minimized $C_j = \left(I_j - 0.013\right)^2$, were the square of the difference between initial beam current 0.013 A and total current making it through various parts of the transport region, at which diagnostics are available. With reference to Fig. 9.1, the current is sampled at four locations, I_1, following Q_6, I_2 following Q_{10}, I_3 following Q_{18} and I_4 at the end of the transport region. The magnets (i = 1,...,22) were then updated according to:

$$Q_i(n+1) = Q_i(n) + \sqrt{\alpha\omega_i}\,\Delta\cos\left(\omega_i\,\Delta n + k S_i(n)\right), \tag{9.9}$$

where $S_i = C_4 + C_3 + C_2 + C_1$ for $Q_1 - Q_6$, $S_i = C_4 + C_3 + C_2$ for $Q_7 - Q_{10}$, $S_i = C_4 + C_3$ for $Q_{11} - Q_{18}$ and $S_i = C_4$ for $Q_{19} - Q_{22}$, so that magnets only saw costs which they were able to influence. For the tuning parameters, we chose k = 2,50,000, so that the amplified costs kS_j in (9.9) took values between 0 and 300. The ω_i were chosen as $\omega_0 r_i$, with $\omega_0 = 1000$ and r_i uniformly distributed between 2.5 and 3.7, $\Delta = \frac{2\pi}{20\omega_{22}}$, and $\alpha = 15$. With these values, $\frac{\omega_{\min}}{kC_{\max}} > 20$.

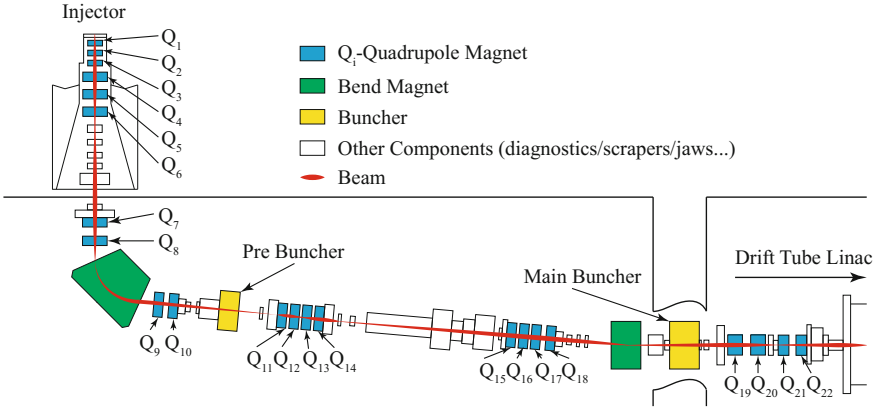

Fig. 9.1 Simplified schematic of the LANSCE H^+ injector and transport region

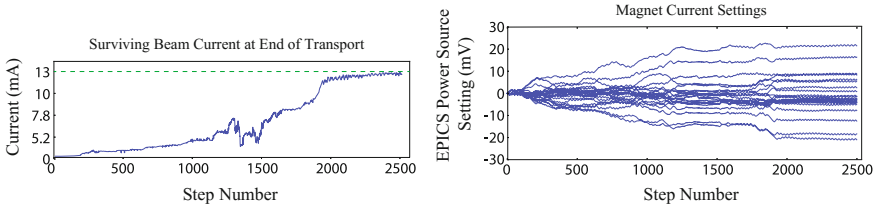

Fig. 9.2 *Left* The surviving current at the end of the beam transport over 2500 iteration steps is shown for an initial beam current of 13 mA. *Right* Evolution of the magnet current settings to the magnets over 2500 iteration steps

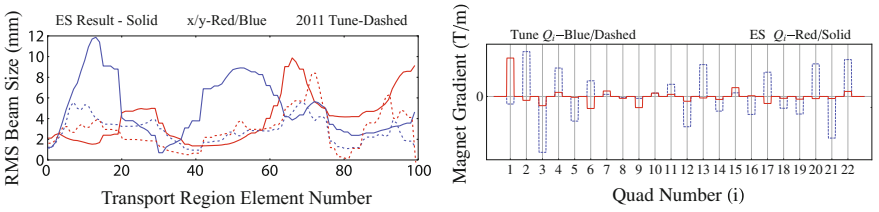

Fig. 9.3 *Left* RMS beam size at the end of the iterative tuning scheme. *Right* Magnet settings at the end of the iterative tuning scheme compared to 2011 tune up settings

Figure 9.2 shows the evolution of the surviving beam current at the end of the transport region during the ES tuning scheme and the evolution of the magnet current inputs. Figure 9.3 shows the RMS beam size through various parts of the transport region at the end of ES tuning and compares the ES found magnet settings to that of the tune up in 2011.

This example demonstrates some of the strengths and limitations of the scheme, and the importance of cost function choice. Although the cost has been minimized and almost all current is making it to the end of the transport region, the beam is beginning to diverge and in this form would not be matched to the DTL following the transport region. In practice it is of course better to start with physics-model based initial parameters, this simulation was conducted starting with all magnet settings at zero in order to fairly demonstrate the model-independent abilities of the ES scheme. The next simulations start with the 2011 tune up for the magnet settings and use current monitors following two tanks of the DTL, in which case surviving beam corresponds with well-matched beam.

9.2.2 Magnet and RF Buncher Cavity Tuning

To demonstrate the use of this scheme for fine tuning of machine settings, we used machine settings found during the 2011 tune up procedure, but with a slightly different beam and incorrectly phased buncher cavities. The magnets were initialized

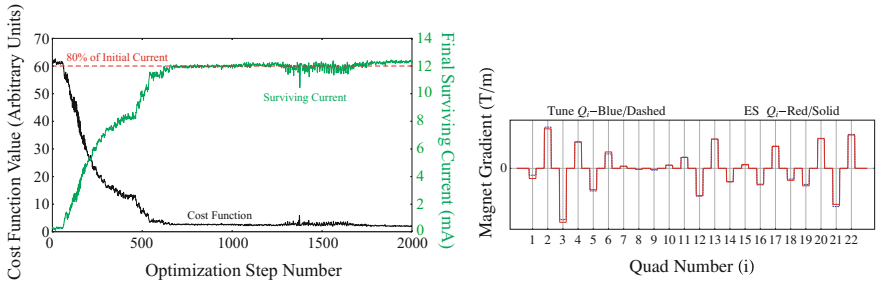

Fig. 9.4 *Left* The surviving current at the end of the beam transport over 2000 iteration steps is shown for an initial beam current of 15 mA. *Right* New magnet settings after optimization

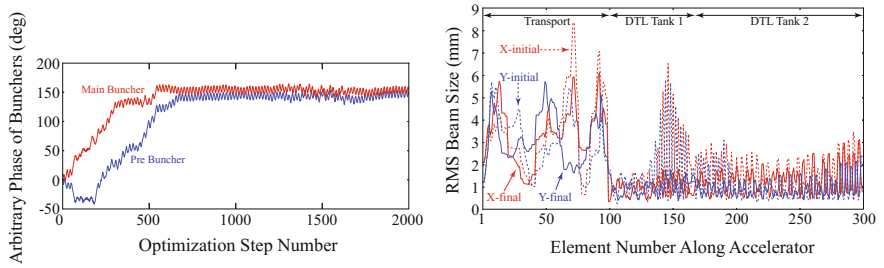

Fig. 9.5 *Left* Evolution of buncher cavity phase settings over 2000 iteration steps. *Right* Comparison of RMS beam size along the accelerator for the 2011 tune-based magnet settings and arbitrary phase *(dashed)* with RMS beam size following ES tune *(solid)*

to the values recorded from one of the 2011 machine turn on tuning periods. We set the phase settings for the buncher and pre-buncher to zero, which typically must be re-tuned at each turn on, by a phase scan, to take care of arbitrary phase shift.

We used only the surviving current at the end of the second tank of the drift tube linac to create our cost, our tuning procedure for the parameters was:

$$Q_i(n+1) = Q_i(n) + \sqrt{\alpha_i \omega_i}\,\Delta \cos\left(\omega_i n \Delta + kC(n)\right), \tag{9.10}$$

where $\alpha_i = \alpha_m$ for the magnets and $\alpha_i = \alpha_b$ for the buncher phases. In both cases $C(n) = (I_{\text{end}} - 15\,\text{mA})^2$. For the tuning parameters, we chose $k = 6{,}05{,}000$, $\alpha_m = 25$, $\alpha_b = 550$. The ω_i were chosen as $\omega_0 r_i$, with $\omega_0 = 2000$ and r_i uniformly distributed between 2.5 and 4.3, $\Delta = \frac{2\pi}{20\omega_{24}}$. With these values, $\frac{\omega_{\min}}{kC_{\max}} > 35$.

With an initial beam current of 15 mA, the typical surviving current after machine tune up is roughly 80 % or 12 mA. After 2000 simultaneous iterations on these 24 parameters (22 quads, 2 buncher phases), the surviving current at the end of Tank 2 was 12.25 mA. The results of the optimization procedure are shown in Figs. 9.4, 9.5 and 9.6. From Figs. 9.4 and 9.5 we see that only minor adjustments are made to magnet settings compared to the RF phases. Figure 9.5 shows that the transverse beam

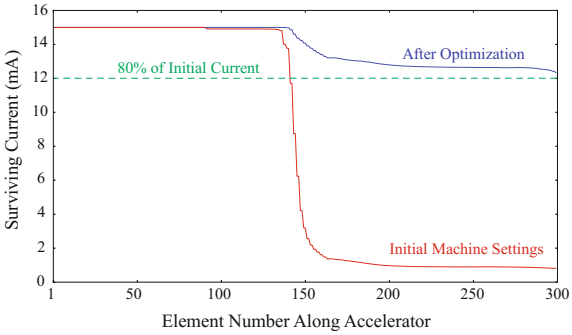

Fig. 9.6 Surviving beam current along the machine with 2011 tune-based magnet settings and arbitrary phase *(red)* and following ES tune *(blue)*

size has further focused throughout the transport region and the transverse match to the DTL has slightly improved. Figure 9.6 compares surviving beam current at the end of Tank 2 of the DTL before and after tuning.

9.2.3 Adaptation to Time Varying Phase Delay and Beam Characteristics

In order to demonstrate the adaptive tuning abilities of the scheme, we started with matched beam settings and varied both the characteristics of the input beam and added a time-varying phase drift to each buncher cavity.

Figure 9.7 shows the initial and final beam properties at the entrance to the transport region, during which ES adaptive tuning maintains beam focus and matching. Figure 9.8 shows the phase shift of the bunchers with and without tuning. These changes took place starting at step 1000 and finished at step 19, 000, with beam properties staying constant before and after the interval. Also, during this beam changing process, the phase of the first buncher was made to drift by 30° and that of the second by 35°, as seen in Fig. 9.8. The drift of beam characteristics and buncher phase shifts took place over 18000 time steps, which for a conservative magnet/phase update rate of 1 Hz translates into drastically changing accelerator and beam properties over the course of just 5 h. All tuning parameters were maintained exactly the same as in the previous example.

Figure 9.8 shows the evolution of the magnet gradients throughout the process, Fig. 9.9 shows the new final magnet settings, and Fig. 9.9 compares the initial and final beam profiles. In Fig. 9.10 we see that adaptive ES tuning is able to maintain $\sim$ 12 mA of surviving beam during the time-varying beam and phase, whereas almost all of the beam is lost without tuning.

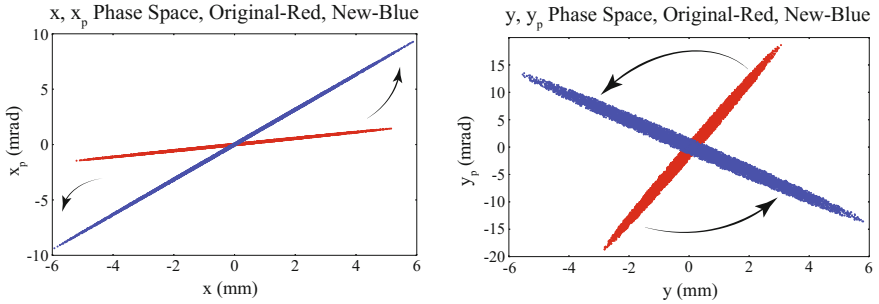

Fig. 9.7 The input beam was gradually changed over 18, 000 time steps

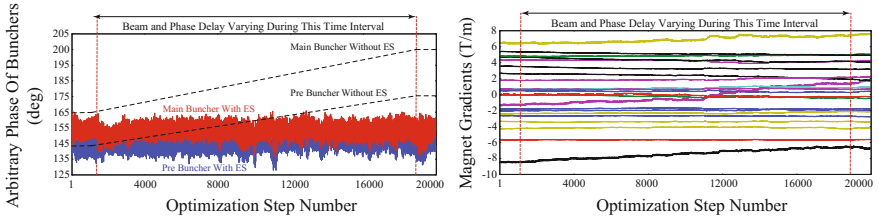

Fig. 9.8 *Left* Evolution of the buncher phase settings, during, and after variation of beam and phase delay parameters. *Right* Evolution of the magnet gradients before, during, and after variation of beam and phase delay parameters

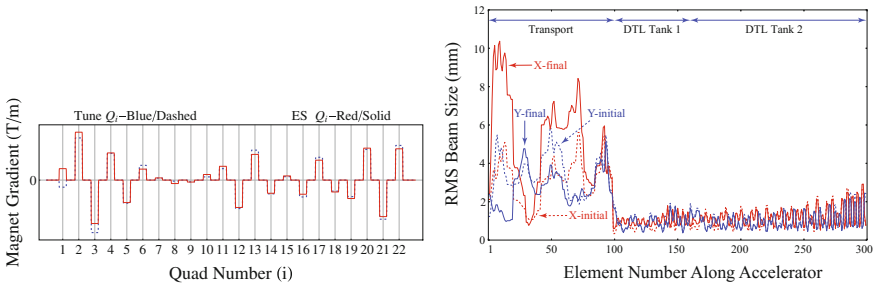

Fig. 9.9 *Left* New magnet settings after optimization. *Right* Comparison of RMS beam size along the accelerator for the 2011 tune-based magnet settings *(dashed)* and after the beam initial conditions have changed and ES tuning has re-focused and matched the beam *(solid)*

9.3 In-Hardware Applicaiton: RF Buncher Cavity Tuning

In this chapter, we present the results of applying ESCO for maintaining RF cavity resonant frequencies at their design values despite unknown external disturbances, such as temperature changes which perturb the resonant frequency of a cavity by changing its geometry [136]. The particles in modern particle accelerators acquire kinetic

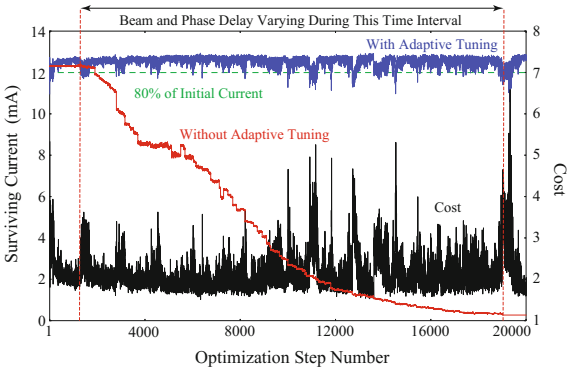

Fig. 9.10 Surviving beam current at the end of the second DTL tank with and without adaptive ES tuning. The cost evolution during the tuning process is also shown

energies of tens to hundreds of gigaelectronvolts (GeV), which require accelerating gradients of tens of megavolts (MV) per meter in order to build machines of reasonable size. Currently, the only efficient way to develop MV gradients while avoiding electrical breakdown is to use resonant radio frequency (RF) cavities. The resonant frequencies of such cavities depend on their geometries. The proposed method automatically compensates for time-varying drifts of cavity resonance despite time varying drifts of the entire RF system, such as arbitrary phase shifts caused by cable length changes, which typically result in periodic manual re-calibration for standard phase-information-dependent resonance control systems to function.

The ES algorithm works by moving a mechanical slug, which changes the resonant frequency of an RF cavity, in such a way that the reflected power from the RF cavity is continuously minimized. By minimizing reflected power, the algorithm is independent of RF field phase measurements. A similar model-independent approach has been applied to a superconducting cavity setup in [137], which requires controlling piezo actuators to compensate for fast phase shifts due to Lorenz force detuning [7, 43, 78, 92, 140].

9.3.1 RF Cavity Background

The resonant mode most useful for acceleration in a right cylindrical conducting cavity has electric and magnetic field components of the form

$$E(r,t) = E_0 J_0\left(\frac{2.405r}{R_c}\right) e^{i\omega_0 t}\hat{z} = E_z(r)e^{i\omega_0 t}\hat{z},$$

$$B(r,t) = -i\sqrt{\frac{\varepsilon}{\mu}} J_1\left(\frac{2.405r}{R_c}\right) e^{i\omega_0 t}\hat{\varphi} = B_\varphi(r)e^{i\omega_0 t}\hat{\varphi},$$

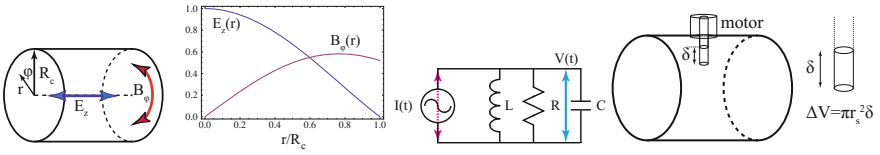

Fig. 9.11 *Left to right* Right cylindrical RF cavity, field strength as a function of distance from cavity center, circuit model of RF cavity mode, and slug tuner setup for resonance control

where J_0 and J_1 are Bessel functions of the first kind with zeroth and first order [64]. The resonant frequency is given by

$$\omega_0 = \frac{2.405c}{R_c}, \tag{9.11}$$

where c is the speed of light and R_c is the radius of the cavity. In this accelerating mode, the electric field has only a z-component, down the axis of the cavity, and is therefore useful for acceleration, while the magnetic field has only azimuthal component and is zero on axis, as shown in Fig. 9.11. For example, the resonant cavities used at the Los Alamos National Laboratory linear particle accelerator have 201.25 MHz RF fields and radii of approximately 0.57 m.

The geometry of an RF cavity is constantly perturbed by, amongst other things, deformations due to temperature change. The high power (megawatts) RF fields in the cavities are sustained by currents in the cavity walls, which, through resistive losses, deposit large amounts of energy into the cavity walls. As a cavity cools or heats up, it's geometry changes, which causes a change in the resonant frequency. The temperature of the cavities must therefore be controlled both to prevent melting, and to sustain a precise, designed resonant frequency, so that the RF source providing power to the cavity is well matched. Another source of temperature change is the time-varying environment in which the cavities are typically located, which undergo temperature fluctuations.

Equation (9.11) is accurate in the case of a perfect cylindrical cavity. In practice, cavity geometries are more complicated, and temperature variations in the cavity walls are uneven, resulting in a non-trivial geometric deformations and complicated resonance shifts. According to the Slater perturbation theorem [141], a small shift in resonance frequency is introduced by removing or adding a small volume Δ V from the cavity volume V, according to

$$\Delta\omega_0 = \omega_0 \frac{\int_{\Delta V} \left(\mu_0 B^2 - \varepsilon_0 E^2\right) dV}{\int_V \left(\mu_0 B^2 + \varepsilon_0 E^2\right) V}. \tag{9.12}$$

Temperature control for RF cavities is typically performed by water cooling systems, which roughly keep the cavities within $\pm 0.1^\circ$ of a desired temperature, with response times on the order of tens of seconds. Such control is sufficient for keeping

the cavities well cooled, and within a rough neighborhood of their required resonance frequency, but is too slow and too inaccurate to maintain the cavities within required bounds of their designed resonance frequencies such that reflected power is acceptably low.

The response of a single mode of a resonant radio frequency (RF) cavity can be fairly accurately modeled as an RLC circuit (Fig. 9.11), with dynamics

$$\ddot{V} = -\omega_0^2 V - \frac{\omega_0}{Q}\dot{V} + \frac{1}{C}\dot{I} \tag{9.13}$$

where $V(t)$ is the cavity's accelerating voltage, $I(t)$ is the driving current, C is a capacitance, and L is inductance, such that $\omega_0 = \frac{1}{\sqrt{LC}}$, and $Q = f_0/f_{1/2}$ is the cavity quality factor where $f_0 = \omega_0/2\pi$ and $f_{1/2}$ is the cavity half-power bandwidth.

For RF driving current of the from $I(t) = \cos(\omega t)$, at steady state, the cavity field is proportional to

$$V \sim \frac{1}{\sqrt{1+\gamma^2}}, \quad \gamma \approx 2Q\frac{\omega - \omega_0}{\omega_0}, \tag{9.14}$$

and reflected power is proportional to

$$P_r(\omega, \omega_0) \sim 1 - \frac{1}{\sqrt{1 + 4Q^2\left(\frac{\omega-\omega_0}{\omega_0}\right)^2}}. \tag{9.15}$$

If the difference between driving frequency ω and resonant frequency ω_0 is too large, the reflected power can result in both damage to the RF source and insufficient power in the cavity to reach desired accelerating field levels.

9.3.2 Phase Measurement Based Resonance Controller

High accuracy, fast resonance control is performed via tuning of mechanical slugs by electric stepper motors, as shown in Fig. 9.11, which modify cavity resonance as estimated by Eq. (9.12). Because the electrical field of the accelerating mode decays to zero, while the magnetic field grows to a maximum amplitude as we approach the outer wall of the cavity, as shown in Fig. 9.11, near the wall of the cavity, for small slug displacement, δ, from some initial position δ_0, we estimate $E \approx 0$ and $B(r) \approx B^2(R_c)$, where R_c is the radius of the cavity.

Considering a slug of radius r_s, for small perturbations δ, we approximate (9.12) as

$$\Delta\omega_0(\delta) \approx \omega_0 K \delta, \quad K = \frac{\pi r_s^2 B^2(R_c)}{\int_V \left(\mu_0 B^2 + \varepsilon_0 E^2\right) V}. \tag{9.16}$$

We also know that for a given frequency offset, $\Delta\omega$, the phase of the cavity field relative to the driving field, is given by ψ, which satisfies

$$\tan(\psi) \approx 2Q\frac{\Delta\omega}{\omega_0}. \tag{9.17}$$

Combining (9.16) and (9.17) one is able to determine in which direction to move the slug in order to compensate for temperature-induced resonance shift. The difficulty with this approach is in its requirement of a precise phase-difference measurement. Although the difficulty in measuring the phase difference between two high frequency RF signals has been overcome, there is always an arbitrary phase shift introduced by the cables through which the RF signals are transported for measurement. Such arbitrary phase offsets can be calibrated out by considering the reflected power from a frequency-perturbed cavity, (9.15), which has a minimum when the cavity is on resonance.

This feedback is then put in place during cavity operation to maintain resonance. However, any time that maintenance is performed and any equipment or cables are changed, the calibration must be re-done. Furthermore, because the RF cables throughout accelerators are constantly experiencing temperature variations, their lengths are time-varying quantities whose slow variations continuously introduce un-calibrated offsets into the feedback system.

Therefore, we utilize the ability of bounded ES to minimize time-varying, uncertain functions, to maintain cavity resonance despite unknown time-varying perturbations of cavity geometry. The main idea of the ES-based resonance controller is to continuously minimize reflected power measurements in order to maintain the cavity on resonance, without needing any phase information. A typical PID-type loop is unable to utilize the reflected power measurement for continuous slug tuning without phase measurements, because of the direction ambiguity; reflected power increases whenever the cavity is too hot or too cold, and only the additional information provided by phase measurement tells one which direction the resonance has moved. Considering reflected power (9.15) together with the influence of the slug on the cavity resonance (9.16), we get the slug-perturbed reflected power:

$$1 - \frac{1}{\sqrt{1 + 4Q^2\left(\frac{\omega - \omega_0(1+K\delta)}{\omega_0(1+K\delta)}\right)^2}}. \tag{9.18}$$

Furthermore, if the resonance of the cavity has shifted from its nominal value, ω_0 to $\omega_0 + \varepsilon(t)$, due to mechanical changes, such as expansion or contraction due to temperature change, the reflected power is proportional to

$$1 - \frac{1}{\sqrt{1 + 4Q^2\left(\frac{\omega - (\omega_0+\varepsilon(t))(1+K\delta)}{(\omega_0+\varepsilon(t))(1+K\delta)}\right)^2}}. \tag{9.19}$$

Typically, an RF system is set up to drive the cavity with a field at its design resonance frequency, ω_0, the reflected power is then proportional to

$$P_r(\varepsilon(t), \delta) = 1 - \frac{1}{\sqrt{1 + 4Q^2 \left(\frac{K\delta(\omega_0 + \varepsilon(t)) + \varepsilon(t)}{\omega_0 + \omega_0 K\delta + \varepsilon(t) + \varepsilon(t) K\delta} \right)^2}}, \tag{9.20}$$

which has a global minimum at

$$\delta^\star(t) = -\frac{\varepsilon(t)}{K(\omega_0 + \varepsilon(t))}. \tag{9.21}$$

We utilize the ES feedback:

$$\dot{\delta} = \sqrt{\alpha \omega_{ES}} \cos\left(\omega_{ES} t + k P_r(\varepsilon(t), \delta, t)\right), \tag{9.22}$$

which has average dynamics

$$\dot{\bar{\delta}} = -\frac{k\alpha}{2} \frac{\partial P_r}{\partial \bar{\delta}}, \tag{9.23}$$

which performs a gradient descent towards the global minimum $d^\star(t)$, when the high frequency ES perturbation ω_{ES} is fast relative to the disturbance dynamics $\varepsilon(t)$.

9.3.3 *Experimental Results*

For the short term test, a heat source was used to periodically heat the cavity and cause it to move drastically off resonance as shown in the first 15 min of Fig. 9.12, where without feedback control, the reflected power is periodically dramatically increased. After 15 min, the ES feedback control 9.22 was activated and no change is seen in reflected power in Fig. 9.12. Figure 9.13 zooms in to show both the reflected power

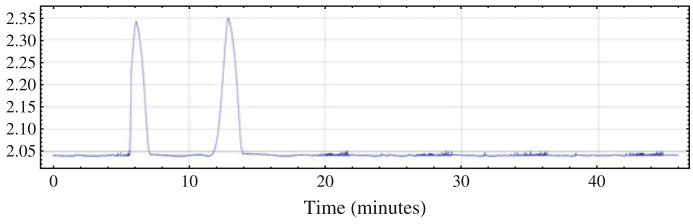

Fig. 9.12 Reflected power is shown as a function of time. for the first 15 min the ES controller is off and a heating element is used to perturb the cavity resonance periodically. After 15 min, feedback control is activated and reflected power is kept at a minimum despite the heater turning on

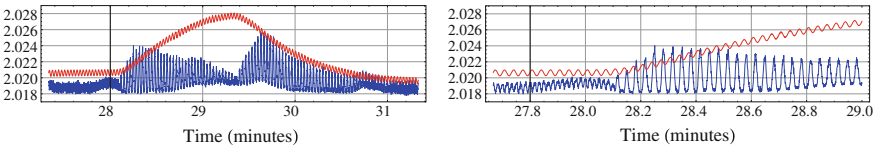

Fig. 9.13 A zoomed in detailed view of the reflected power *(blue)* and the position of the control slug *(red)*. The controller can be seen activating every time that the heater is turned on, to maintain minimal reflected power

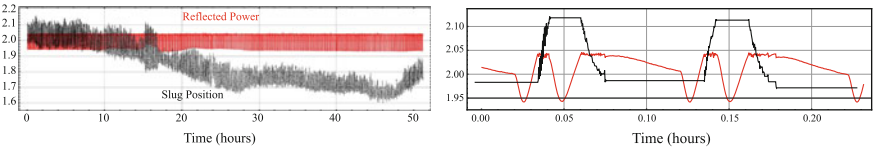

Fig. 9.14 Reflected power *(red)* is shown next to slug tuner position *(black)* with implementation of dead zone to prevent slug from continuously moving

and slug tuner position when the heater was activated and the motor had to respond to keep the cavity on resonance.

Finally, Fig. 9.14 shows results of implementation of ES combined with a dead zone so that the controller only responded when reflected power exceeded a prescribed threshold, resulting in the motor moving only for small periods of time when required, instead of the persistent motion typical of ES feedback which could degrade the mechanical motor over time. A long term test was conducted over 2 days for 50 + h. While the reflected power is maintained below a prescribed threshold, the slug tuner position is seen to move in a repeatable fashion to compensate for short heater-induced temperature variations, and a slower, further motion takes place over a longer time scale as the room temperature slowly drifted.

Chapter 10
Conclusions

This book presents a new application of Extremum Seeking, as a method for stabilization of unknown systems as well as trajectory tracking and optimization. The stabilization of unknown systems is possible due to the controller's ability to perform a gradient descent of unknown functions or of purposely chosen Lyapunov-like functions.

The extremum seeking algorithm creates a closed loop system that is independent of the control vector's direction. This is a useful property which allows us to stabilize and perform trajectory tracking with unknown, unstable, control direction-varying systems using a particular form of time-varying nonlinear high-gain feedback.

In Chap. 5, we showed that the ES controllers may be chosen such that they turn themselves off as equilibrium is approached, in Chap. 6 we showed that they may be chosen so that they are bounded, with all unknowns entering the ES scheme as arguments of a-priori known, bounded functions, in Chap. 7, we showed that we are not limited to systems affine in control, and in Chap. 8 we concluded that we may replace smooth perturbing functions such as $\sin(\cdot)$ or $\cos(\cdot)$, with a general class of integrable functions, such as square waves with dead time or triangle waves, signals which are more naturally implemented in digital logic. Finally, in Chap. 9 we described a few cases of implementation of these methods, in hardware, for tuning various components of a particle accelerator.

One of the main challenges of ESS, as with all other ES approaches, is that it is an existence result. For any system, for any given compact set and any desired degree of accuracy, there exists some $\omega^\star$, such that for all $\omega > \omega^\star$, the desired results hold. Finding concrete bounds on $\omega^\star$ based on a given system's parameters and a set of initial conditions would be an interesting result. Another possible topic of future research may be in creating an auto-tuning ESC controller, which iteratively or dynamically adjusts its own k, α, and ω values, in order to stabilize or optimize an unknown system.

A. Scheinker and M. Krstić, *Model-Free Stabilization by Extremum Seeking*,
SpringerBriefs in Control, Automation and Robotics,
DOI 10.1007/978-3-319-50790-3_10

Series Editor Biography

Tamer Başar is with the University of Illinois at Urbana-Champaign, where he holds the academic positions of Swanlund Endowed Chair, Center for Advanced Study Professor of Electrical and Computer Engineering, Research Professor at the Coordinated Science Laboratory, and Research Professor at the Information Trust Institute. He received the B.S.E.E. degree from Robert College, Istanbul, and the M.S.,M.Phil, and Ph.D. degrees from Yale University. He has published extensively in systems, control, communications, and dynamic games, and has current research interests that address fundamental issues in these areas along with applications such as formation in adversarial environments, network security, resilience in cyber-physical systems, and pricing in networks.

In addition to his editorial involvement with these Briefs, Basar is also the Editor in Chief of Automatica, Editor of two Birkhäuser Series on Systems & Control and Static & Dynamic Game Theory, the Managing Editor of the Annals of the International Society of Dynamic Games (ISDG), and member of editorial and advisory boards of several international journals in control, wireless networks, and applied mathematics. He has received several awards and recognitions over the years, among which are the Medal of Science of Turkey (1993); Bode Lecture Prize (2004) of IEEE CSS; Quazza Medal (2005) of IFAC; Bellman Control Heritage Award (2006) of AACC; and Isaacs Award (2010) of ISDG. He is a member of the US National Academy of Engineering, Fellow of IEEE and IFAC, Council Member of IFAC (2011-2014), a past president of CSS, the founding president of ISDG, and president of AACC (2010–2011).

Antonio Bicchi is Professor of Automatic Control and Robotics at the University of Pisa. He graduated from the University of Bologna in 1988 and was a postdoc scholar at M.I.T. A.I. Lab between 1988 and 1990. Following are his main research interests:

- dynamics, kinematics, and control of complex mechanical systems, including robots, autonomous vehicles, and automotive systems;
- haptics and dextrous manipulation; and theory and control of nonlinear systems, in particular hybrid (logic/dynamic, symbol/signal) systems;

A. Scheinker and M. Krstić, *Model-Free Stabilization by Extremum Seeking*,
SpringerBriefs in Control, Automation and Robotics,
DOI 10.1007/978-3-319-50790-3

- theory and control of nonlinear systems, in particular hybrid (logic/dynamic, symbol/ signal) systems.

He has published more than 300 papers in international journals, books, and refereed conferences.

ProfessorBicchi currently serves as the Director of the Interdepartmental Research Center "E. Piaggio" of the University of Pisa, and President of the Italian Association or Researchers in Automatic Control. He has served as Editor in Chief of the Conference Editorial Board for the IEEE Robotics and Automation Society (RAS), and as Vice President of IEEE RAS, Distinguished Lecturer, and Editor for several scientific journals including the *International Journal of Robotics Research, the IEEE Transactions on Robotics and Automation, and IEEE RAS Magazine.* He has organized and co-chaired the firstWorldHapticsConference (2005), and Hybrid Systems: Computation and Control (2007). He is the recipient of several best paper awards at various conferences, and of an Advanced Grant from the European Research Council. Antonio Bicchi has been an IEEE Fellow since 2005.

Miroslav Krstic holds the Daniel L. Alspach chair and is the founding director of the Cymer Center for Control Systems and Dynamics at University of California, San Diego. He is a recipient of the PECASE, NSF Career, and ONR Young Investigator Awards, as well as the Axelby and Schuck Paper Prizes. Professor Krstic was the first recipient of the UCSD Research Award in the area of engineering and has held the Russell Severance Springer Distinguished Visiting Professorship at UC Berkeley and the HaroldW. Sorenson Distinguished Professorship at UCSD. He is a Fellow of IEEE and IFAC. Professor Krstic serves as Senior Editor for *Automatica and IEEE Transactions on Automatic Control and as Editor for the Springer series Communications and Control Engineering.* He has served as Vice President for Technical Activities of the IEEE Control Systems Society. Krstic has co-authored eight books on adaptive, nonlinear, and stochastic control, extremum seeking, control of PDE systems including turbulent flows and control of delay systems.

References

1. A. Abrishamifar, Fixed switching frequency sliding mode control for single-phase unipolar inverters. IEEE Trans. Power Electron. **27**, 2507–2514 (2012)
2. V. Adetola, M. Guay, Adaptive output feedback extremum seeking receding horizon control of linear systems. J. Process Control **16**, 521–533 (2006)
3. V. Adetola, M. Guay, Guaranteed parameter convergence for extremum-seeking control of nonlinear systems. Automatica **43**, 105–110 (2007)
4. S. Almer, S. Mariethoz, M. Morari, Dynamic phasor model predictive control of switched mode power converters. IEEE Trans. Control Syst. Technol. **23**, 349–356 (2015)
5. R. Antonello, M. Carraro, M. Zigliotto, Maximum-torque-per-ampere operation of anisotropic synchronous permanent-magnet motors based on extremum seeking control. IEEE Trans. Industr. Electron. **61**, 5086–5093 (2014)
6. K.B. Ariyur, M. Krstić, *Real-Time Optimization by Extremum-Seeking Control* (Wiley-Interscience, Hoboken, NJ, 2003)
7. V. Ayvazyan, S. Simrock, Dynamic Lorentz Force Detuning Studies in Tesla Cavities, in *Proceedings of European Particle Accelerator Conference*, Lucerne (2004)
8. R. Bartolini, M. Apollonio, I.P.S. Martin, Phys. Rev. ST Accel. Beams **15**, 030701 (2012)
9. I. Bazarov, C. Sinclair, Phys. Rev. ST Accel. Beams **8**, 034202 (2005)
10. A.M. Bazzi, P.T. Krein, Concerning 'Maximum power point tracking for photovoltaic optimization using ripple-based extremum seeking control'. IEEE Trans. Power Electron. **26**, 1611–1612 (2011)
11. M. Borland, V. Sajaev, L. Emery, A. Xiao, Direct methods of optimization of storage ring dynamic and momentum aperture. in *Proceedings PAC 2009*, 2009
12. R. Becker, R. King, R. Petz, W. Nitsche, Adaptive closed-loop separation control on a high-lift configuration using extremum seeking. AIAA Paper 2006–3493 (2006)
13. R. Becker, R. King, W. Petz, W. Nitsche, Adaptive closed-loop separation control on a high-lift configuration using extremum seeking. AIAA J. **45**, 1382–1392 (2007)
14. N. Bizon, Global maximum power point tracking (GMPPT) of photovoltaic array using the extremum seeking control (ESC): a review and a new GMPPT ESC scheme. Renew. Sustain. Energy Rev. **57**, 524–539 (2016)
15. A. Brunn, W. Nitsche, L. Henning, R. King, Application of slope-seeking to a generic car model for active drag control, preprint
16. S.L. Brunton, C.W. Rowley, S.R. Kulkarni, C. Clarkson, Maximum power point tracking for photovoltaic optimization using extremum seeking, in *34th IEEE Photovoltaic Specialists Conference (PVSC)*, Philadelphia, 2009

A. Scheinker and M. Krstić, *Model-Free Stabilization by Extremum Seeking*,
SpringerBriefs in Control, Automation and Robotics,
DOI 10.1007/978-3-319-50790-3

17. S.L. Brunton, C.W. Rowley, S.R. Kulkarni, C. Clarkson, Maximum power point tracking for photovoltaic optimization using ripple-based extremum seeking control. IEEE Trans. Power Electron. **25**, 2531–2540 (2010)
18. D. Carnevale, A. Astolfi, C. Centioli, S. Podda, V. Vitale, L. Zaccarian, A new extremum seeking technique and its application to maximize RF heating on FTU. Fusing Eng. Design **84**, 554–558 (2009)
19. C. Centioli, F. Iannone, G. Mazza, M. Panella, L. Pangione, S. Podda, A. Tuccillo, V. Vitale, L. Zaccarian, Maximization of the lower hybrid power coupling in the Frascati Tokamak Upgrade via extremum seeking. Control Eng. Pract. **16**, 1468–1478 (2008)
20. J.-Y. Choi, M. Krstić, K.B. Ariyur, J.S. Lee, Extremum seeking control for discrete-time systems. IEEE Trans. Autom. Control **47**, 318–323 (2002)
21. S.K. Chung, H.B. Shin, H.W. Lee, Precision control of single-phase PWM inverter using PLL compensation. IEE Proc. Electr. Power Appl. **152**, 429–436 (2005)
22. J. Cochran, E. Kanso, S.D. Kelly, H. Xiong, M. Krstić, Source seeking for two nonholonomic models of fish locomotion. IEEE Trans. ŁRobotics **25**(5), 1166–1176 (2009)
23. J. Cochran, M. Krstić, Nonholonomic source seeking with tuning of angular velocity. Trans. Autom. Control **54**(4), 717–731 (2009)
24. J. Conway, *A Course in Functional Analysis* (Springer-Verlag, New York, 1990)
25. J. Creaby, Y. Li, J.E. Seem, Maximizing wind turbine energy capture using multivariable extremum seeking control. Wind Eng. **33**, 361–387 (2009)
26. S. Dasgupta, S.K. Sahoo, S.K. Panda, Single-phase inverter control techniques for interfacing renewable energy sources with micro gird—Part I: Paralle-connected inverter topology with active and reactive power flow control along with grid current shaping. IEEE Trans. Power Electron. **26**, 717–731 (2011)
27. S. Dasgupta, S.K. Sahoo, S.K. Panda, Single-phase inverter control techniques for interfacing renewable energy sources with micro gird—Part II: Series-connected inverter topology to mitigate voltage-related problems along with active power flow control. IEEE Trans. Power Electron. **26**, 732–746 (2011)
28. D. DeHaan, M. Guay, Extremum-seeking control of state-constrained nonlinear systems. Automatica **41**, 1567–1574 (2005)
29. P. Dower, P.M. Farrel, D. Nesic, Extremum seeking control of cascaded Raman optical amplifiers. IEEE Trans. Control Syst. Technol. **16**, 396–407 (2008)
30. C.S. Draper, Y.T. Li, Principles of optimalizing control systems and an application to the internal combustion engine, in *Optimal and Self-optimizing Control*, ed. by R. Oldenburger (The M.I.T. Press, Boston, MA, 1951)
31. H. Dürr, M. Stanković, C. Ebenbauer, K. Johansson, Lie bracket approximation of extremum seeking systems. Automatica **49**, 1538–1552 (2013)
32. H.B. Dürr, M.S. Stankovć, K.H. Johansson, C. Ebenbauer, Extremum seeking on submanifords in the Euclidian space. Automatica **50**, 2591–2596 (2014)
33. H.B. Dürr, M. Krstic, A. Scheinker, C. Ebenbauer, Singularly perturbed lie bracket approximation. IEEE Trans. Autom. Control **60**, 3287–3292 (2015)
34. L. Emery, Global optimization of damping ring designs using a multi-objective evolutionary algorithm, in *PAC 2005* (2005)
35. A. Favache, M. Guay, M. Perrier, D. Dochain, Extremum seeking control of retention for a microparticulate system. Can. J. Chem. Eng. **86**, 815–827 (2008)
36. R. Freeman, P. Kokotović, *Robust Nonlinear Control Design* (Birkhauser, 1996)
37. P. Frihauf, M. Krstić, T. Başar, Nash equilibrium seeking for games with non-quadratic payoffs, in *Proceeding IEEE Conference on Decision and Control*, Atlanta, GA, 2010
38. W. Gao, L. Wang, W. Li, Phys. Rev. ST Accel. Beams **14**, 094001 (2011)
39. S. Ge, C. Yang, T. Lee, Adaptive robust control of a class of nonlinear strict-feedback discrete-time systems with unknown control directions. Syst. Control Lett. **57**, 888–895 (2008)
40. M.A. Ghadiri-Modarres, M. Mojiri, H.R.Z. Zangeneh, New schemes for GPS-denied source localization using a nonholonomic unicycle. IEEE Trans. Control Syst. Technol. (2016, to appear)

41. A. Ghaffari, M. Krstic, D. Nesic, Multivariable Newton-based extremum seeking. Automatica **48**, 1759–1767 (2012)
42. A. Ghaffari, M. Krstić, S. Seshagiri, Power optimization for photovoltaic micro-converters using multivariable Newton-based extremum seeking. IEEE Trans. Control Syst. Technol. **22**, 2141–2149 (2014)
43. M. Grecki, J. Andryszczak, T. Pozniak, K. Przygoda, P. Sekalski, Compensation of Lorentz Force Detuning, in *Proceedings of EPAC 2008*, Genoa, 2008
44. M. Guay, T. Zhang, Adaptive extremum seeking control of nonlinear dynamics systems with parametric uncertainties. Automatica **39**, 1283–1293 (2003)
45. M. Guay, D. Dochain, M. Perrier, Adaptive extremum seeking control of continuous stirred tank bioreactors with unknown growth kinetics. Automatica **40**, 881–888 (2004)
46. M. Guay, M. Perrier, D. Dochain, Adaptive extremum seeking control of nonisothermal continuous stirred reactors. Chem. Eng. Sci. **60**, 3671–3681 (2005)
47. M. Guay, D. Dochain, M. Perrier, N. Hudon, Flatness-based extremum-seeking control over periodic orbits. IEEE Trans. Autom. Control **52**, 2005–2012 (2007)
48. M. Guay, A time-varying extremum-seeking control approach for discrete-time systems. J. Process Control **24**, 98–112 (2014)
49. M. Guay, E. Moshksar, D. Dochain, A constrained extremum-seeking control approach. Int. J. Robust Nonlinear Control **25**, 3132–3153 (2014)
50. M. Guay, D. Dochain, A time-varying extremum-seeking control approach. Automatica **51**, 356–363 (2015)
51. M. Guay, D. Dochain, A multi-objective extremum-seeking controller design technique. Int. J. Control **88**, 38–53 (2015)
52. M. Guay, A perturbation-based proportional integral extremum-seeking control approach. IEEE Trans. Autom. Control (2016, to appear)
53. L. Gurvits, Averaging approach to nonholonomic motion planning, in *Proceeding IEEE Conference, Robotics and Automation*, Nice, France, 1992
54. L. Gurvits, Z. Li, Smooth time-periodic solutions for non-holonomic motion planning. NYU, Technical report TR-598, 1992
55. L. Gurvits, Z. Li, in Smooth time-periodic solutions for non-holonomic motion planning, ed. by Z. Li, J.F. Canny, Nonholonomic Motion Planning (Kluwer, 1992)
56. R. Hajima, N. Taked, H. Ohashi, M. Akiyama, Nucl. Instrum. Methods Phys. Res., Sect. A **318**, 822 (1992)
57. M. Haring, N. Wouw, D. Nesic, Extremum-seeking control for nonlinear systems with periodic steady-state outputs. Automatica **49**, 1883–1891 (2013)
58. L. Henning, R. Becker, G. Feuerbach, R. Muminovic, A. Brunn, W. Nitsche, R. King, Extensions of adaptive slope-seeking for active flow control. J. Syst. Control Eng
59. H. Heydari-doostabad, R. Keypour, M.R. Khalghani, M.H. Khooban, A new approach in MPPT for photovoltaic array based on extremum seeking control under uniform and non-uniform irradiances. Sol. Energy **94**, 28–36 (2013)
60. A. Hofler, B. Terzic, M. Kramer, A. Zvezdin, V. Morozov, Y. Roblin, F. Lin, C. Jarvis, Phys. Rev. ST Accel. Beams **16**, 010101 (2013)
61. L. Hsu, T.R. Oliveira, J.P.V.S. Cunha, Extremum seeking control via monitoring function and time-scaling for plants of arbitrary relative degree, in *Proceeding of 13th International Workshop on Variable Structure Systems*, Nantes, 2014
62. X.Y. Gu, C. Shao, Robust adaptive control of time-varying linear plants using polynomial approximation. in *IEE Proceedings D. Control Theory and Applications*, vol. 140, no. 2 (IET, 1993)
63. P. Ioannou, J. Sun, *Robust Adaptive Control* (Prentice Hall, 1996)
64. J. Jackson, *Classical Electrodynamics* (Wiley, NJ, 1999)
65. P.L. Kapitza, Dynamic stability of a pendulum when its point of suspension vibrates. Soviet Phys. JETP **21**, 588592 (1951)
66. V.V. Kazakevich, Technique of automatic control of different processes to maximum or to minimum, Avtorskoe svidetelstvo. (USSR Patent). No **66335**, 25 (1943)

67. V.V. Kazakevich, On extremum seeking, Ph.D. Thesis, Moscow High Technical University (1944)
68. H. Khalil, *Nonlinear Systems* (Upper Saddle River, Prentice -Hall, 2002)
69. S.Z. Khong, D. Nesic, Y. Tan, C. Manzie, Unified frameworks for sampled-data extremum seeking control: global optimisation and multi-unit systems. Automatica **49**, 2720–2733 (2013)
70. K. Kim, C. Kasnakoglu, A. Serrani, M. Samimy, Extremum-seeking control of subsonic cavity flow. AIAA J. **47**, 195–205 (2009)
71. R. King, R. Becker, G. Feuerbach, L. Henning, R. Petz, W. Nitsche, O. Lemke, W. Neise, Adaptive flow control using slope seeking, in *14th IEEE Mediterranean Conference on Control Automation*, Ancona, Italy, 2006
72. J. Kurzweil, J. Jarnik, Limit processes in ordinary differential equations. J. Appl. Math. Phy. **38**, 241–256 (1987)
73. M. Krstić, I. Kanellakopoulos P.V. Kokotović, *Nonlinear and Adaptive Control Design*, 1995
74. M. Krstić, H. Deng, *Stabilization of Nonlinear Uncertain Systems* (Springer-Verlag, NY, 1998)
75. M. Krstić, Z. Li, Inverse optimal design of input-to-state stabilizing nonlinear controllers. IEEE Trans. Automat. Control **43**, 336–350 (1998)
76. M. Krstić, H. Wang, Stability of extremum seeking feedback for general dynamic systems. Automatica **36**, 595–601 (2000)
77. N. Kryloff, N. Bogoliuboff, *Introduction to Nonlinear Mechanics* (Princeton University Press, NJ, 1943)
78. A. Kumar, A. Jana, V. Kumar, A study of Dynamic Lorentz Force Detuning of 650 MHz g = 0.9 superconducting radiofrequency cavity. Nuclear Instrum. Methods Phy. Res. A **24**(6), 69–77 (2014)
79. J. Kurzweil, J. Jarnik, Iterated lie brackets in limit processes in ordinary differential equations. RM **14**, 125–137 (1988)
80. K. Kvaternik, L. Pave, Interconnection conditions for the stability of nonlinear sampled-data extremum seeking schemes, in *Proceedings of IEEE Conference on Decision and Control*, Florida, 2011
81. K. Kvaternik, L. Pavel, An analytic framework for decentralized extremum seeking control, in *Proceedings of American Control Conference*, Montreal, 2012
82. K. Kvaternik, L. Pavel, Analysis of decentralized extremum-seeking schemes, Technical Report 1201, University of Toronto Systems Control Group, 2012
83. M. Leblanc, "Sur l'electri"cation des chemins de fer au moyen de courants alternatifs de frequence elevee, *Revue Generale de l'Electricite*, 1922
84. R. Leyva, C. Alonso, I. Queinnec, A. Cid-Pastor, D. Lagrange, L. Martinez-Salamero, MPPT of photovoltaic systems using extremum-seeking control. IEEE Trans. Aerosp. Electron. Syst. **42**, 249–258 (2006)
85. R. Leyva, P. Artillan, C. Cabai, B. Estibals, C. Alonso, Dynamic performance of maximum power point tracking circuits using sinusoidal extremum seeking control for photovoltaic generation. Int. J. Electron. **98**, 529–542 (2011)
86. R. Leyva, C. Olalla, H. Zazo, C. Cabal, A. Cid-Pastor, I. Queinnec, C. Alonso, MPPT based on sinusoidal extremum-seeking control in PV generation. Int. J. Photoenergy **2012**, 1-7
87. P. Lei, Y. Li, Q. Chen, J.E. Seem, Extremum seeking control based integration of MPPT and degradation detection for photovoltaic arrays, in *Proceedings of 2010 American Control Conference*
88. P. Li, Y. Li, J. E. Seem, Extremum seeking control for efficient and reliable operation of air-side economizers, in *Proceedings of 2009 American Control Conference*
89. Y. Li, M.A. Rotea, G. Chiu, L. Mongeau, I. Paek, Extremum seeking control of tunable thermoacoustic cooler. IEEE Trans. Control Syst. Technol. **13**, 527–536 (2005)
90. X. Li, Y. Li, J.E. Seem, P. Lei, Maximum power point tracking for photovoltaic systems using adaptive extremum seeking control, in *ASME 2011 Dynamic Systems and Control Conference and Bath/ASME Symposium on Fluid Power and Motion Control*, Virginia, 2011

91. X. Li, Y. Li, J.E. Seem, P. Lei, Detection of internal resistance change for photovoltaic arrays using extremum-seeking control MPPT signals. IEEE Trans. Control Syst. Technol. **24**, 325–333 (2016)
92. M. Liepe, W. Moeller, S. Simrock, Dynamic Lorentz Force compensation with a fast piezo-electric tuner, in *Proceedings of the 2001 Particle Accelerator Conference*, Chicago, 2001
93. S.-J. Liu, M. Krstić, Newton-based stochastic extremum seeking. Automatica **50**, 952–961 (2014)
94. L. Luo, E. Schuster, Mixing enhancement in 2D magnetohydrodynamic Łchannel flow by extremum seeking boundary control, in *Proceeding American Control Conference*, St. Louis, MO, 2009
95. J. Luxat, L. Lees, Stability of peak-holding control systems. IEEE Trans. Ind. Electron. Control Instrum., pp. 11–15 (1971)
96. R. Marino, P. Tomei, Robust stabilization of feedback linearizable time-varying uncertain nonlinear systems. Automatica **29**, 181–189 (1993)
97. S.M. Meerkov, Asymptotic methods for investigating a class of forced states in extremal systems. Autom. Remote Control **12**, 1916–1920 (1967)
98. I.S. Morosanov, Method of extremum control. Autom. Remote Control **18**, 1077–1092 (1957)
99. W.H. Moase, C. Manzie, M.J. Brear, Newton-like extremum-seeking part I: Theory, in *Proceeding IEEE Conference on Decision and Control*, Shanghai, China, 2009
100. W.H. Moase, C. Manzie, D. Nesic, I.M.Y. Mareels, Extremum seeking from 1922 to 2010, in 29th *Chinese Control Conference*, 14, 2010
101. W.H. Moase, C. Manzie, M.J. Brear, Newtown-like extremum-seeking for the control of thermoacoustic instability. IEEE Trans. Autom. Control **55**, 2094–2105 (2010)
102. W.H. Moase, C. Manzie, Fast extremum-seeking for Wiener-Hammerstein plants. Automatica **48**, 2433–2443 (2012)
103. W.H. Moase, C. Manzie, Semi-global stability analysis of observer-based extremum-seeking for Hammerstein plants. IEEE Trans. Autom. Control **57**, 1685–1695 (2012)
104. J.P. Moeck, M.R. Bothien, C.O. Paschereit, G. Gelbert, R. King, Two-parameter extremum seeking for control of thermoacoustic instabilities and characterization of linear growth, AIAA Paper 2007–1416
105. L. Moreau, D. Aeyels, Practical stability and stabilization. IEEE Trans. Autom. Control **45**, 1554–1558 (2000)
106. D. Mudgett, S. Morse, Adaptive stabilization of linear systems with unknown high-frequency gains. IEEE Trans. Automat. Control **30**, 549–554 (1985)
107. D. Nešić, Y. Tan, W.H. Moase, C. Manzie, A unifying approach to extremum seeking: Adaptive schemes based on estimation of derivatives, in *Proceeding IEEE Conference on Decision and Control*, Atlanta, GA, December 2010
108. D. Nesic, A. Mohammadi, C. Manzie, A framework for extremum seeking control of systems with parameter uncertainties. IEEE Trans. Autom. Control **58**, 435–448 (2013)
109. D. Nesic, T. Nguyen, Y. Tan, C. Manzie, A non-gradient approach to global extremum seeking: an adaptation of the Shubert algorithm. Automatica **49**, 809–815 (2013)
110. M. Nordin, P.-O. Gutman, Controlling mechanical systems with backlash, a survey. Automatica **38**, 1633–1649 (2002)
111. R. Nussbaum, Some remarks on a conjecture in parameter adaptive control. Syst. Control Lett. **3**, 243–246 (1985)
112. V.K. Obabkov, Theory of multichannel extremal control systems with sinusoidal probe signals. Autom. Remote Control **28**, 48–54 (1967)
113. T. Roux Oliveira, A.J. Peixoto, L. Hsu, Global real-time optimization by output-feedback extremum-seeking control with sliding modes. J. Franklin Inst. **349**, 1397–1415 (2012)
114. T. Roux Oliveira and M. Krstić, Gradient extremum seeking with delays, in *12th IFAC Workshop on time delay systems*, 2015
115. T. Roux Oliveira, M. Krstić, Newton-based extremum seeking under actuator and sensor delays, in *12th IFAC Workshop on time delay systems*, Michigan, 2015

116. T. Roux Oliveira, M. Krstić, D. Tsubakino, Extremum seeking for static maps with delays, IEEE Trans. Autom. Control (2016, to appear)
117. I.I. Ostrovskii, Extremum regulation. Autom. Remote Control **18**, 900–907 (1957)
118. A.J. Peixoto, T.R. Oliveira, Global output-feedback extremum seeking for a class of nonlinear dynamic systems with arbitrary relative degree. Int. J. Control, 1–17 (2016)
119. K. Peterson, A. Stefanopoulou, Extremum seeking control for soft landing of an electromechanical valve actuator. Automatica **29**, 1063–1069 (2004)
120. A. Poklonskiy, D. Neuffer, Int. J. Modern. Phys. A **24**, 5 (2009)
121. D. Popović, M. Janković, S. Magner, A. Teel, Extremum seeking methods for optimization of variable CAM timing engine operation. IEEE Trans. Control Syst. Technol. **14**, 398–407 (2006)
122. D.A. Recker, et al., Adaptive nonlinear control of systems containing a deadzone, in *Proceedings of the 30th IEEE Conference on Decision and Control*, (IEEE, 1991)
123. A.R. Reisi, M.H. Moradi, S. Jamasb, Classification and comparison of maximum power point tracking techniques for photovoltaic system: a review. Renew. Sustain. Energy Rev. **19**, 433–443 (2013)
124. M.A. Rotea, Analysis of multivariable extremum seeking algorithms, in *Proceedings of the 2000 American Control Conference*
125. A. Scheinker, Extremum seeking for stabilization, Ph.D. Thesis, University of California, San Diego, 2012
126. A. Scheinker, M. Krstić, A universal extremum seeking-based stabilizer for unknown LTV systems with unknown control directions, in *Proceeding ACC*, Montreal, Canada, 2012
127. A. Scheinker, M. Krstić, Extremum seeking-based tracking for unknown systems with unknowns control directions, in *Proceeding CDC*, Maui, HI, 2012
128. A. Scheinker, M. Krstić, Maximum-seeking for CLFs: universal semiglobally stabilizing feedback under unknown control directions. IEEE Trans. Autom. Control **58**, 1107–1122 (2013)
129. A. Scheinker, M. Bland, M. Krstić, J. Audia, Rise-time optimization of high voltage converter modulator rise-time. IEEE Trans. Control Syst. Technol. **22**, 34–43 (2013)
130. A. Scheinker, X. Pang, L. Rybarcyk, Model-independent particle accelerator tuning. Phy. Rev. Accel. Beams **16**(10), 102803 (2013)
131. A. Scheinker, M. Krstić, Non-C^2 Lie bracket averaging for nonsmooth extremum seekers. J. Dyn. Syst. Meas. Control **136**(1), 011010 (2014)
132. A. Scheinker, M. Krstić, Extremum seeking with bounded update rates. Syst. Control Lett. **63**, 25–31 (2014)
133. A. Scheinker, S. Gessner, Adaptive method for electron bunch profile prediction. Phy. Rev. Accel. Beams **18**(10), 102801 (2015)
134. A. Scheinker, D. Scheinker, Bounded extremum seeking with discontinuous dithers. Automatica **69**, 250–257 (2016)
135. A. Scheinker, D. Scheinker, Extremum seeking for systems not affine in control, arXiv preprint arXiv:1608.04587 (2016)
136. A. Scheinker, Extremum seeking for RF Cavity resonance control, in *Proceeding ACC*, Boston, USA, 2016
137. A. Scheinker, Application of extremum seeking for time varying systems to resonance control of RF cavities. IEEE Trans. Control Syst. Technol. (submitted)
138. R.R. Selmic, F.L. Lewis, Deadzone compensation in motion control systems using neural networks. IEEE Trans. Autom. Control **45**(4), 602–613 (2000)
139. R. Sepulchre, M. Jankovic, P.V. Kokotović, *Constructive Nonlinear Control* (Springer, 1997)
140. S. Simrock, Lorentz force compensation of pulsed SRF Cavities, in *Proceedings of LINAC 2002*, Gyeongju, 2002
141. J.C. Slater, Microwave electronics. Rev. Modern Phy. **18**(4), October 1946
142. E. Sontag, A "universal" construction of Artstein's theorem on nonlinear stabilization. Syst. Contr. Lett. **13**, 117–123 (1989)

143. M.S. Stanković, K.H. Johansson, D.M. Stipanović, Distributed seeking of Nash equilibria in mobile sensor networks. in *Proceeding IEEE Conference On Decision and Control*, Atlanta, GA, 2010
144. M.S. Stanković, D.M. Stipanović, Extremum seeking under stochastic noise and applications to mobile sensors. Automatica **46**, 1243–1251 (2010)
145. H.J. Sussmann, W. Liu, Limits of highly oscillatory controls and the approximation of general paths by admissible trajectories, in *Proceeding IEEE Conference on Decision and Control*, Brightonm England, 1991
146. H.J. Sussmann, New differential geometric methods in nonholonomic path finding, in *Progress Systems and Control Theory*, pp. 365–384 (1992)
147. Y. Tan, D. Nešić, I. Mareels, On non-local stability properties of extremum seeking control. Automatica **42**, 889–903 (2006)
148. Y. Tan, D. Nesic, I. Mareels, On the choice of dither in extremum seeking systems: a case study. Automatica **44**, 1446–1450 (2008)
149. Y. Tan, D. Nesic, I.M.Y. Mareels, A. Astolfi, On global extremum seeking in the presence of local extrema. Automatica **45**, 245–251 (2009)
150. P. Tomei, R. Marino, *Nonlinear Control Design* (Prentice Hall, London, 1995)
151. O. Wiederhold, L. Neuhaus, R. King, W. Niese, L. Enghardt, B.R. Noack, M. Swoboda, Extensions of extremum-seeking control to improve the aerodynamic performance of axial turbomachines, in *Proceedings of the 39th AIAA Fluid Dynamics Conference*, AIAA 2009–4175, San Antonio, Texas, U.S.A., 2009
152. Y. Xudong, Asymptotic regulation of time-varying uncertain nonlinear systems with unknown control directions. Automatica **35**, 929–935 (1999)
153. Y. Xudong, Z. Ding, Robust tracking control of uncertain nonlinear systems with unknown control directions. Syst. Control Lett. **42**, 1–10 (2001)
154. L. Yang, D. Robin, F. Sannibale, C. Steier, W. Wan, Nucl. Instrum. Methods Phys. Res., Sect. A **609**, 50 (2009)
155. H.T. Yau, C.H. Wu, Comparison of extremum-seeking control techniques for maximum power point tracking in photovoltaic systems. Energies **4**, 2190–2195 (2011)
156. X. Ye, J. Jiang, Adaptive nonlinear design without a priori knowledge of control directions. IEEE Trans. Autom. Control **43**, 1617–1621 (1998)
157. C. Zhang, D. Arnold, N. Ghods, A. Siranosian, M. Krstić, Source seeking with nonholonomic unicycle without position measurement and with tuning of forward velocity. Syst. Control Lett. **56**, 245–252 (2007)
158. C. Zhang, A. Siranosian, M. Krstić, Extremum seeking for moderately unstable systems and for autonomous vehicle target tracking without position measurements. Automatica **43**, 1832–1839 (2007)
159. X.T. Zhang, D.M. Dawson, W.E. Dixon, B. Xian, Extremum-seeking nonlinear controllers for a human exercise machine. IEEE/ASME Trans. Mechatron. **11**, 233–240 (2006)
160. Y. Zhang, C. Wen, Y. Soh, Adaptive backstepping control design for systems with unknown high-frequency gain. IEEE Trans. Automat. Control **45**, 2350–2354 (2000)
161. C. Zhang, R. Ordonez, *Extremum-Seeking Control and Applications* (Springer-Verlag, London, 2012)